Function of Plasma Membrane V-ATPases in Breast Tumor Cell Invasion

A Thesis

Submitted by

Joseph Capecci

In partial fulfillment of the requirements
for the degree of

Doctor of Philosophy

in

Cellular and Molecular Physiology

TUFTS UNIVERSITY

Sackler School of Graduate Biomedical Sciences

February 2014

ADVISOR: Dr. Michael Forgac

Abstract

The vacuolar H^+ ATPases (V-ATPases) are a family of ATP-driven proton pumps that couple ATP hydrolysis with translocation of protons across membranes. V-ATPases are expressed in intracellular compartments, such as endosomes and lysosomes, where they participate in processes such as membrane trafficking and protein degradation. They are also present in the plasma membrane of specialized cells, such as osteoclasts and renal cells, where they function in bone resorption and urinary acidification, respectively. Previous studies have implicated V-ATPases in human cancer cell invasion. The a subunit, which controls cellular targeting of V-ATPases, is expressed as four isoforms in mammalian cells (a1-a4). The a3 and a4 isoforms target V-ATPases to the plasma membrane of osteoclasts and renal intercalated cells, respectively. Prior work from our laboratory comparing a subunit expression in human breast cancer cell lines has shown that both a3 and a4 are highly expressed in highly invasive MDA-MB231 cells compared to poorly invasive MCF7 cells and that knockdown of either isoform using isoform-specific siRNAs significantly inhibits invasion of MDA-MB231 cells. To further examine whether expression of particular a subunit isoforms is critical to invasiveness of breast tumor cells, two closely related cell lines have been examined. MCF10a is a non-invasive, immortalized, human breast epithelial cell line and MCF10CA1a is a highly invasive, H-Ras-transformed derivative of the MCF10a cell line that has been selected for its ability to form metastases in mice. We find that inhibition of V-ATPase activity by concanamycin reduced *in vitro* invasion of MCF10CA1a cells, but not the parental MCF10a cells. MCF10CA1a cells expressed higher levels of the a3 isoform and higher levels of plasma membrane V-ATPases relative to MCF10a cells, and knockdown of a3

(but not other isoforms) using isoform-specific siRNAs inhibits invasion of MCF10CA1a cells. Importantly, overexpression of the a3 isoform in the parental MCF10a cells significantly increased both the level of plasma membrane V-ATPases and *in vitro* invasion. To determine whether expression of V-ATPases at the plasma membrane is important in breast cancer cell invasion, we have employed an inhibitory antibody that selectively blocks plasma membrane V-ATPase activity. Inhibition of plasma membrane V-ATPases is shown to significantly reduce invasion of MDA-MB231 cells. These studies suggest that human breast tumor cells employ particular a subunit isoforms to target V-ATPases to the plasma membrane, where they aid in tumor cell invasion.

Acknowledgements

This work would not have been possible without contributions of numerous people. My committee members, Drs. Vladimir Marshansky, Brent Cochran, Daniel Jay and Peter Juo have provided experimental guidance and many helpful ideas. I am grateful to our collaborators Drs. Souad Sennoune and Raul Martinez-Zaguilan, who have provided experimental expertise that has been essential to this work. I am thankful to my colleagues, including Sarah Bond, Kristina Cotter, Ayana Hinton, Rachel Liberman, Regina Saum, Laura Stransky, Masashi Toei and Satoko Toei who have made the Forgac lab a pleasant and intellectually stimulating place to work. I am extremely grateful to have Dr. Michael Forgac as my thesis advisor. Mike has always been willing to spend time helping me with my projects and has taught me a great deal about conducting and writing about science. Mike has been an excellent example of how to excel as a scientist. Finally I would like to thank the members of my family, who have been extremely supportive during my time at Tufts. In particular, I would like to thank my wife Katie, who has always been willing to listen and offer encouragement during the challenges I have faced conducting the work of this thesis. Her support has been essential to this work.

Table of Contents

Appendix

List of Figures

Function of Plasma Membrane V-ATPases in Breast Tumor Cell Invasion

Chapter 1

Introduction

Proton transport into intracellular compartments is largely accomplished through the activity of Vacuolar H^+ ATPases (V-ATPases). V-ATPases are a family of large, membrane-embedded, ATP-dependent proton pumps that localize to a variety of cellular membranes, including lysosomes, endosomes, Golgi-derived vesicles, secretory vesicles and (for certain cell types) the plasma membrane (Forgac, 2007). The activity of V-ATPases is critical for a multitude of biological processes and is exploited in several disease processes. V-ATPases are structurally and mechanistically related to F-ATP synthases (F-ATPases) found in mitochondria, chloroplasts and bacteria and archaeal A-ATP synthases (A-ATPases) (Cross and Muller, 2004). However, V-ATPases are distinct from other rotary enzymes in that they function solely as proton pumps and do not synthesize ATP under physiological conditions. Thus, V-ATPases function in transport of protons out of the cytosol and into the lumen of membrane vesicles or into the extracellular space when expressed at the plasma membrane. V-ATPases contain multiple subunits that are organized into two functional domains; a peripheral V_1 domain that hydrolyzes ATP and a membrane embedded V_0 domain that transports protons across the membrane. This introductory chapter will review the current understanding of V-ATPase function, structure and mechanism and discuss the rational for this thesis.

Functions of V-ATPases

Intracellular Functions of V-ATPases

V-ATPases within early endosomes play a critical role in receptor-mediated endocytosis by facilitating the uncoupling of ligands, such as low-density lipoprotein, from their receptor complexes (Figure 1.1). This uncoupling allows for degradation of

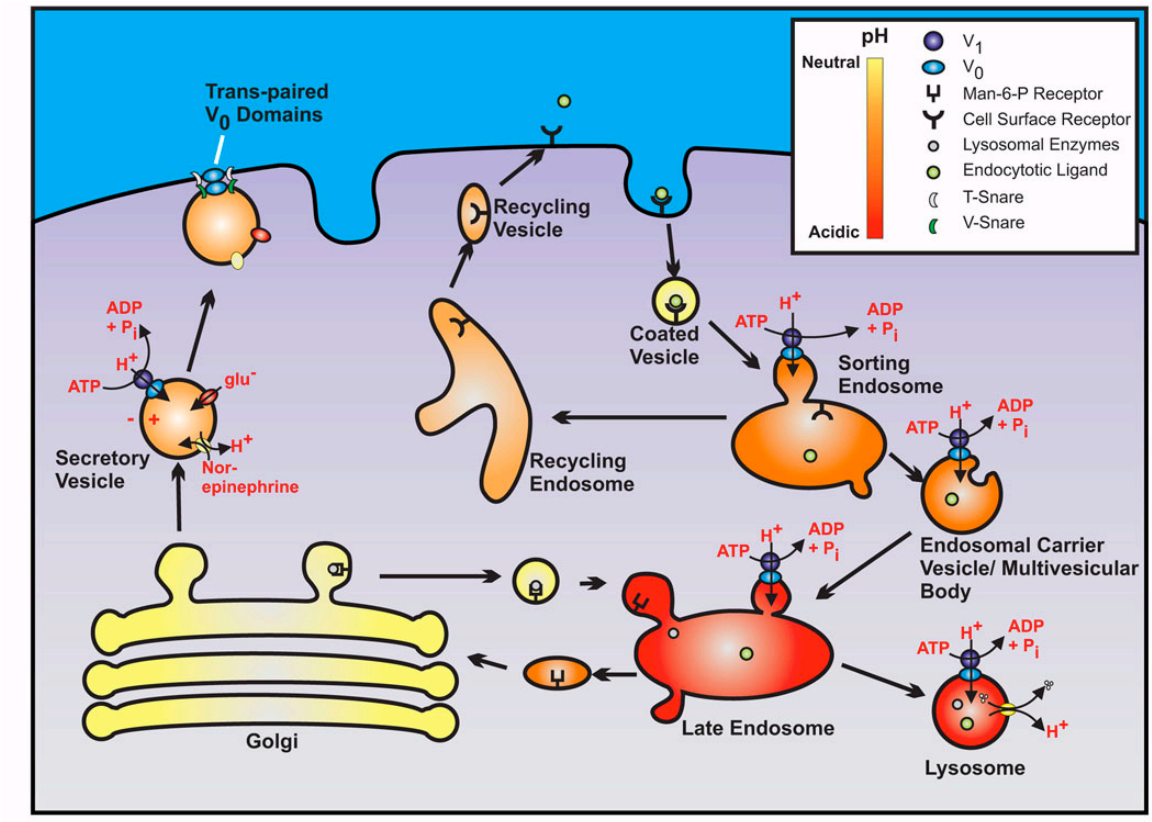

Figure 1.1. Functions of V-ATPases in Intracellular Compartments. Acidification of endosomes by V-ATPases is crucial for dissociation of internalized ligands from receptors and recycling of receptors back to the cell surface. Budding of endosomal carrier vesicles depends on low luminal pH. Lysosomal proteins are released from mannose-6-phosphate receptors in the acidic late endosomes. Protein degradation by cathepsins and other proteases within the lysosomes depends on the low pH established by V-ATPases. The pH gradient within secretory vesicles drives uptake of neurotransmitters and other molecules in the secretory pathway. It has been proposed that V_0 domains play a direct role in membrane fusion (From Jefferies et al., 2008).

internalized ligands and recycling of receptors back to the cell surface (Hinton et al., 2009a). Neutralization of endosomal compartments prevents dissociation of ligand-receptor complexes and receptor recycling. V-ATPases are also required for the budding of endosomal carrier vesicles from early endosomes and the delivery of internalized material to late endosomes. Formation of endosomal carrier vesicles relies on activity of the small GTPase Arf1, which recuites β-Cop to the membrane of early endosomes (Gu and Gruenberg, 2000). This process requires an acidic pH in the lumen of the early endosome that is generated by V-ATPases. Additionally, V-ATPases were shown to be the docking site for Arf6 and its guanine exchange factor ARNO (Hurtado-Lorenzo et al., 2006). Interactions between V-ATPases and Arf6/ARNO are dependent on low endosomal pH and blocking these interactions abrogates trafficking between early and late endosomes (Hurtado-Lorenzo et al., 2006).

The low pH of endosomes is exploited by a variety of enveloped viruses and bacterial toxins that enter cells through endosomal compartments (Gruenberg and van der Goot, 2006). For example, influenza enters cells through clathrin-coated vesicles and is delivered to early endosomes where the acidic pH induces a large conformational change in the viral coat protein hemagglutinin (HA) that exposes a hydrophobic domain of HA. Oligomers of HA form within the endosomal membrane that lead to the development of a fusion pore, which ultimately releases viral RNA into the cytoplasm of the host cell. One example of a bacterial toxin that exploits the low pH of the endocytic pathway is anthrax toxin. It is composed of two cytoactive polypeptides, edema factor (EF) and lethal factor (LF) that enter cells through the activity of a third polypeptide, protective antigen (PA) (Gruenberg and van der Goot, 2006). In a low pH-dependent process, PA creates a

fusion pore in the late endosomal membrane that allows EF and LF to enter into the cytoplasm of the infected cell (Abrami et al., 2004). Thus, neutralizing acidic endosomes may be an effective way to block viral infection or toxin pathology in exposed cells.

V-ATPases generate the low pH of lysosomes (5.0-5.5), which activates acid-dependent proteases that degrade internalized proteins (Mindell, 2012). The low pH of lysosomes is necessary for the efflux of degradation products out of the lumen of the lysosome through H^+/amino acid cotransporters (Hinton et al., 2009a). V-ATPase activity is also necessary for the trafficking of newly synthesized lysosomal enzymes to the lysosome. In the trans-Golgi network, lysosomal enzymes are attached to mannose 6-phosphate (Man-6-P) receptors that traffic these enzymes to late endosomes (Ghosh et al., 2003). The low pH of late endosomes allows for release of lysosomal enzymes from Man-6-P receptors. Lysosomal enzymes are then delivered to the lysosome, while Man-6-P receptors are recycled back to the trans-Golgi network.

V-ATPase mediated acidication of secretory vesicles is essential in both neuronal and endocrine systems. Activation of prohormones to their mature forms depends on proteases that require an acidic pH for activity. For example, blocking acidification of secretory vesicles with V-ATPase inhibitors prevents the processing of proinsulin to insulin in pancreatic beta cells (Sun-Wada et al., 2006). The internally positive membrane potential across the secretory vesicle membrane is also used to drive uptake of small molecules (Forgac, 2007). Examples of this include the loading of negatively charged ATP into chromaffin granules and glutamate uptake into secretory vesicles within glutamatergic neurons. The pH gradient generated by V-ATPases is also used to

drive uptake of norepinephrine into synaptic vesicles through a norepinephrine/H^+ antiporter.

A role for the V_0 domain of the V-ATPase has been proposed in membrane fusion that is independent of acidification (El Far and Seager, 2011). This function was initially proposed in studies showing that V_0 domains contribute to homotypic vacuole fusion in yeast (Peters et al., 2001). After tethering of SNARE proteins, trans-V_0 domains from adjacent membranes that are primed to be fused were suggested to bind each other and catalyze the mixing of lipids required for membrane fusion. Further support for an acidification-independent role of V_0 in membrane fusion has come from studies of synaptic vesicle release in *Drosophila* (Hiesinger et al., 2005), exosome release of cuticle proteins in *C. elegans* (Liégeois et al., 2006), secretion of insulin from pancreatic beta cells (Sun-Wada et al., 2006) and lysosome-phagosome fusion in zebrafish (Peri and Nusslein-Volhard, 2008). Moreover, V_0 subunits interact with proteins involved in membrane fusion, such as VAMP-2, synaptobrevin 2 and syntaxin-1 (Galli et al., 1996; Hiesinger et al., 2005; Di Giovanni et al., 2010). Despite numerous reports implicating V_0 in fusion, this role remains controversial.

V-ATPase activity is essential for several signaling pathways. mTor complex 1 (mTorc1) is a nutrient sensor and a central regulator of cell growth. Amino acids are one of the signals that lead to mTorc1 activation by promoting its binding to Rag GTPases, which recruit mTorc1 to the surface of the lysosome (Zoncu et al., 2011a). mTorc is anchored at the lysosomal membrane through interactions between the Rag GTPases and a multi-protein complex known as the Ragulator. V-ATPases have recently been identified as the Ragulator/Rag GTPase docking site and are required for mTorc1

activation and recruitment to lysosomal membranes upon amino acid stimulation (Zoncu et al., 2011b). Moreover, V-ATPase activity is necessary for epidermal growth factor (EGF)-mediated mTorc1 activation (Xu et al., 2012). Interestingly, mTorc1 also regulates V-ATPase expression, suggesting that a feedback loop exists in which mTorc1 can regulate lysosomal function (Peña-Llopis et al., 2011).

The Notch signaling pathway is important for development and cell differentiation in multicellular organisms (Kopan and Ilagan, 2009). After ligand binding, Notch receptors expressed at the plasma membrane are internalized into endosomes where a series of cleavage events are required for downstream signaling to occur. Several reports have demonstrated that inhibiting V-ATPase activity by disrupting expression of the V-ATPase regulator Rabconnectin-3 blocks Notch cleavage and inhibits Notch signaling (Yan et al., 2009; Sethi et al., 2010). The role of V-ATPases in Notch signaling occurs upstream of a gamma-secretase mediated cleavage event (Vaccari et al., 2010). Thus, inhibition of V-ATPase activity in endosomes may be an effective way to block pathological gamma-secretase activity that occurs in Altzheimer's disease.

Plasma Membrane Functions of V-ATPases

Plasma membrane V-ATPases play important roles in a number of specialized cell types. V-ATPases located on the plasma membranes of renal epithelial cells are critical for maintaining acid-base homeostasis (Wagner et al., 2004). V-ATPases are highly expressed in apical membranes of alpha intercalated cells of the late distal tubule and collecting duct where they participate in proton transport into the lumen of the tubule

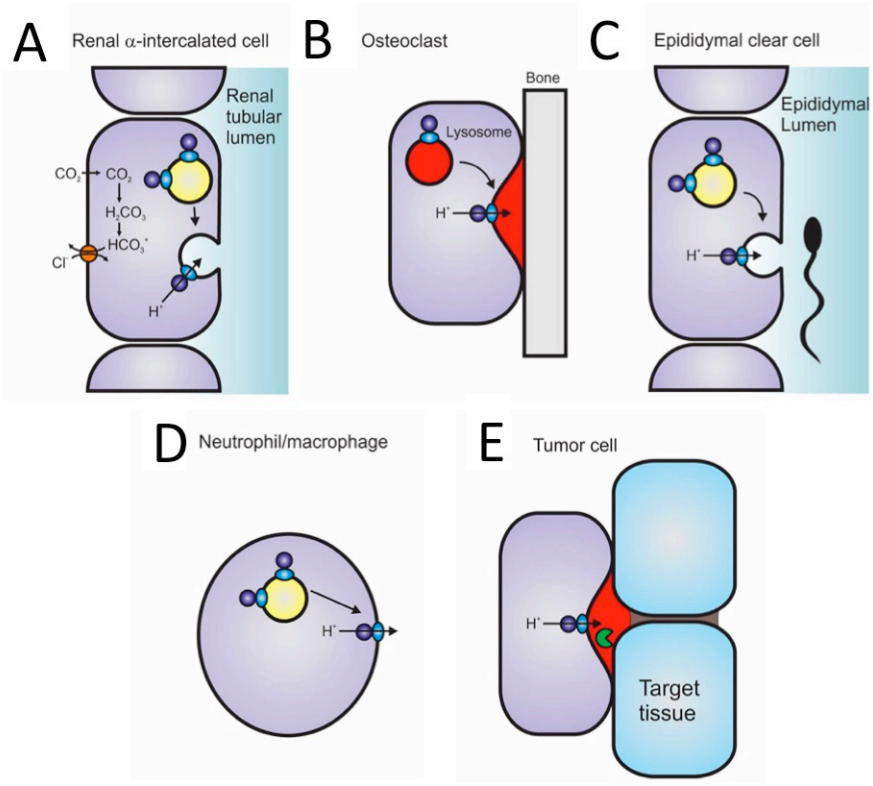

Figure 1.2. Functions of V-ATPases at the Plasma Membrane. A, V-ATPases in alpha intercalated cells of the kidney secrete H^+ into the urine. B, plasma membrane V-ATPases in osteoclasts acidify the extracellular space in contact with bone, promoting activity of acid-dependent proteases that are necessary for bone resorption. C, in epididymal clear cells, V-ATPases expressed at the apical membrane generate the acidic luminal pH required for sperm maturation. D, plasma membrane V-ATPases are involved in pH homeostasis in neutrophils and macrophages. E, plasma membrane V-ATPases have been implicated in tumor cell invasion (From Jefferies et al., 2008).

(Figure 1.2A) (Brown et al., 2009). Decreased plasma pH leads to increased density of V-ATPases in the apical membrane of intercalated cells and increased in H^+ secretion into the urine. Along with Na^+/H^+ exchangers, V-ATPases expressed in the plasma membrane of proximal tubule cells participate in the resorption of HCO^-_3 from the lumen of the renal tubule. Carbonic anhydrase IV in the lumen of the renal tubule catalyzes the conversion of secreted H^+ and HCO^-_3 to H_2O and CO_2. The CO_2 then diffuses into the cell, is converted back to HCO^-_3 by cytosolic carbonic anhydrase II and is transported across the basolateral membrane by a $C1^-/HCO^-_3$ exchanger.

Osteoclasts are specialized cells that function in bone resorption. This is accomplished by the binding of osteoclasts to the surface of the bone followed by secretion of acid and degradative enzymes that will dissolve bone matrix within a sealed extracellular region (Qin et al., 2012). V-ATPases localize to the region of the cell surface involved in bone resorption and secrete protons out of the cell, which lowers the extracellular pH, facilitating the dissolution of the mineral portion of bone and activation of pH-dependent proteases (Figure 1.2B). Mutations or deletions in V-ATPase subunits expressed in osteoclasts leads to defective bone resorption associated with osteopetrosis (Li et al., 1999; Frattini et al., 2000; Scimeca et al., 2000; Ochotny et al., 2011). This function also makes V-ATPases an attractive target in the development of drugs to treat osteoporosis.

Clear cells are one of the major cell types found in the epithelium of the epididymis and the distal vas deferens. V-ATPases are highly expressed in the apical membranes of clear cells where they participate in the luminal acidification of the epididymis (Figure 1.2C) (Shum et al., 2009). Acidic luminal pH is critical for sperm

maturation and the maintenance a quiescent state during sperm storage. The importance of V-ATPases in sperm maturation has been demonstrated by the observation that blocking expression of particular subunit isoforms causes infertility (Blomqvist et al. 2006; Vldarsson et al. 2009). Due to their important role in sperm maturation, V-ATPases located in the plasma membranes of clear cells are potential targets for a male contraceptive.

Plasma membrane V-ATPases are necessary for the functions of several types of immune cells. Macrophages and neutrophils are highly metabolic cells that often reside in acidic environments and, as such, they require greater acid secretion capacity than other cell types to maintain a neutral cytosolic pH. Because of this, these cells localize V-ATPases to the plasma membrane where they assist Na^+/H^+ exchangers in proton efflux from the cytosol (Figure 1.2D)(Nanda et al., 1996).

Finally, plasma membrane V-ATPases have been implicated in tumor cell invasion (Figure 1.2E). The role of V-ATPases in promoting the invasion of breast cancer cells is investigated in Chapters 2 and 3 of this thesis. A detailed discussion of the role in V-ATPases in tumor cell invasion will be presented later in this chapter.

V-ATPase Structure and Mechanism of Proton Pumping

Structure of V_0 Subunits

The V_0 domain is a membrane embedded complex composed of six subunits in yeast (a, c, c', c", d, and e) and mammals (a, c, c", d, e and Ac45) that is responsible for the transport of protons out of the cytoplasm and into the lumen or extracellular space (Figure 1.3). The c subunits are predicted to form a 10 membered proteolipid ring

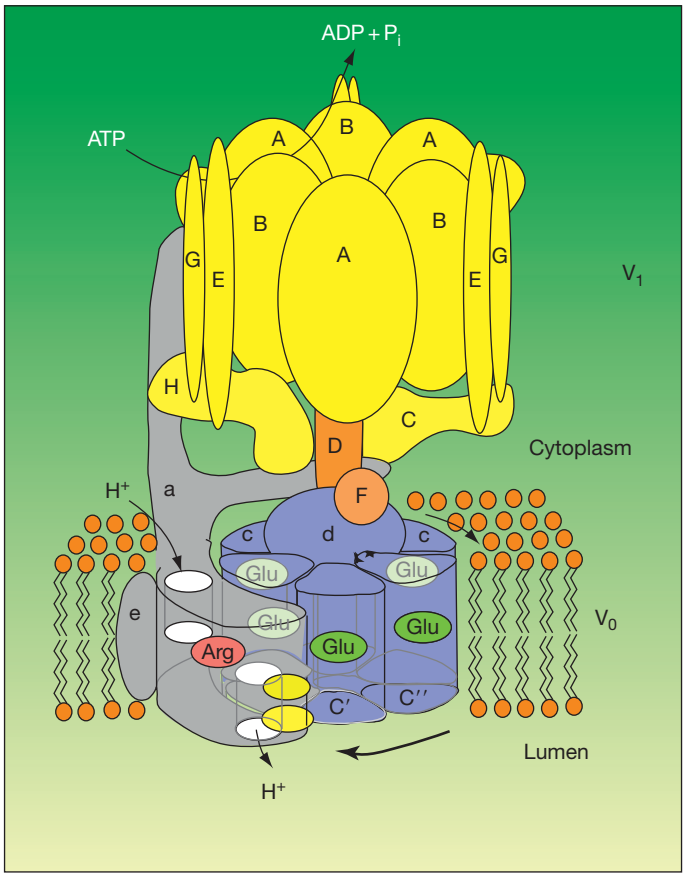

Figure 1.3. Structure of the V-ATPases. The V-ATPase contains two domains. The V_1 domain is responsible for ATP hydrolysis and the V_0 domain carriers out proton transport across the membrane. Like the F-ATPases, the V-ATPases operate by a rotary mechanism in which ATP hydrolysis in V_1 drives rotation of the central stalk, which is connected to a ring of proteolipid subunits in V_0. It is the movement of the proteolipid ring relative to subunit a that drives proton transport. An arginine (Arg) residue on subunit a and glutamic acid (Glu) residues on the ring of proteolipid subunits are crucial to proton translocation and are shown in red and green, respectively. Charge residues on subunit a that contribute to the proton-conducting hemichannels are shown in yellow (From Capecci and Forgac, 2013).

containing 8 copies of c and one copy each of c' and c'' (Murata et al., 2005). The c subunits are homologous to each other and the c subunit of the F-ATPase (Hirata et al., 1997). Subunits c and c' are 16 kDa proteins that contain four transmembrane helices with both the C- and N-termini located in the lumen (Flannery et al., 2004). Subunit c'' is a 23 kDa subunit containing 5 transmembrane helices with a cytoplasmic N-terminus and a luminal C-terminus (Flannery et al., 2004). Each proteolipid subunit contains a glutamic acid residue (or aspartic acid in F-ATPases) that is essential for proton translocation (Hirata et al., 1997). Multiple crystal structures of proteolipid rings from rotary ATPases have been resolved in recent years demonstrating that the critical carboxylates are located in the center of the membrane within alpha helices on the periphery of the c rings (Murata et al., 2005; Meier et al., 2005; Pogoryelov et al., 2009; Pogoryelov et al., 2010).

The 100 kDa a subunit is the largest V-ATPase subunit and contains two domains; an N-terminal hydrophilic domain that interacts with V_1 subunits in the cytosol and a highly hydrophobic C-terminal transmembrane domain consisting of eight alpha helices (Wang et al., 2008). Many buried charged or polar residues within the C-terminal domain of subunit a have been identified whose mutation leads to a partial or complete loss of proton translocation (Leng et al., 1996; Leng et al., 1998; Kawasaki-Nishi et al, 2001b). These hydrophilic residues are predicted to form two aqueous, proton-conducting hemichannels, one of which is in contact with the cytoplasm while the second is in contact with the lumen or extracellular space (Toei et al., 2011).

The N- terminal domain of subunit a is critical for the targeting of V-ATPases to specific cellular locations (Kawasaki Nishi et al., 2001c). Additionally, the N-terminal

domain functions in regulated assembly of the V-ATPase, which is an important mechanism of controlling V-ATPase activity in yeast and higher eukaryotes (discussed below). Multiple studies have identified structural interactions between the N-terminus of subunit a and various V_1 subunits. During dissociation of V_1 and V_0, such interactions must be broken, which suggests that these interactions are dependent on signaling molecules that regulate V-ATPase assembly. A structure for the N-terminal domain of subunit I (an subunit a homologue) from the archaebacterium *Meiothermus ruber* A-ATPase was recently solved that is predicted to have high secondary structure similarity to subunit a of the V-ATPase (Srinivasan et al., 2011; Finnigan et al., 2012). Based on the secondary structure conservation, models of the N-terminal domain of yeast a subunits have been constructed showing a hairpin structure with globular proximal and distal lodes connected by a flexible alpha helical linker region (Finnigan et al. 2012; Liberman et al, 2013).

Mechanism of proton translocation through V_0 and proposed role of helical swiveling

A mechanism for proton transport relying on aqueous hemichannels through subunit a was first proposed for F-ATPases (Vik and Antonio, 1994; Cain, 2000; Fillingame et al., 2002). A similar mechanism is predicted to be employed by V-ATPases (Forgac, 2007). Protons are predicted to enter into the membrane through the cytoplasmic hemichannel and are brought into contact with the buried glutamic acid on one of the proteolipid subunits (Figure 1.3). Following protonation of the glutamic acid, ATP hydrolysis in V_1 (discussed below) drives rotation of the proteolipid ring, ultimately bringing the protonated glutamic acid into contact with the luminal hemichannel.

Interaction between the glutamic acid and an essential arginine residue in subunit a displaces the proton into the luminal hemichannel, leaving the deprotonated glutamic acid free to bind another proton. Consistent with this model, direct rotation of the proteolipid ring has been observed in the presence of ATP by fluorescence microscopy (Yokoyama et al., 2003). Additional support for this model of proton transport comes from cross-linking studies showing that transmembrane (TM) helix 7 of subunit a, which contains the critical arginine residue, comes into close proximity with TM4 of subunit c' and TM3 of subunit c'', which contain the essential glutamic acid residues (Kawasaki-Nishi et al., 2003; Wang et al., 2004).

Interestingly, the cross-links obtained between TM7 of subunit a and TM4 of c' or TM3 of c'' occur over a wide range of helical faces, suggesting the helices within subunit a and the proteolipid ring are able to swivel (Kawasaki-Nishi et al. 2003; Wang et al., 2004). Helical swiveling within subunit a was previously hypothesized to be mechanistically important for proton translocation based on the predicted positions of residues in the proton-conducting hemichannels (Toei et al., 2011). Supporting this hypothesis, helical movements within subunit a were recently demonstrated to be critical for proton transport in the F-ATPase (Moore and Fillingame, 2013). The role of swiveling within subunit a of the V-ATPases has not yet been evaluated.

While evidence for helical rotation in the c subunits exists, it is not known whether this helical mobility is mechanistically important for proton translocation (Kawasaki-Nishi et al. 2003; Wang et al., 2004). Helical rotation in a c subunit may serve as a way to shield the hydrophilic glutamic acid from the hydrophobic membrane environment during rotation of the proteolipid ring, while providing the glutamic acid

with access to the aqueous hemichannels when in contact with subunit a. Consistent with this hypothesis, differences in the orientation of helices in F-ATPase c subunits that are dependent on the protonation state of the critical carboxyl group have been observed in NMR structures (Rastogi and Girvin, 1999). Moreover, cross-linking studies with the proteolipid ring of F-ATPases are supportive of helical swiveling (Vincent et al., 2007).

Alternatively, it has also been suggested that large-scale helical movements are not necessary for proton translocation. This hypothesis is supported by a crystal structure of the c15 ring from the F-ATPase of *Spirulina platensis* obtained in the presence N,N′-dicyclohexylcarbodiimide (DCCD) (Pogoryelov et al., 2010). DCCD selectively attacks protonated carboxyl groups, but cannot enter into the proteolipid ring due to its large size. In the DCCD-bound crystal structure, the side chain of the aspartic acid is reoriented outward compared to the unbound crystal structure without changes in helical orientation. These results suggest that side chain movements of the critical aspartic group may be sufficient to provide aqueous access to the carboxyl group. However, this structure was obtained in the absence of subunit a and does not properly mimic the environment in which c interacts with the aqueous hemichannels in the intact enzyme. Therefore, whether or not helical swiveling in subunit c is important for proton translocation remains an open question. The mechanistic importance of helical swiveling within the c ring during proton translocation of V-ATPases is addressed in Appendix 1 of this thesis.

a Subunit Isoforms

Multiple isoforms of subunit a are found in both yeast and mammals (Toei et al., 2010). In yeast, subunit a is the only subunit with multiple isoforms and is encoded by

two genes (*VPH1* and *STV1*). Vph1p and Stv1p are 54% identical at the amino acid level and have higher sequence identity in the transmembrane domain than in the cytosolic domain (Manolson et al., 1994). V-ATPases containing Vph1p localize to the vacuole while those containing Stv1p localize to the Golgi. Chimeric proteins containing different parts of Vph1p and Stv1p have shown that the targeting signal exists in the N-terminal domain of subunit a (Kawasaki-Nishi et al., 2001c). A short signaling sequence ($W^{83}KY$) located in the N-terminus of Stv1p has been shown to be necessary for retention in the Golgi (Finnigan et al., 2012). In addition to differences in targeting, V-ATPases containing Vph1p or Stv1p differ in the degree of assembly between V_1 and V_0 and in their efficiency in coupling proton transport to ATP hydrolysis (Kawasaki-Nishi et al. 2001a, Kawasaki-Nishi et al., 2001c). These differences are likely to be partially responsible for the lower pH of the vacuole relative to the Golgi.

In mammals, four subunit a isoforms are expressed (a1-a4) that also containing targeting information. The human a isoforms have 47−61% sequence identity at the amino acid level (Wagner et al., 2004). a1 localizes to synaptic nerve terminals where it is expressed within synaptic vesicles and presynaptic membranes (Morel et al., 2003). siRNA-mediated a1 knockdown reduces acidification of dense-core vesicles and neurotransmitter uptake in neurosecretory PC12 cells (Saw et al., 2011). In addition to a probable role in the acidification of synaptic vesicles, a1 has been shown to have a critical role in exocytosis of synaptic vesicles in *Drosophila* (Hiesinger et al., 2005). The a2 isoform has been shown to target V-ATPases to the Golgi (Toyomura et al., 2003). Additionally, a2 is present in the apical endosomes of proximal tubule cells in the kidney, where the low pH that is generated releases endocytosed peptides from the receptors

megalin and cubilin (Hurtado-Lorenzo et al., 2006). This process is critical for the absorption of filtered peptides present in the tubular lumen.

a3 is highly expressed in osteoclasts where it plays a critical role in bone resorption. In pre-osteoclasts, a3 localizes to lysosomes, but is transported to the plasma membrane upon differentiation into mature osteoclasts (Toyomura et al., 2003). Mutations in a3 are frequently found in individuals with osteopetrosis (Frattini et al., 2000) and genetic disruption of a3 in mouse models causes severe osteopetrosis (Li et al., 1999; Scimeca et al., 2000; Ochotny et al., 2011). Because of its role in bone resorption, drugs targeting a3 have been proposed as a potential treatment for osteoporosis.

a3 is expressed in pancreatic beta cells where it localizes to the membranes of insulin-containing secretory granules (Sun-Wada et al., 2006). Interestingly, beta cells from a3 knockout mice are deficient in insulin secretion, but are still able to acidify secretory granules and process insulin (Sun-Wada et al., 2006). a2 was found to localize to insulin-containing secretory granules in a3 knockout mice, but not in wild-type mice, suggesting that a2 may compensate for the loss a3 in secretory granule acidification. However, a2 localized in secretory granules cannot compensate for loss of a3 in regulated exocytosis. These results suggest that V_0 domains containing a3 may have a role in membrane fusion that is necessary for insulin release.

a4 was the last a isoform discovered and its expression is restricted to a limited number of cell types (Wagner et al., 2004). In renal alpha-intercalated cells of the late distal tubule and collecting duct, a4 targets V-ATPases to apical membranes and mutations in a4 cause defective urinary acid secretion associated with renal tubular acidosis (Smith et al., 2000). a4 similarily targets V-ATPases to the apical membrane of

epididymal cells of the male reproductive system (Shum et al., 2009). In addition to renal tubular acidosis, loss of a4 has been associated with hearing loss in both humans and mice, due to its function in hair cells (Stover et al., 2002; Norgetta et al., 2012). Moreover, a4 localizes to the apical pole of the olfactory epithelium and a4 knockout mice have an impaired sense of smell (Norgetta et al., 2012). These studies show that while a4 has a restricted expression pattern, it plays critical physiological roles in a number of specialized epithelia.

The structure and function of V_1 subunits

The cytoplasmic V_1 domain is a 650 kDa complex composed of eight subunits (A-H) in a likely stoichiometry of $A_3B_3CDE_3FG_3H$ that is responsible for ATP hydrolysis (Zhang et al., 2008). The A and B subunits form a hexameric ring (A_3B_3), with three copies of each subunit in alternating positions (Maher et al., 2009). ATP hydrolysis occurs on subunit A at its interface with subunit B (Lui et al., 1996; Lui et al., 1997; MacLeod et al., 1998). Additional ATP binding sites are found on subunit B at its interface with subunit A, but these sites are not competent for ATP hydrolysis (MacLeod et al., 1998). Subunit B contains actin-binding sites that are important for regulating V-ATPase targeting (Holliday et al., 2000; Zuo et al., 2006; Shum et al., 2011). A large, protruding bulge is present at the top of subunit A known as the nonhomologous region that is absent in the F-ATPase A homolog. The non-homologous region is important for coupling of ATP hydrolysis with proton translocation and is involved in the regulation of V-ATPase activity (Shao and Forgac, 2004).

While only one isoform of the A subunit is found in mammals, two isoforms of subunit B are expressed (B1 and B2). Whereas B2 is ubiquitously expressed and is associated with intracellular compartments, B1 has a more restricted expression pattern and is associated with V-ATPases that are targeted to the plasma membrane (Toei et al., 2010). B1 is expressed in renal cells, epididymal clear cells and hair cells of the inner ear. Loss of B1 expression causes renal tubular acidosis as well as deafness (Karet et al., 1999). B1 localizes to the apical membrane of renal intercalated cells where it is involved in the proton secretion into the urine (Brown et al., 2009). While the expression patterns of B1 and B2 are different, B2 is able to compensate for some of the consequences of B1 loss, including being retargeted to the plasma membrane (Da Silva et al., 2007; Paunescu et al., 2007). The factors involved in the differential targeting and activity of B1 and B2 are not understood.

Central and peripheral stalks bridge the V_1 and V_0 domains. The central stalk, composed of the V_1 subunits D, F and the V_0 subunit d, functions to couple the energy of ATP hydrolysis to rotation of the proteolipid ring. Subunit D is highly helical and is predicted to extend into the center of the A_3B_3 ring (Jefferies et al., 2008). ATP hydrolysis within the A_3B_3 head induces a conformation change in these subunits that causes rotation of the central stalk. Direct rotation of subunits D and F from the eubacterium *Thermus thermophilus* has been observed by fluorescence microscopy (Imamura et al., 2003). The central stalk components interact with and drive rotation of the proteolipid ring, thereby coupling ATP hydrolysis to proton transport.

Each V-ATPase contains three peripheral stalks that bridge the A_3B_3 head and V_0 (Zhang et al., 2008). Peripheral stalks are composed of one EG heterodimer, as well as

non-identical interactions with subunits C, H and the N-terminal domain of subunit a (Zhang et al., 2008; Oot and Wilkens, 2010; Oot and Wilkens 2012). A recent crystal structure of the EG dimer complexed with the head region of C demonstrates that the N-terminal ends of the E and G subunits fold together in a non-canonical right-handed coil-coil (Oot et al., 2012). The peripheral stalks serve as a stator to prevent rotation of the A_3B_3 head relative to subunit a (the stator portion of V_0) during catalysis and serve as a structural bridge between V_1 and V_0 (Zhang et al., 2008).

High-resolution structures of subunits C and H have been resolved. Subunit C is an elongated protein with globular head and foot domains, each of which is able to interact with separate EG heterodimers (Drory et al., 2004; Inoue and Forgac, 2005; Oot and Wilkens, 2010). The foot domain of C also interacts with the N-terminal domain of subunit a (Oot and Wilkens, 2012). Like subunit C, subunit H has an elongated structure with N- and C-terminal globular domains (Sagermann et al., 2001). Subunit H has been shown to be largely responsible for inhibiting ATPase activity of dissociated V_1 through interactions with subunit F (Parra et al., 2000; Jefferies and Forgac, 2008). Moreover, V-ATPases lacking subunit H are much less stable and the N-terminal domain of subunit H has been shown to bind to the N-terminal domain of subunit a, suggesting that subunit H is important for stabilizing V-ATPases (Diab et al., 2009).

Mechanisms of V-ATPase regulation

Reversible Dissociation

An important mechanism of V-ATPase regulation is the reversible dissociation of the V_0 and V_1 domains and the subsequent inhibition of ATP hydrolysis and proton

transport (Figure 1.4A). Reversible dissociation has been extensively studied in yeast and has also been observed in insect and mammalian cells. This process was first observed in midgut cells of the tobacco hornworm *Manduca sexta,* where dissociation of V-ATPases occurs during molting as an energy conservation mechanism (Sumner et al., 1995). In yeast, dissociation occurs in response to decreasing glucose levels and is also thought to be an energy conservation mechanism (Kane, 2006; Kane, 2012). In addition to glucose concentration, factors such as extracellular and cytosolic pH can also affect V-ATPase assembly state in yeast (Diakov and Kane, 2010; Dechant et al., 2010). V-ATPase assembly in mammalian cells can also be regulated by glucose levels, although the physiological importance of this is not well understood (Sautin et al., 2005; Kohio and Adamson, 2013). During maturation of dendritic cells, an increase in V-ATPase assembly onto lysosomal membranes enhances lysosomal acidification and antigen processing (Trombetta et al., 2003).

In the past several years, the signal pathways modulating reversible dissociation have begun to be elucidated. In yeast, glucose-dependent assembly is mediated by the activity of the Ras/cAMP/Protein Kinase A (PKA) pathway (Bond and Forgac, 2008). At high glucose levels, Ras is active and stimulates adenylate cyclase, which causes an increase in cAMP that in turn activates PKA and increases V-ATPase assembly. This pathway is suppressed upon glucose depletion. It is not currently known whether PKA activates V-ATPases by directly phosphorylating a pump subunit or whether the regulation is indirect. In insect cells, PKA has been shown to directly phosphorylate subunit C (Voss et al., 2007). Uniquely, subunit C separates from both V_0 and V_1 during reversible dissociation (Kane, 1995), suggesting the possibility that phosphorylation of

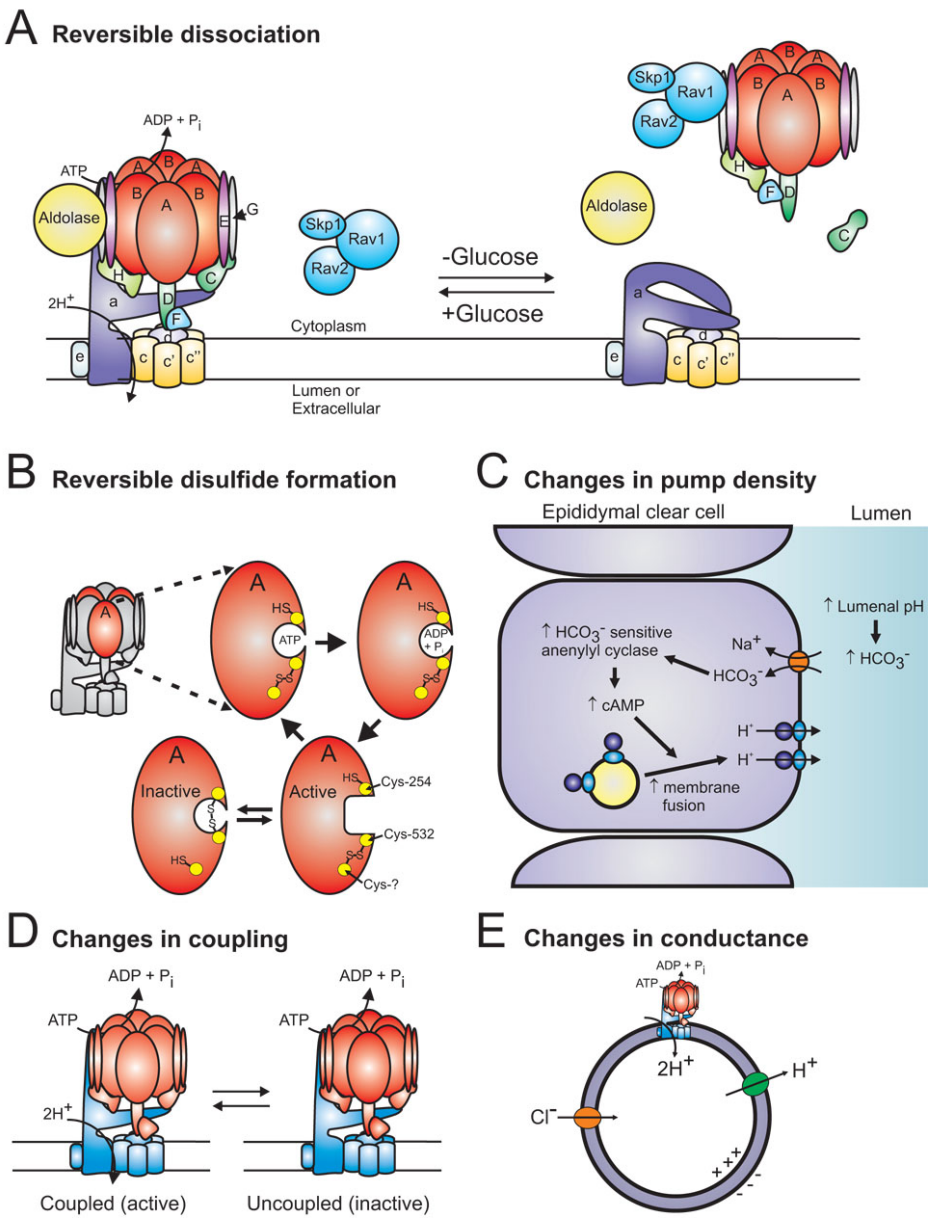

Figure 1.4. Regulation of V-ATPase Activity. A, V-ATPase activity is inhibited by the separation of complexes into free V_0, free V_1 without subunit C, and free subunit C. Free V_1 is enzymatically inactive and free V_0 is unable to transport protons. Reversible dissociation has been shown to occur in response to glucose depletion. Dissociation requires intact microtubules whereas reassembly requires aldolase and the Rave complex, suggesting that these processes occur by distinct mechanisms. B, reversible disulfide bond formation between cysteine residues in subunit A locks the catalytic site into a conformation that cannot undergo ATP hydrolysis. C, changes in pump density in epididymal clear cells are regulated by luminal pH. D, changes in coupling efficiency can alter activity of the pump. E, vesicle pH can be altered by changing the conductance of Cl^- or H^+ through distant channels (From Jefferies et al., 2008).

subunit C by PKA may induce pump assembly. However, in insect cells phosphorylation of subunit C by PKA was not observed in assembled V-ATPases, suggesting that the phosphorylation event triggering assembly may be transient (Voss et al., 2007). Additional signaling pathways appear to be involved in assembly. Phosphatidylinositol 3-kinase has been shown to mediate glucose-dependent V-ATPase assembly in renal cells (Sautin et al., 2005) and EGF has been shown to increase V-ATPase assembly in primary hepatocytes (Xu et al., 2012).

A number of interactions have been shown to be important for reversible dissociation. Firstly, intact microtubules are required for glucose-dependent disassembly in yeast, but not for reassembly when glucose is added back to the media (Xu and Forgac, 2001). Secondly, the trimeric Rave complex (composed of Skp1, Rav1 and Rav2) binds to V_1 through interactions with the peripheral stalks and subunit C and has been shown to be required for V-ATPase assembly, but not disassembly (Seol et al., 2001). Interactions between Rave and V_1 are preserved in disassembled V-ATPases, suggesting that RAVE may be functioning to maintain V_1 in an assembly competent state (Smardon et al., 2002; Smardon and Kane, 2007). Rav1 is a homolog of Rabconnectin-3, which regulates V-ATPase-dependent organelle acidification in *Drosophila* and mammalian cells, implying that the role of the Rave complex in V-ATPase assembly and activity is conserved (Yan et al., 2009; Sethi et al., 2010).

Intriguingly, glucose-dependent interactions between V-ATPases and the glycolytic enzyme aldolase have been observed. Aldolase catalyzes the formation of dihydroxyacetone phosphate and glyceraldehyde 3-phosphate from fructose 1,6-bisphosphate. Deletion of aldolase in yeast causes dissociation of V-ATPases (Lu et al.,

2001; Lu et al., 2004). This interaction raised the possibility that glycolytic generation of ATP may directly regulate consumption of ATP by affecting V-ATPase assembly state. However, it was subsequently demonstrated that enzymatically inactive aldolase mutants that preserved V-ATPase binding maintained normal V-ATPase assembly and activity, indicating that only physical interactions between V-ATPases and aldolase are necessary (Lu et al., 2007). Interactions have also been observed between subunit a and phosphofructokinase-1 (Su et al., 2003; Su et al., 2008).

The non-homologous region of subunit A also appears to be involved in reversible dissociation. Mutational analysis of the non-homologous region demonstrated that particular residues in this region are necessary for dissociation upon glucose removal, but are not important for pump activity (Shao et al., 2003). When expressed by itself, the non-homologous region can independently bind to V_0 in a glucose-dependent manner (Shao and Forgac, 2004). Thus the non-homologous region of A may serve as a glucose sensor and mediate V_1 interactions with V_0.

Membrane composition is likely to be a critical, but less well understood regulator of V-ATPase activity. In yeast, reversible dissocation is dependent on membrane environment. V-ATPases containing Stv1p, which target the pump to the Golgi, do not dissociate in response to glucose depletion, while those containing Vph1p, which targets pumps to the vacuole, do dissociate. However, when targeted to the vacuole by overexpression, Stv1p-containing V-ATPases undergo dissociation in response to glucose depletion (Kawaski-Nishi et al., 2001a). Conversely, when Vph1p-containing V-ATPases are localized to prevacoular compartments instead of the vacuole, glucose-dependent dissociation is reduced (Qi and Forgac, 2007). The precise factors within

these membranes that contribute to the control of reversible dissociation are not yet known.

Additional Methods of V-ATPase Regulation

A second mechanism of V-ATPase regulation is disulfide bond formation within the nucleotide-binding site of the catalytic subunit A (Figure 1.4B). This mechanism was first identified in V-ATPases purified from bovine clathrin-coated vesicles, where formation of disulfide bonds between Cys254 and Cys532 reversibly inactivates V-ATPases (Feng and Forgac, 1992; Feng and Forgac, 1994). This mechanism of regulation is thought to be evolutionarily conserved, since the cysteine residues involved are conserved in all eukaryotic species sequenced and mutation of Cys261 in yeast (corresponding to the bovine Cys254) abolished sensitivity of V-ATPase activity to sulfhydryl reagents and oxidation by hydrogen peroxide (Liu et al., 1997). Furthermore, the redox state of the cell can affect V-ATPase activity *in vivo* through reversible disulfide bond formation within subunit A (Oluwatosin and Kane, 1997). It is not known under what conditions reversible disulfide bond formation is an important physiological regulator of V-ATPase activity.

Cells that express V-ATPases at the plasma membrane can modulate proton secretion by regulating the density of V-ATPases at the cell surface. This is accomplished through the reversible exocytosis of vesicles containing high quantities of V-ATPases, which increases the total number of V-ATPases on the plasma membrane and thereby increases proton efflux (Brown et al., 2009). This mechanism is utilized in the apical membranes of renal cells to control acid/base balance. The number of plasma

membrane V-ATPases in alpha intercalated cells is tightly regulated. A pool of intracellular vesicles containing V-ATPases resides near the apical surface of intercalated cells that will fuse with the cell membrane in response to an acid load within the cytoplasm of the cell (Brown et al., 2009). Similarly, expression of V-ATPases in the apical membranes of epididymal clear cells is tightly regulated by the recycling of V-ATPase from the plasma membrane to intracellular vesicles that reside near the apical surface (Shum et al., 2009). In clear cells, vesicle exocytosis is regulated by soluble adenylyl cyclase, which is activated by alkaline luminal pH (Figure 1.4C) (Pastor-Soler et al., 2003). The subsequent increase in cAMP levels increases exocytosis of V-ATPase containing vesicles in a PKA-dependent manner (Pastor-Soler et al., 2008).

V-ATPases localized to different compartments differ in the efficiency in which proton transport is coupled to ATP hydrolysis (Figure 1.4D). Differences in coupling efficiency have been observed in yeast, where Stvp1-containing V-ATPases localized to the Golgi have a much lower efficiency of proton transport than Vph1p-containing V-ATPases that are localized to the vacuole (Kawasaki-Nishi et al., 2001a), thus contributing to the more alkaline pH of the Golgi.

Lastly, V-ATPase-mediated acidification can be indirectly modulated through changes in ion conductance of distinct channels (Figure 1.4E). Mutations in chloride channel proteins have been associated with defects in acidification of endosomes in renal cells (Gunther et al., 1998), impairment of bone resorption by osteoclasts (Kornak et al., 2001) and impaired proteolytic activity of macrophages (Jiang et al., 2012). In these compartments, the activity of chloride channels is essential to dissipate the membrane potential generated by the V-ATPase.

V-ATPases and Tumor Cell Invasion

The metastatic dissemination of tumor cells is responsible for the vast majority of cancer mortalities (Nguyen et al., 2009). Metastasis is a complex multistep process that involves intravasation of tumor cells out of a primary tumor site, dissemination through the circulatory or lymphatic system, and finally extravasation of cells into secondary sites within the body (Nguyen et al., 2009). Metastasis is initiated as tumor cells acquire mutations in genes that promote cell detachment, cell motility and invasion. Cell detachment can be achieved by disrupting expression of proteins involved in cellular adhesion, such as E-Cadherin and integrins (Gupta and Massague, 2006; Canel et al., 2013). Proteolysis of cell-matrix and cell-cell adhesions is important for tumor cell detachment from the primary tumor environment. Unidirectional cell migration occurs through cell polarization followed by Rac and Cdc42-regulated leading edge protrusion of lamellipodia and filopodia (Ridley et al., 2003). The leading edge will transiently adhere to extracellular matrix (ECM) components as the rear of the cell retracts. The ECM is a compact network of glycoproteins and proteoglycans that acts as a scaffold to stabilize tissue structures. Invasive cancer cells must be able to breakdown the ECM to create a path for tumor cells to enter into the circulation during intravasation and enter into the site of metastasis upon leaving the circulation during extravasation. This is partially accomplished through the activity of martix metalloproteases (MMPs), a large family of zinc-binding endopeptidases that degrade a wide array of ECM components and promote many aspects of tumor metastasis (Chabottaux and Noel, 2007).

A second class of proteases that have been shown to participate in tumor cell invasion is cathepsins (Gocheva and Joyce, 2007). Cathepsins are synthesized as inactive

precursors and require an acidic environment for activation and activity, both of which typically occur in lysosomes, where cathepsins function in degradation of proteins. Several cathepsins have been implicated in cancer invasion. Increased expression of cathepsin B correlates with poor prognosis in many cancer types (Berdowska, 2004). Moreover, knockout of cathepins B, L or S significantly reduces invasion of pancreatic cancer cells in mice (Gocheva et al., 2006; Gocheva and Joyce, 2007). Consistent with this finding, numerous studies have demonstrated that cancer cells secrete cathepsins that are capable of degrading ECM components (Frosch et al., 1999; Hashimoto et al., 2006). Cathepsins have also been shown to increase the activity of MMPs by directly activating pro-MMPs and by degrading MMP inhibitors (Gondi and Rao, 2013).

Typical cellular pH values are disrupted in metastatic cancer cells, such that the intracellular pH is more alkaline and the extracellular pH is more acidic in cancer cells when compared to normal cells (Sennoune & Martinez-Zaguilan, 2012). Multiple reports have demonstrated that an acidic extracellular pH enhances tumor cell invasiveness (Martinez-Zaguilan et al., 1996; Gillet et al., 2009). Neutralization of extracellular pH in tumors has been shown to limit the formation of metastases and reduce activity of cathepsins and MMPs in mice (Robey et al., 2009; Robey and Nesbit 2013). Since cathepsins rely on an acidic pH for optimal activity, understanding the mechanisms by which the low extracellular pH of tumors is regulated can lead to the identification of anti-metastatic therapeutics.

In recent years, multiple studies have suggested that V-ATPase activity is important for cancer cell invasion. Many of these studies have been conducted in breast cancer models. Highly invasive MDA-MB231 human breast cancer cells express much

higher levels of V-ATPase at the plasma membrane than poorly invasive MCF7 cells (Sennoune et al., 2004). Moreover, *in vitro* invasion by MDA-MB231 but not MCF7 cells is inhibited by the specific V-ATPase inhibitors bafilomycin and concanamycin (Sennoune et al., 2004). More recent studies from our laboratory have shown that MDA-MB231 cells express much higher levels of the a3 and a4 isoforms relative to MCF7 cells and that siRNA knockdown of both a3 and a4 inhibit invasion by MDA-MB231 cells (Hinton et al., 2009b). Knockdown of a4 in these cells appears to significantly reduce plasma membrane localization of V-ATPases. However, a limitation of these studies is that MDA-MB231 and MCF7 cells are independently derived cell lines that differ in many phenotypic and genetic properties (Soule et al., 1973; Cailleau et al., 1974).

Haeme-responsive-1 (HRG-1) is an insulin-like growth factor 1 (IGF-1) responsive gene that interacts with and enhances the activity of V-ATPases (O'Callaghan et al., 2010). A recent report has shown that HRG-1 associates with V-ATPases at the plasma membrane of MDA-MB231 cells and knockdown of HRG-1 reduced invasion and MMP activity (Fogarty et al., 2013). Conversely, overexpression of HRG-1 in the minimally invasive MCF7 cell line increased extracellular acidification, MMP expression and invasiveness (Fogarty et al., 2013). Thus, high expression of V-ATPases appears to be pivotal for extracellular acidification and MMP activity in invasive breast cancer cell lines.

The involvement of V-ATPases in invasiveness is not limited to breast cancer cells. In human pancreatic ductal adenocarcinoma, high V-ATPase expression correlates with increasing cancer grade and V-ATPases localize to the plasma membrane in the invasive Panc-1 pancreatic cancer cell line (Chung et al., 2011). Furthermore, blocking

V-ATPase activity inhibits pancreatic cancer cell invasion and reduces MMP-9 activity (Chung et al., 2011). The highly metastatic mouse melanoma cell line B16-F10 expresses more a3 than the less metastatic B16 cell line (Nishisho et al., 2011). B16-F10 cells also localize V-ATPases to the plasma membrane and knockdown of a3 suppresses invasion. Importantly, siRNA knockdown of a3 blocks bone metastasis of B16-F10 cells in mice (Nishisho et al., 2011). A recent report has demonstrated that inhibition of V-ATPases blocks invasion of prostate cancer cell lines as well (Michel et al., 2013). The results of these studies are consistent with a role for plasma membrane V-ATPases in cancer cell invasion. However, whether or not specific inhibition of plasma membrane V-ATPases alone is sufficient to inhibit invasion has not yet been tested.

The major goal of the studies discussed in this thesis is to further investigate the role of V-ATPases is in breast cancer cell invasion. Chapter 2 expands on previous work evaluating the role of a subunit isoforms in tumor invasion by studying two closely related cell lines (MCF10a and MCF10CA1a cells) that vary in invasive potential. Chapter 3 studies the role of plasma membrane V-ATPases in invasion of MDA-MB231 cells by specifically ablating the activity of plasma membrane V-ATPases and analyzing the effects on invasion and cellular pH regulation.

Chapter 2

The Function of Vacuolar ATPase (V-ATPase) a Subunit Isoforms in Invasiveness of MCF10a and MCF10CA1a Human Breast Cancer Cells

Published in *The Journal of Biological Chemistry*
Vol. 288, pp. 32731-32741, November 8, 2013

Rationale

Previous studies have shown that highly invasive MDA-MB231 cells have higher expression of the a3 and a4 subunit a isoforms in comparison to less invasive MCF7 cells (Hinton et al., 2009b). Moreover, siRNA-mediated knockdown of a3 or a4 significantly reduced invasion of MDA-MB231 cells, indicating that V-ATPases containing these isoforms are critical for invasion. However, a comparison of a subunit isoform expression in genetically related breast cells lines with varying invasive potential has not previously been conducted. Furthermore, it is currently unknown which a subunit isoforms are expressed at the plasma membrane in breast cancer cells and whether plasma membrane V-ATPase expression is directly involved in the invasive phenotype. To better examine whether expression of particular a subunit isoforms is critical to invasiveness of breast tumor cells, two closely related breast cancer cell lines have been examined. The MCF10a cell line is a non-invasive, immortalized human breast epithelial cell line and the MCF10CA1a cell line is a highly invasive, H-Ras transformed derivative of MCF10a selected for its ability to form metastases in mice (Soule et al., 1990; Santer et al., 2001). We have compared the invasiveness of these lines and their dependence on V-ATPases for invasion using V-ATPase inhibitors and knockdown of specific a subunit isoforms. We have also investigated the effect of overexpression of particular a subunit isoforms on invasiveness and plasma membrane localization of V-ATPases. The results suggest a role for the a3 isoform in both plasma membrane localization and invasiveness of human breast cancer cells.

Experimental Procedures

Cell Culture

MCF10a cells were purchased from American Type Culture Collection (ATCC). MCF10CA1a cells were generously provided by Dr. Yibin Kang (Princeton University). MCF10a and MCF10CA1a cells were cultured as previously described (Debnath et al., 2003) in DMEM/F12 medium (Invitrogen) containing 5% horse serum (Invitrogen), 20 ng/ml epidermal growth factor (Peprotech), 0.5 μg/ml hydrocortisone (Sigma), 100 ng/ml cholera toxin (Sigma), 10 μg/ml insulin (Sigma), 60 μg/ml penicillin and 125 μg/ml streptomycin (Invitrogen). Cells were grown in a 95% air, 5% CO_2 humidified environment at 37 °C.

Real Time Reverse Transcription-PCR

Quantitative Real Time Reverse Transcription-PCR was conducted as previously described (Hinton et al., 2009b). Cells were harvested and lysed, and RNA was isolated using RNeasy® mini kit (Qiagen). After RNA isolation, mRNA was isolated with the MicroPoly(A) Purist^{TM} kit from Ambion. Total RNA or mRNA concentration was quantified using Quant-iT RiboGreen RNA reagent (Molecular Probes). One-step quantitative RT-PCR was performed in a 96-well format on a Stratagene MX-3000P QPCR system using Brilliant SYBR Green QRT-PCR master mix kit (Stratagene). The PCR cycling sequence consisted of 30 min at 50 °C to allow for reverse transcription and then a heat inactivation and denaturation step for 10 min at 95 °C; this was followed by 40 cycles of 30 s at 95 °C, 1 min at 55 °C, and 30 s at 72 °C to allow for denaturation, annealing, and extension, respectively. To quantitate the results, cDNA clones were

obtained from ATCC (a1 and a2 isoforms), Open Biosystems (a3 and a4 isoforms) and Thermo Scientific (A). The cDNA sequences were verified by sequencing. Plasmid DNA for each isoform isolated from Escherichia coli was quantitated by measuring the absorbance at 260 nm; serial dilutions were made, and these DNA standards were used to facilitate quantification of the initial mRNA levels for each experimental sample by use of a standard curve.

RNA Interference

siRNA pools specific for the a1, a2, a3, or a4 isoform were purchased from Dharmacon. Each pool contained four siRNAs specific for the appropriate a subunit isoform. MCF10CA1a cells were plated in 60-mm dishes at 4×10^5 cells/dish in the media described above without antibiotics and incubated overnight. Cells were transfected with 20 nM siRNA directed against a1 or a2, 100 nM siRNA directed against a3, or 10 nM siRNA directed against a4 according to the manufacturer's directions. Briefly, the siRNA was mixed 1:1 with Opti-MEM^{TM} (Invitrogen), allowed to incubate for 5 min, and then mixed with Dharmafect 1 transfection reagent (Dharmacon). The siRNA/transfection reagent mix was incubated for 20 min at room temperature and then added to the appropriate volume of DMEM/F12 + serum, and 4 ml was added to each dish. After incubation of cells with siRNA for 24 hr, the media were changed to siRNA-free media, and cells were incubated for additional time (depending upon the assay) prior to harvesting. For all experiments, data were collected 96 hr post-transfection. To quantitate reduction in the a subunit isoform mRNA levels, quantitative RT-PCR was performed as described above using RNA isolated from cells after siRNA treatment. To

confirm the specificity of knockdown, we used primers specific for each isoform tested. The effect of siRNA treatment on cell viability was assessed by trypan blue exclusion. Insignificant staining with trypan blue was observed with all siRNA treatments, indicating that siRNA knockdown of a isoforms did not reduce cell viability.

Plasmid Transfection

cDNAs for each human a subunit isoform were separately cloned into the pTracer™-CMV/Bsd plasmd (Invitrogen). In all cases, insertion was verified by sequencing. 15 μg of the resultant plasmids, as well as the empty vector, were separately transfected into MCF10a cells using Lipofectamine 2000 (Invitrogen) in accordance with the manufacturers recommendations. Stable transfection was achieved by treatment of cells with 7.5 μg/ml Blasticidin S (Invitrogen) for 21 days, beginning 3 days post-transfection. After selection for stable transfection, overexpression of the appropriate a subunit isoform was verified using quantitative RT-PCR as described above.

Invasion Assay

Assays for *in vitro* invasion were performed using Fluoroblok inserts (BD Biosciences) with an 8-μm pore size membrane and coated with Matrigel™ (BD Biosciences) (Partridge and Flaherty, 2009). A chemoattractant (FBS) was added to the *trans*-side of the membrane to induce invasive cells to digest the coating and invade through the pores to the *trans*-side. Matrigel™ was diluted in PBS to a final concentration of 0.3 μg/μl, and a total of 18 μg was coated onto the membrane in each well. The membrane was allowed to dry overnight under vacuum at room temperature.

Matrigel™-coated membrane was re-hydrated with 60 µl of DMEM + 4.5 g/liter D-glucose, without phenol red, l-glutamine, or sodium pyruvate (Invitrogen) (termed Media) for at least two hr. 500 µl of the Media containing 5% FBS were added to wells plate in a 24 well plate to act as a chemoattractant. Cells were harvested by trypsinization and were brought to a concentration of 2×10^5 cells/ml in Media. For experiments testing the effects of concanamycin on invasion, cells were resuspended in Media containing either DMSO or 100 nM concanamycin A in DMSO and allowed to incubate for 15 min at 37 °C. 5×10^4 cells were seeded onto the rehydrated membrane, which was then placed onto the wells containing chemoattractant. After 15 hr, membranes were placed onto wells containing 4 µg/mL Calcein AM in Hank's Balance Salt Solution (Invitrogen) and incubated for 30 min at 37°C in 5% CO_2. Cells that had migrated to the trans-side of the membrane were quantitated using a Zeiss Axiovert 10 fluorescence microscope. The number of invading cells was averaged over three wells (15 images per well). Invasion for treated cells was measured relative to control cells. For concanamycin or DMSO treated samples, cell viability was assessed by trypan blue exclusion 24 hours after treatment was initiated: less than 1% of harvested cells stained with trypan blue in either treatment group, indicating minimal cell death.

Immunocytochemistry

A monoclonal antibody raised against the V-ATPase subunit A (Sigma, clone 4F5) was used to determine the *in situ* localization of V-ATPases. Cells were plated onto 24 x 24 mm coverslips. Approximately 24 hrs later, cells were washed, fixed with 4% paraformaldehyde and permeabilized with 0.1% Triton X-100. Nonspecific binding was

blocked by incubation with 1% bovine serum albumin in PBS for 1 hr and then incubated with the anti-A subunit antibody at a 1:1000 dilution overnight. The cells were next rinsed with PBS, and then incubated with Alexa Fluor® 488-conjugated goat anti-rabbit secondary antibody (1:500 dilution) and Alexa Fluor® 594 phalloidin (to stain F-actin, 1:250 dilution) (Invitrogen) in 1% bovine serum albumin/PBS. After 2 hr of incubation at room temperature, the cells were rinsed with PBS. The cells were prepared for viewing using ProLong® Gold (Invitrogen) mounting medium and allowed to cure at room temperature for 24 hr. The stained cells were imaged on a Leica TCS SP2 confocal microscope. To quantify plasma membrane staining, 60 cells from three separate batches of immunostained images were counted and the percentage of cells showing plasma membrane V-ATPase localization was determined.

Cell Lysis and Western Blotting

Cells were harvested, resuspended in lysis buffer with protease inhibitors (PBS-EDTA containing 137 mM NaCl, 1.2 mM KH_2PO_4, 15.3 mM Na_2HPO_4, 2.7 mM KCl, 2 mM EDTA (pH 7.2), 2 μg/ml aprotinin, 5 μg/ml leupeptin, 0.7 μg/ml pepstatin, and 1 mM PMSF) and lysed by sonication. Cell lysates were centrifuged for 10 minutes at 4°C at 15,000 × g to remove cellular debris. Protein concentrations were determined using the Lowry method. SDS sample buffer was added to the lysates and aliquots containing 20 μg of protein were separated by SDS-PAGE on 4–15% gradient acrylamide gels. The presence of subunit A or α-Tubulin was detected by Western blotting using monoclonal antibodies from Sigma or GenScript, respectively, followed by a horseradish peroxidase-

conjugated secondary antibody (Bio-Rad). Blots were developed using the Amersham Biosciences ECL Western blotting analysis system from GE Healthcare.

Statistical Analysis

All results are expressed as means. Error bars represent standard deviation. Significance was determined by analysis of variance for each experiment, followed by pairwise t test to compare individual treatments to the appropriate controls.

Results

Effect of V-ATPase inhibition on in vitro invasion of MCF10a and MCF10CA1a cells

In order to determine the role of V-ATPases in breast tumor cell invasion, we have compared V-ATPase involvement in two closely related human breast cancer cell lines. MCF10a cells are spontaneously immortalized breast epithelial cells derived from a patient with fibrocystic disease that are unable to form tumors in immunocompromised mice (Soule et al., 1990). MCF10CA1a is a highly invasive cell line derived from H-Ras transformed MCF10a cells (MCF10AT) after selection for the ability to forms tumors in mice (Dawson et al., 1996; Santer et al., 2001). The effect of treatment of MCF10a and MCF10CA1a cells with the specific V-ATPase inhibitor concanamycin (100 nM) on invasion was determined using an *in vitro* Matrigel invasion assay (Partridge and Flaherty, 2009). MCF10CA1a cells are significantly more invasive than the parental MCF10a cell line (Figure 2.1). Moreover, treatment with concanamycin

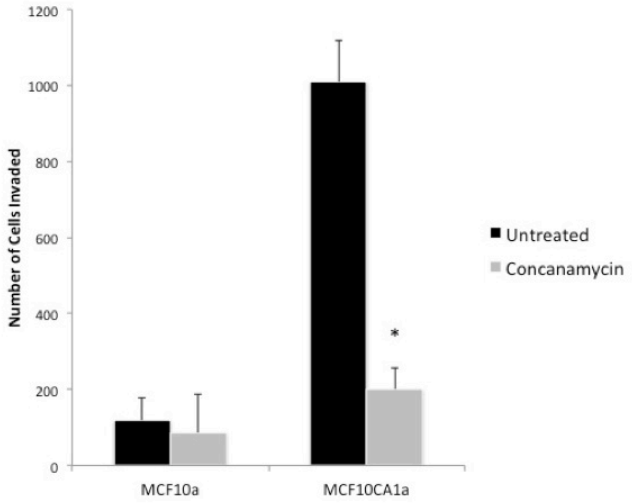

Figure 2.1. ***In vitro*** **invasion of MCF10a and MCF10CA1a cells after concanamycin treatment.** *In vitro* invasion was assayed using Matrigel™-coated FluoroBlok™ inserts as described under Experimental Procedures. Cells were treated with or without 100 nM concanamycin, allowed to invade toward a chemotractant and stained with Calcein-AM. An equal amount of solvent (DMSO) was added to untreated cells. Cells which had migrated to the trans-side were counted, with three wells analyzed per sample and 15 images analyzed per well. Values are the mean of three independent experiments and error bars indicate standard deviation. *, $p < 0.01$ compared to the untreated control.

dramatically reduced invasion by MCF10CA1a cells but did not significantly affect invasion by MCF10a cells. Measurement of cell viability using trypan blue exclusion revealed that treatment with 100 nM concanamycin for 24 hrs (a period longer than the 15 hrs employed in the cell invasion assay), did not induce cell death in either MCF10a or MCF10CA1a cells (data not shown), indicating that inhibition of invasion by concanamycin is not a consequence of decreased cell viability. These data show that V-ATPase activity is important for *in vitro* invasion by MCF10CA1a cells but not MCF10a cells.

mRNA levels of a subunit isoforms in MCF10a and MCF10CA1a cells.

We next compared expression levels of isoforms of subunit a in MCF10a and MCF10CA1a cells using quantitative RT-PCR. We had previously demonstrated that the highly invasive MDA-MB231 cells expressed higher levels of both the a3 and a4 isoforms of subunit a as compared to the poorly invasive MCF7 cells (Hinton et al., 2009b). The significance of these results was limited, however, by the fact that MB231 and MCF7 cells are independently derived lines and thus likely differ in many functional and genetic properties. The parental MCF10a cells expressed the highest levels of mRNA encoding the a2 and a3 isoforms (Figure 2.2A). Relative to MCF10a cells, MCF10CA1a cells expressed 8 and 3-fold higher levels of the a1 and a3 mRNA respectively (Figure 2.2B). We are not able at present to confirm the relative protein expression of a subunit isoforms due to the lack of antibodies that are specific for particular a subunit isoforms.

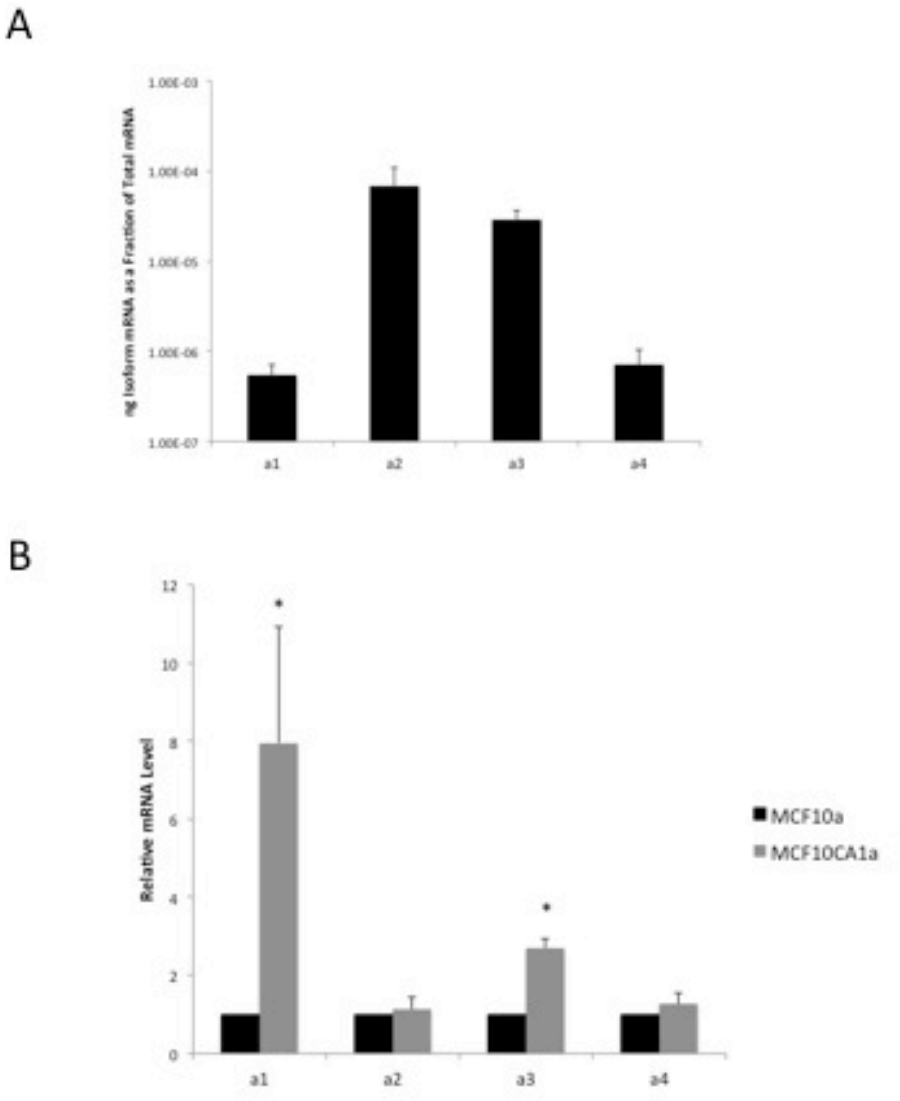

Figure 2.2. **mRNA levels of a subunit isoforms in MCF10a and MCF10CA1a cells.** mRNA levels were determined using quantitative RT-PCR for each a subunit isoform on mRNA isolated from each cell line, as described under Experimental Procedures. Plasmids expressing the cDNA of each a subunit isoform were used to establish a standard curve. Values were normalized to the total mRNA loaded and are the averages of four separate experiments. Error bars are standard deviation. A, a subunit isoform levels in MCF10a cells reported as the ratio of a subunit isoform mRNA to the total mRNA. B, ratio of a subunit isoform mRNA levels in MCF10CA1a cells verses MCF10a cells. *, $p < 0.01$ compared to MCF10a mRNA level.

Effect of knockdown of a subunit isoforms using isoform-specific siRNAs on invasion of MCF10CA1a cells

To determine the role of various a subunit isoforms in invasion by MCF10CA1a cells, cells were transfected with pools of siRNAs specific for each a subunit isoform for 81 hours prior to measuring *in vitro* invasion as described above. The effect of siRNA treatment on mRNA levels for each isoform was assessed by quantitative RT-PCR. siRNAs targeting a1, a2 or a3 resulted in a 50% or greater reduction in mRNA levels for the corresponding isoforms without significantly affecting expression levels of the other a subunit isoforms (Figure 2.3A). Treatment of cells with siRNAs targeting a4 decreased a4 subunit mRNA levels to 20% of untreated cells. However, this treatment also resulted in measurable decreases in a1 and a2 mRNA levels and a compensatory increase in a3 mRNA levels. With respect to invasion, knockdown of a3 but not a1, a2 or a4 significantly inhibited invasion by approximately 30% (Figure 2.3B). To determine whether the increase in a3 levels observed upon treatment with a4 siRNAs might be relevant for invasion, MCF10CA1a cells were transfected simultaneously with siRNAs targeting a3 and a4. Co-transfection of a3 and a4 siRNAs led to a decrease in expression of both a3 and a4, without affecting a1 and a2 levels (Figure 2.3A). Concurrent knockdown of a3 and a4 inhibited invasion to a much greater extent than knockdown of a3 alone (Figure 2.3B). These results suggest that both a3 and a4 expression contribute to the invasion by MCF10CA1a cells.

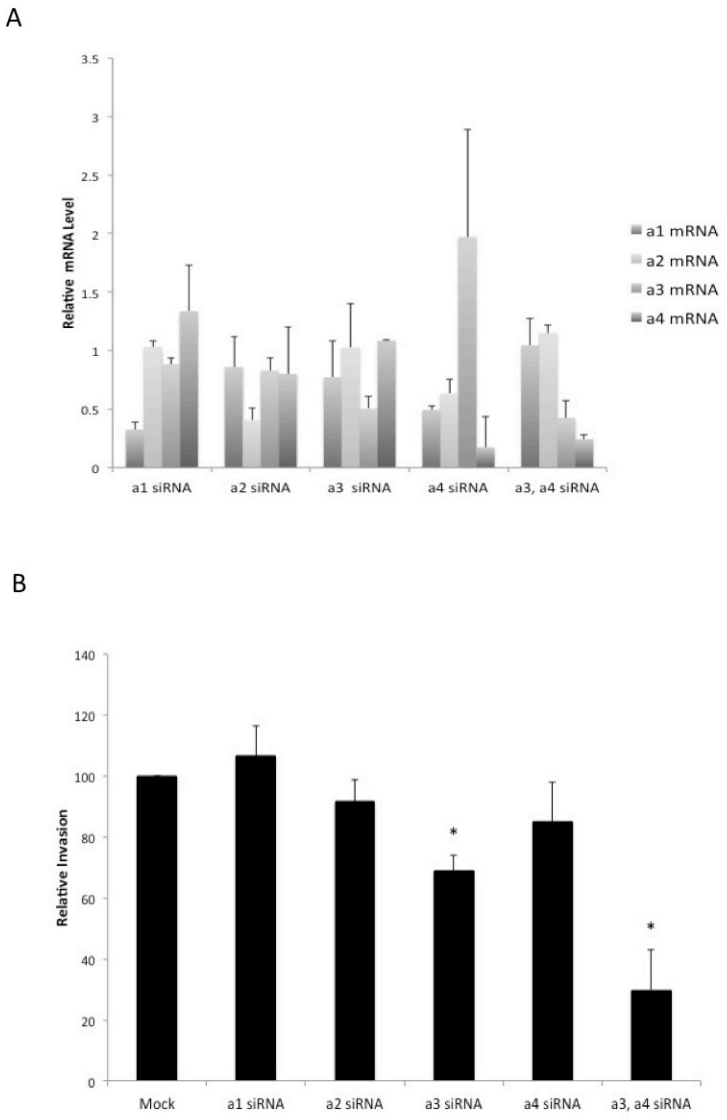

Figure 2.3. ***In vitro*** **invasion of MCF10CA1a cells after siRNA treatment.** A, mRNA levels of a subunit isoforms in MCF10CA1a cells after siRNA treatment. Cells were exposed to a subunit isoform-specific siRNA pools for 96 hrs prior to measuring mRNA levels, as described under Experimental Procedures. Quantitative RT-PCR was conducted as described in the legend to Figure 2.2. Knockdown is reported as the ratio of a subunit isoform mRNA in cells treated with siRNA verses a subunit isoform mRNA in untreated cells (NT). Values are the mean of three separate experiments. Error bars indicate standard deviation. B, Cells were exposed to a subunit isoform-specific siRNAs for 81 hrs prior to measuring invasion through Matrigel^{TM}- coated FluoroBlok^{TM} wells. Invasion is reported as the percentage of invasion observed for siRNA-treated cells relative to untreated cells (Mock). Three wells were counted per sample, with 15 images analyzed per well. Values are the mean of three independent experiments and error bars indicate standard deviation. *, $p < 0.005$ compared to Mock

Effect of a subunit isoform overexpression on the invasiveness of MCF10a cells

To assay the effect of overexpression of each a subunit isoform on invasion by the parental MCF10a cells, MCF10a cells were stably transfected with plasmids encoding each a subunit isoform. As a control, cells were stably transfected with the empty vector. Stable transfection of cells resulted in significant increases of the corresponding a subunit mRNA levels relative to vector transfected cells (Figure 2.4A). In the case of a4 transfected cells, there was also a measurable decrease in the levels of a1 mRNA. Overexpression of the a3 isoform, but not a1, a2 or a4, significantly increased invasion of MCF10a cells (Figure 2.4B). To determine whether high expression of a3 led to increased overall V-ATPase expression, A subunit expression levels were determined using RT-PCR. No significant difference in A expression was observed in a subunit isoform overexpressing MCF10a cells when compared to vector transfected controls (Figure 2.5A). To confirm this result, Western blotting was performed on whole cell lysates of cells expressing the vector alone or the various a subunit isoforms. As seen in Figure 2.5B, no significant difference in A subunit protein levels was observed between these cell lines. These data suggest that upregulation of a3 is sufficient to significantly increase the invasiveness of the parental MCF10a cell line, and highlight the importance of a subunit isoform expression in breast cancer cell invasion.

Effect of a subunit expression on cellular distribution of V-ATPases using immunocytochemistry

Previous studies have correlated plasma membrane V-ATPase distribution with invasive potential in breast cancer cell lines (Sennoune et al., 2004; Hinton et al., 2009b)

A

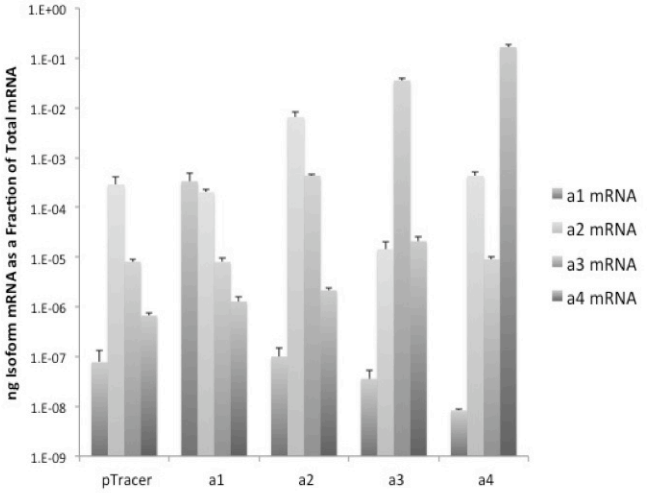

B

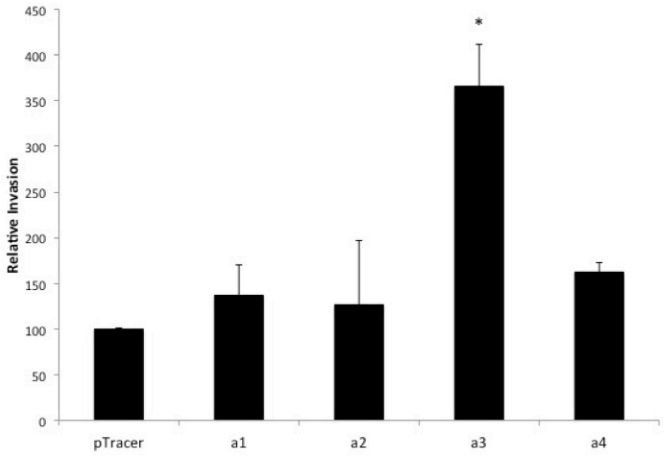

Figure 2.4. ***In vitro*** **invasion assay of MCF10a cells selectively overexpressing each a subunit isoform.** Each a subunit isoform was separately cloned into an overexpression vector and the vectors were stably transfected into MCF10a cells individually. A, mRNA levels of a subunit isoforms in MCF10a cells expressing a subunit isoform overexpression vectors. mRNA levels were determined using quantitative RT-PCR for each a subunit isoform with mRNA isolated from each stable cell line. Plasmids expressing the cDNA of each a subunit isoform were used to establish a standard curve. The values reported are the ratio of isoform-specific mRNA to the total mRNA. Values represent the mean of three experiments. Error bars are standard deviation. B, *In vitro* invasion of MCF10a cells selectively overexpressing each a subunit isoform through Matrigel™-coated FluoroBlok™ wells. Invasion is reported as the percentage of invasion observed for cells overexpressing particular a subunit isoforms relative to cells expressing empty vector. Three wells

were counted per sample, with 15 images analyzed per well. Values are the mean of three independent experiments. Error bars indicate standard deviation. The X-axis is labeled as follows: pTracer- MCF10a cells transfected with an empty pTracer vector; a1- MCF10a cells overexpressing a1; a2- MCF10a cells overexpressing a2; a3- MCF10a cells overexpressing a3; a4- MCF10a cells overexpressing a4. *, $p < 0.01$ compared to pTracer.

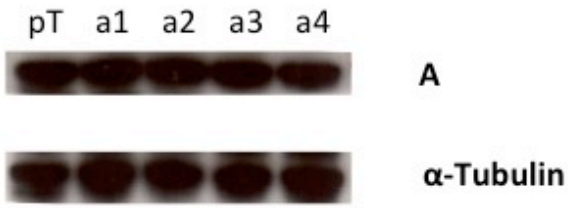

Figure 2.5. Protein levels of subunit A in MCF10a cells overexpressing various a subunit isoforms. The Western blot analysis shows protein levels of subunit A in MCF10a cells overexpressing various subunit a isoforms. *pT*, MCF10a cells transfected with the empty pTracer vector; *a1*, MCF10a cells overexpressing a1; *a2*, MCF10a cells overexpressing a2; *a3*, MCF10a cells overexpressing a3; *a4*, MCF10a cells overexpressing a4. The Western blot displayed is representative of data obtained from two separate experiments.

and migration of microvascular endothelial cells (Rojas et al., 2006). To determine whether this correlation applies to the cell lines employed in the present study, immunocytochemistry was performed using antibodies directed against the A subunit of the V-ATPase. This subunit is part of the V_1 domain and is common to all V-ATPases in the cell (Forgac, 2007). When images were assessed by confocal microscopy, V-ATPases were observed at the cell periphery in MCF10CA1a cells but only rarely in the parental MCF10a cells (Figure 2.6A). Phalloidin staining of F-actin was used to outline cells. V-ATPase staining observed at the periphery of the cell was interpreted as plasma membrane localization. Quantitation revealed an approximately 3-fold increase in the abundance of cell periphery V–ATPases in MCF10CA1a cells relative to the parental line (Figure 2.6B).

We next compared V-ATPase distribution in the MCF10a cells stably transfected with each of the a subunit isoforms by confocal microscopy (Figure 2.7A). MCF10a cells transfected with the empty vector or overexpressing a4 showed a primarily diffuse pattern of staining, whereas cells overexpressing a1 or a2 showed both punctate and diffuse patterns of staining. By contrast, MCF10a cells overexpressing a3 showed not only diffuse and punctate intracellular staining, but also staining at the cell periphery that we interpret as plasma membrane localization. Quantitation revealed a 2.5-4-fold increase in the fraction of cells displaying cell periphery V-ATPase localization relative to cells transfected with the empty vector or overexpressing a1, a2 or a4 (Figure 2.7B). These results suggest that a3 likely targets the V-ATPase to the plasma membrane in a3-transfected MCF10a cells and that it is plasma membrane V-ATPases that likely contribute to the increased invasiveness of these cells.

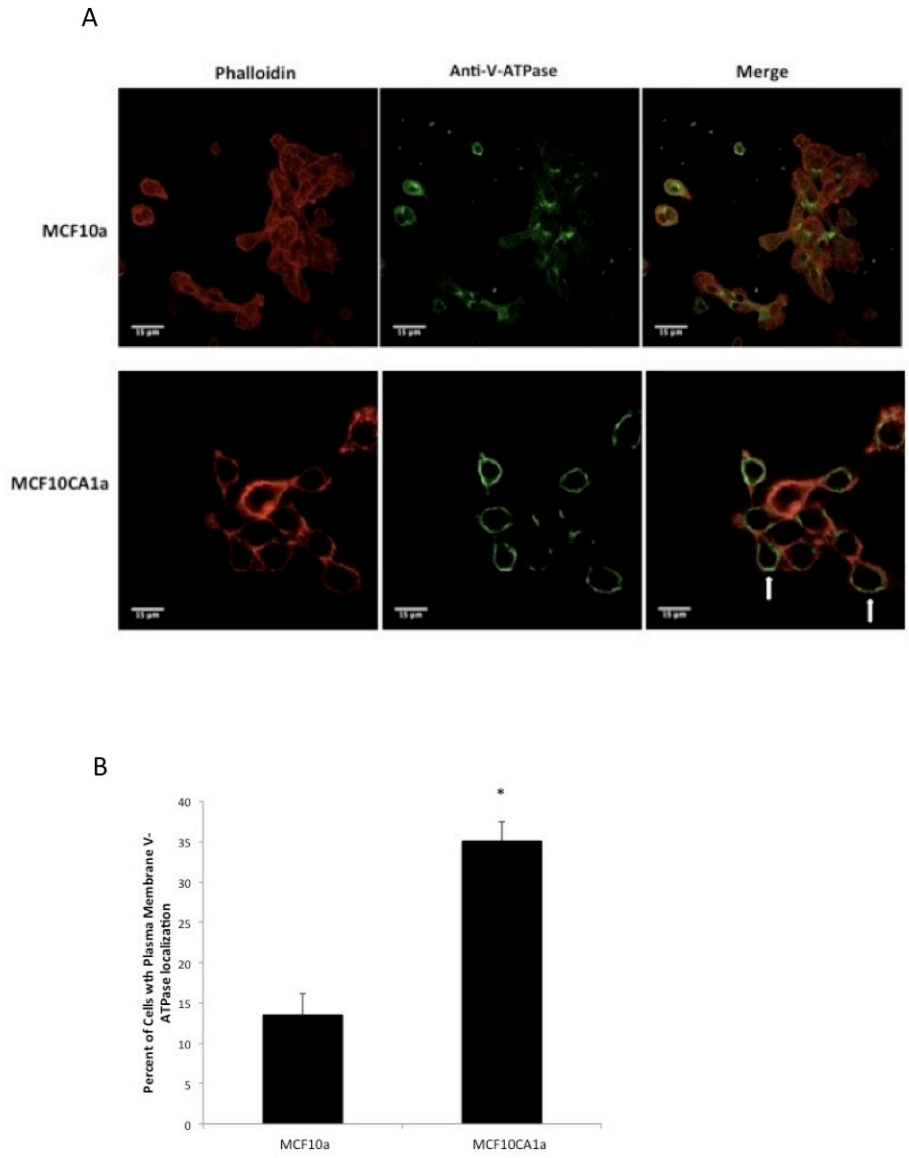

Figure 2.6. Immunostaining of MCF10a and MCF10CA1a cells using an antibody against the V-ATPase. MCF10a and MCF10CA1a cells were grown as a monolayer on coverslips in 6 well plates. Cells were immunostained using an antibody against subunit A of the V-ATPase (part of the V_1 domain, which stains all the V-ATPases in the cell), as well as phalloidin to stain actin. Images were taken with identical exposure times and antibody concentrations. A, three panels of MCF10a (top) and MCF10CA1a (bottom) cells showing fluorescence staining of actin (left), V-ATPase (middle), and the merge (left). B, quantification of plasma membrane staining in cells from immunostained images. 60 cells from each of three separate batches of immunostained images were counted and the number of cells showing plasma membrane V-ATPase localization (as indicated by arrows above) was determined. The values represent the average percentage of cells displaying plasma membrane staining. Error bars indicate standard deviation. *, $p < 0.01$

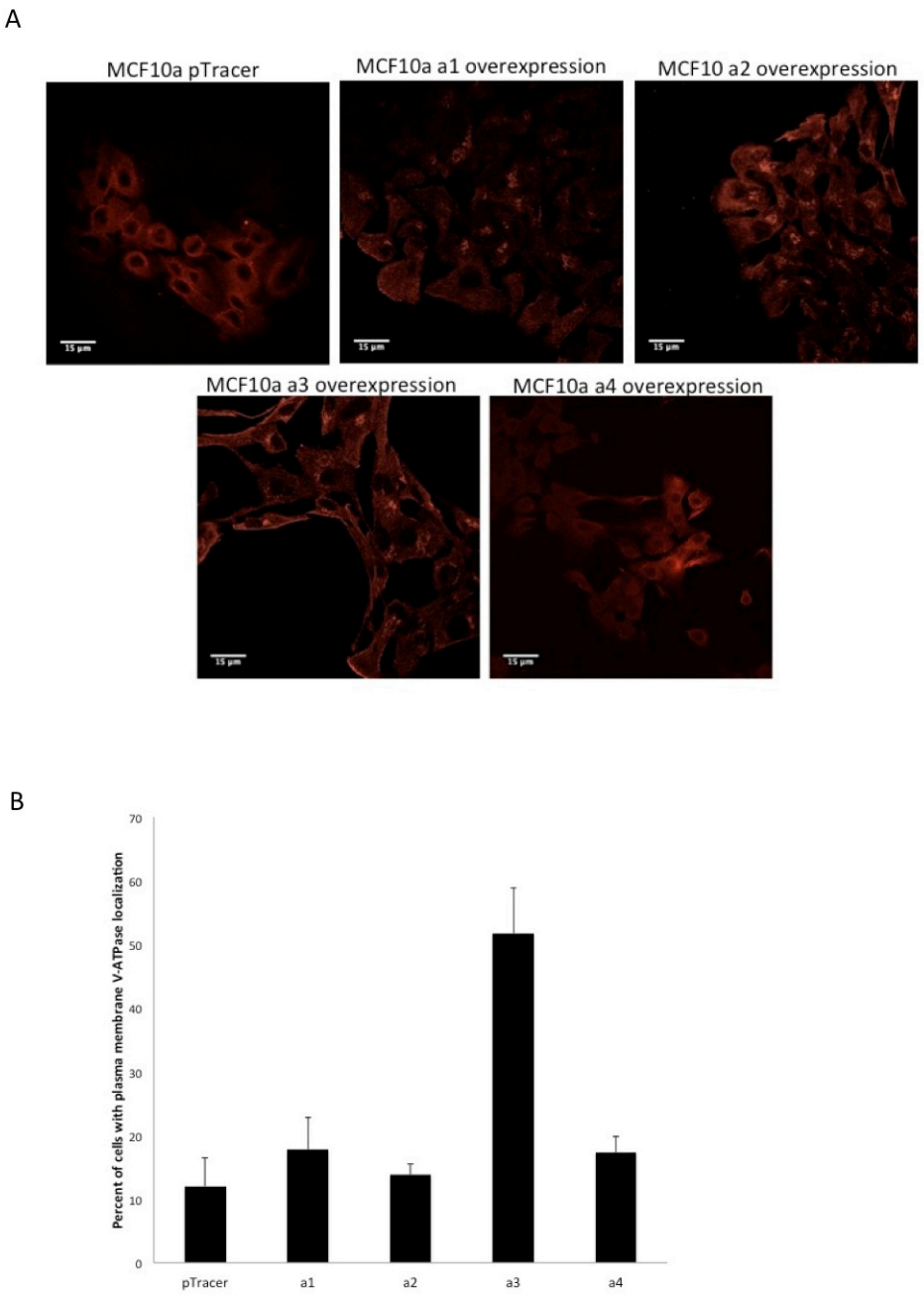

Figure 2.7. Immunostaining of MCF10a cells overexpressing subunit a isoforms using an antibody against the V-ATPase. MCF10a cells were grown as a monolayer on coverslips in 6 well plates. Cells were immunostained using an antibody against subunit A of the V-ATPase. Images were taken with identical exposure times and antibody concentrations. A, 5 panels of MCF10a cells expressing the empty pTracer vector or overexpressing the subunit a isoform indicated. B ,quantification of plasma membrane staining in cells from immunostained images. 60 cells from each of two or three separate batches of immunostained images were counted and the number of cells showing plasma membrane V-ATPase localization was determined. The values represent the average percentage of cells displaying plasma membrane staining. Error bars indicate standard deviation. The X-axis is labeled as follows: a1- MCF10a cells overexpressing a1; a2- MCF10a cells overexpressing a2; a3- MCF10a cells overexpressing a3; a4- MCF10a cells overexpressing a4.

Conclusions

The data presented in this chapter demonstrate that activity of V-ATPases is crucial for invasion of MCF10 cell lines. Inhibiting V-ATPases largely abolished invasion of MCF10CA1a cells without affecting invasion of the parental MCF10a cells. MCF10CA1a cells expressed much higher levels of both a1 and a3 subunit isoforms relative to the parental line. siRNA knockdown of a3 alone or a3 and a4 together significantly reduced invasion of MCF10CA1a cells. Importantly, overexpression of a3, but not other a subunit isoforms, in parental MCF10a cells increased *in vitro* invasion and peripheral V-ATPase localization. These results suggest that a3 is targeting V-ATPases to the plasma membrane in MCF10 cells and that a3-containing V-ATPases are the population of V-ATPases critical for invasion. In agreement with previous studies, these results suggest a role for plasma membrane V-ATPases in tumor cell invasion. The role of plasma membrane V-ATPases is further investigated in Chapter 3 of this thesis.

Chapter 3

Activity of Plasma Membrane V-ATPases is Critical for the Invasion of MDA-MB231 Breast Cancer Cells

The experiments displayed in Figures 3.3, 3.5 and 3.6 were conducted by Souad Sennoune and Raul Martinez-Zaguilan

Rationale

Although a correlation between plasma membrane V-ATPases and tumor cell invasiveness has been demonstrated, direct involvement of plasma membrane V-ATPases in tumor cell invasion has not yet been shown. Inhibitors such as bafilomycin and concanamycin are membrane permeant, and thus inhibit all the V-ATPases in the cell. This is important as acidification of secretory vesicles is V-ATPase dependent and may be required for the processing and secretion of pro-invasive factors, such as proteases or growth factors (Wiedmann et al., 2012; Hendrix et al., 2013). Moreover, knockdown of particular a subunit isoforms may indirectly affect plasma membrane localization of V-ATPases or secretion of proinvasive factors by effecting membrane trafficking.

To more directly assess the role of plasma membrane V-ATPases in tumor cell invasion, we have expressed a recombinant form of the V-ATPase c subunit containing an epitope tag exposed on the extracellular surface of tumor cells. We have then demonstrated that an antibody against the extracellular tag, added to living cells, inhibits both plasma membrane V-ATPase activity and invasion. These results suggest that plasma membrane V-ATPase activity is important for the invasiveness of at least some tumor cells.

Experimental Procedures

Cell Culture

The human breast cancer cell line MDA-MB231 was purchased from American Type Culture Collection (ATCC). Cells were grown in Falcon^{TM} T-75 flasks in Dulbecco's Modified Eagle's Medium (DMEM) with phenol red, 25 mM D-glucose, 4

mM l-glutamine, and 1 mM sodium pyruvate (Invitrogen) supplemented with 10% FBS (Invitrogen), 60 μg/ml penicillin, and 125 μg/ml streptomycin (Invitrogen). Cells were grown in a 95% air, 5% CO_2 humidified environment at 37 °C.

Plasmid Transfection

cDNA encoding the human c subunit was amplified by PCR and cloned into the pcDNA™ 3.1/V5-His TOPO® TA Expression vector (Invitrogen) to allow for C-terminal expression of the V5 epitope. Successful insertion was verified by sequencing. 15 μg of the resultant plasmid was transfected into MDA-MB231 cells using Lipofectamine 2000 (Invitrogen) in accordance with the manufacturer's recommendations. Stable transfection was achieved by treatment of cells with 7.5 μg/ml Blasticidin S (Invitrogen) for 21 days, beginning 3 days post-transfection. Cells were subsequently maintained under selective conditions.

Cell Lysis and Western Blotting

Cells were harvested with trypsin, resuspended in lysis buffer with protease inhibitors (PBS-EDTA containing 137 mM NaCl, 1.2 mM KH_2PO_4, 15.3 mM Na_2HPO_4, 2.7 mM KCl, 2 mM EDTA (pH 7.2), 2 μg/ml aprotinin, 5 μg/ml leupeptin, 0.7 μg/ml pepstatin, and 1 mM PMSF) and lysed by sonication. Cell lysates were centrifuged for 10 minutes at 4°C at 15,000 × g to remove cellular debris. Protein concentrations were determined using the Lowry method. SDS sample buffer was added to the lysates and aliquots containing 20 μg of protein were separated by SDS-PAGE on 4–15% gradient acrylamide gels or 12% acrylamide gels. The presence of the V5 epitope, subunit A or α-

Tubulin was detected by Western blotting using monoclonal antibodies from Invitrogen, Sigma or GenScript, respectively, followed by a horseradish peroxidase-conjugated secondary antibody (Bio-Rad). Blots were developed using the Amersham Biosciences ECL Western blotting analysis system from GE Healthcare.

Immunocytochemistry

A mouse monoclonal antibody raised against the V5 epitope (Invitrogen) was used to localize the V5-tagged subunit c in transfected cells. Cells were plated onto 24 x 24 mm coverslips. Approximately 24 hrs later, cells were washed, fixed with 4% paraformaldehyde and either permeabilized with 0.1% Triton X-100 or incubated in phosphate buffered saline (PBS) for non-permeabilized cells. Nonspecific binding was blocked by incubation with 1% bovine serum albumin in PBS for 1 hr. Cells were then incubated with the anti-V5 antibody at a 1:5000 dilution overnight, rinsed with PBS, and then incubated with Alexa Fluor® 488-conjugated goat anti-rabbit secondary antibody (1:500 dilution) and Alexa Fluor® 594 phalloidin (to stain F-actin, 1:250 dilution) (Invitrogen) in 1% bovine serum albumin/PBS. After 2 hr of incubation at room temperature, the cells were rinsed with PBS. The cells were prepared for viewing using ProLong® Gold (Invitrogen) mounting medium and allowed to cure at room temperature for 24 hr. The stained cells were imaged using a Zeiss Axiovert 10 fluorescence microscope.

Cytosolic and endosomal/lysosomal pH measurements

Cells growing on rectangular coverslips (8 x 22 mm) and treated overnight with or without the anti-V5 antibody were loaded with pyranine (8-hydroxypyrene-1,3,6-trisulfonic acid, trisodium salt) and SNARF-1 (5-[and-6] carboxy-SNARF-1-AM) (Life Science Molecular Probes, Eugene, OR) to simultaneously measure endosome/lysosome and cytosolic and pH, respectively (Hinton et al., 2009b). Cells were transferred to the cell perfusion system and were continuously perfused at 3.0 ml/min at 37°C with Cell Superfusion Buffer (CSB) containing: 1.3 mM $CaCl_2$, 1 mM $MgSO_4$, 5.4 mM KCl, 0.44 mM KH_2PO_4, 110 mM NaCl, 0.35 mM NaH_2PO_4, 5 mM glucose, 2 mM glutamine, and 20 mM HEPES at pH_{ex} 7.4. After steady state cytosolic pH (pH_{cyt}) was reached (5 min), the perfusate was exchanged for one containing 50 mM KOAc in a Na^+-free buffer, where Na^+ was substituted with 60 mM N-methylglucamine. The excitation spectra of pyranine (450/405 nm) in endosomes/lysosomes were acquired using an emission wavelength of 514 nm; and the emission spectra of SNARF-1 (644/584 nm) were acquired using 534 nm as excitation wavelength. The conversion of ratio values to cytosolic pH (pH^{cyt}) and endosomal/lysosomal pH ($pH^{E/L}$) were performed as described previously (Hinton et al., 2009b). The fluorescence was monitored with a SLM-8100/DMX spectrofluorometer (Spectronics Instruments, Rochester, NY) equipped for sample perfusion. The sample temperature was maintained at 37°C by keeping both the water jacket and perfusion media at 37°C using an iso-temperature immersion circulator water bath (Lauda model RM20, Brinkmann Instruments, Westbury, NY). All measurements were performed using 4 nm-bandpass slits and an external rhodamine standard as a reference. Fluorescence data were converted to ASCII format for analyses.

In situ calibration of SNARF-1

In situ calibration curves were generated as described previously (Hinton et al., 2009b). Briefly, the cells attached to cover slips were perfused with High K^+ buffer (10 mM NaCl, 146 mM KCl, 10 mM HEPES, 10 mM MES, 10 mM Bicine, 2 μM valinomycin and 6.8 μM nigericin, 5 mM glucose, 2 mM Glutamine, pH 5.5 to 8.0 adjusted with NaOH). The buffer contains high K^+ to approximate the intracellular K^+ concentration. Nigericin is an ionophore that exchanges H^+ and K^+ across the membrane, rendering the pH_{cyt} equal to the extracellular pH (pH_{ex}). Valinomycin is an ionophore that moves K^+ across the plasma membrane and, together with nigericin, helps to equilibrate pH_{cyt} and pH_{ex}. The pH of the buffers was determined using a Beckman pH meter with a glass electrode (Corning Inc., Horseheads, NY) calibrated at 37°C with commercially available standard solutions (VWR Scientific, San Francisco, CA). The ratios (R=644/584) of SNARF-1 were converted to pH using a modified Henderson-Hasselbalch equation (Martinez-Zaguilan et al., 1993). The equation was solved using nonlinear least squares analysis with Sigma Plot to obtain the values of pK_a, R_{min}, and R_{max} for SNARF-1 in these cells.

Plasma Membrane Proton Flux Measurements

The initial rate of pH_{cyt} recovery from an acid load induced by K^+-acetate was measured as the dpH/dt, which is the slope of the linear regression curve relating time and pH_{cyt}. Cells were loaded with SNARF-1 were perfused with CSB until the steady-state pH_{cyt} was reached. The cells were then perfused with 50 mM K^+-acetate in HCO_3^- and Na^+-free CSB to eliminate the contribution of potential HCO_3^- transporters and

Na^+/H^+ exchanger. The perfusion with K^+-acetate will cause a rapid intracellular acidification followed by a subsequent pH_{cyt} recovery. We then evaluated the pH_{cyt} recovery from this acidification within the first 3 minutes. The individual pH_{cyt} data points were then used to plot a linear regression curve relating time and DpH_{cyt}. To quantify the pH_{cyt} recovery, we expressed the recoveries as proton flux (J_{H+}) which is given by the apparent H^+ buffering (B_{H+} capacity multiplied by the dpH/dt)(Roos and Boron, 1981).

Invasion Assay

Assays for *in vitro* invasion were performed using Fluoroblok inserts (BD Biosciences) with an 8-μm pore size membrane and coated with Matrigel™ (BD Biosciences) (Patridge and Flaherty, 2009). Matrigel™ was diluted in PBS to a final concentration of 0.3 μg/μl, and a total of 18 μg was coated onto the membrane in each well. The membrane was allowed to dry overnight under vacuum at room temperature. Matrigel™-coated membrane was re-hydrated with 60 μl of DMEM plus 25 mM D-glucose, without phenol red, l-glutamine, or sodium pyruvate (Invitrogen) (termed Media) for at least two hr. 500 μl of the Media containing 5% FBS were added to wells plate in a 24 well plate to act as a chemoattractant. Prior to performing the invasion assay, cells were harvested by trypsinization and were brought to a concentration of 2×10^5 cells/ml in Media. For experiments testing the effects of the anti-V5 antibody, cells were resuspended in Media either with or without the monoclonal anti-V5 antibody (Invitrogen) at a dilution of 1:500 and allowed to incubate with cells for 15 min on ice. The bafilomycin-biotin conjugate was kindly provided by Dr. Marcus Huss. For

experiments conducted with biotin-bafilomycin, the inhibitor was incubated with streptavidin (Sigma) at a 2-fold molar excess of binding sites for 1 hr at 4°C on a Nutator. After this, the streptavidin-conjugated inhibitor was added to cells at a final concentration of 1.5 μM and incubated at 37°C for 15 min. An equal concentration of streptavidin along with an equal volume of DMSO was added to control cells. After incubation with the appropriate inhibitor, 5×10^4 cells were seeded onto the rehydrated membrane, which was then placed onto the wells containing chemoattractant. After 8 hr, membranes were placed onto wells containing 4 μg/mL Calcein AM in Hank's Balance Salt Solution (Invitrogen) and incubated for 30 min at 37°C in 5% CO_2. Cells that had migrated to the trans-side of the membrane were quantitated using a Zeiss Axiovert 10 fluorescence microscope. The number of invading cells was averaged over three wells (15 images per well), with all experiments performed at least three times.

Statistical Analysis

All results are expressed as means. Error bars represent standard deviation. Significance was determined by a pairwise t test.

Results

MDA-MB231 cells stably transfected with a V5-tagged construct of subunit c of the V-ATPase express the V5 epitope at the plasma membrane

To determine whether plasma membrane V-ATPases were critical to invasion of MDA-MB231 cells, cells were first stably transfected with a construct expressing the proteolipid c subunit of the V-ATPase tagged with the V5 epitope at the C-terminus

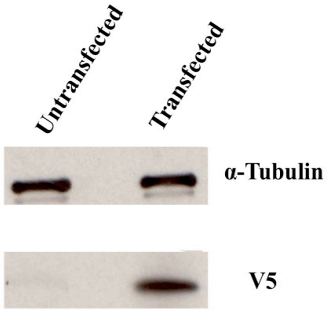

Figure 3.1. Expression of V5-tagged c subunit in untransfected and c-V5 transfected MDA-MB231 cells. Cell lysates were prepared from untransfected cells and cells transfected with the V5-tagged construct of subunit c. For each preparation, 20 μg of protein was separated by SDS-PAGE using 4-15% gradient acrylamide gels and proteins were transferred to nitrocellulose. Immunoblotting was conducted using monoclonal antibodies against V5 (Invitrogen) and alpha-tubulin (GenScript) as described under Experimental Procedures. The blot displayed is representative of data obtained from two separate experiments.

(termed c-V5). The C-terminus of subunit c has previously been shown to be present on the luminal surface of the protein such that, for a V-ATPase complex present at the plasma membrane, this epitope would be exposed on the extracellular surface of the membrane (Flannery et al., 2004). Expression of the c-V5 construct in the transfected cells was verified by Western blotting of whole cell lysates (Figure 3.1). We next wanted to determine whether c-V5 containing V-ATPases were present at the plasma membrane. To address this, immunocytochemistry was conducted using a V5 antibody in cells that either were or were not permeabilized by treatment with 0.1% Triton X-100. Fluorescence images are shown in Figure 3.2 demonstrating that permeabilized cells were readily stained with phalloidin, which stains F-actin, an intracellular marker, whereas non-permeabilized cells showed no phalloidin staining, confirming that cells remained impermeable to antibodies under the conditions of fixation employed. Staining with the anti-V5 antibody was observed in both permeabilized and non-permeabilized c-V5 cells. In permeabilized cells, both diffuse and punctate staining was observed, with significant perinuclear staining, consistent with localization to intracellular compartments, such as the Golgi and lysosomes. By contrast, in non-permeabilized cells, only diffuse staining with the V5 antibody was observed, indicating the presence of V5-tagged V-ATPase complexes diffusely distributed over the surface of cells (Figure 3.2). No staining with the V5 antibody was observed in untransfected cells (Figure 3.2), indicating that the antibody specifically targets the V5 epitope.

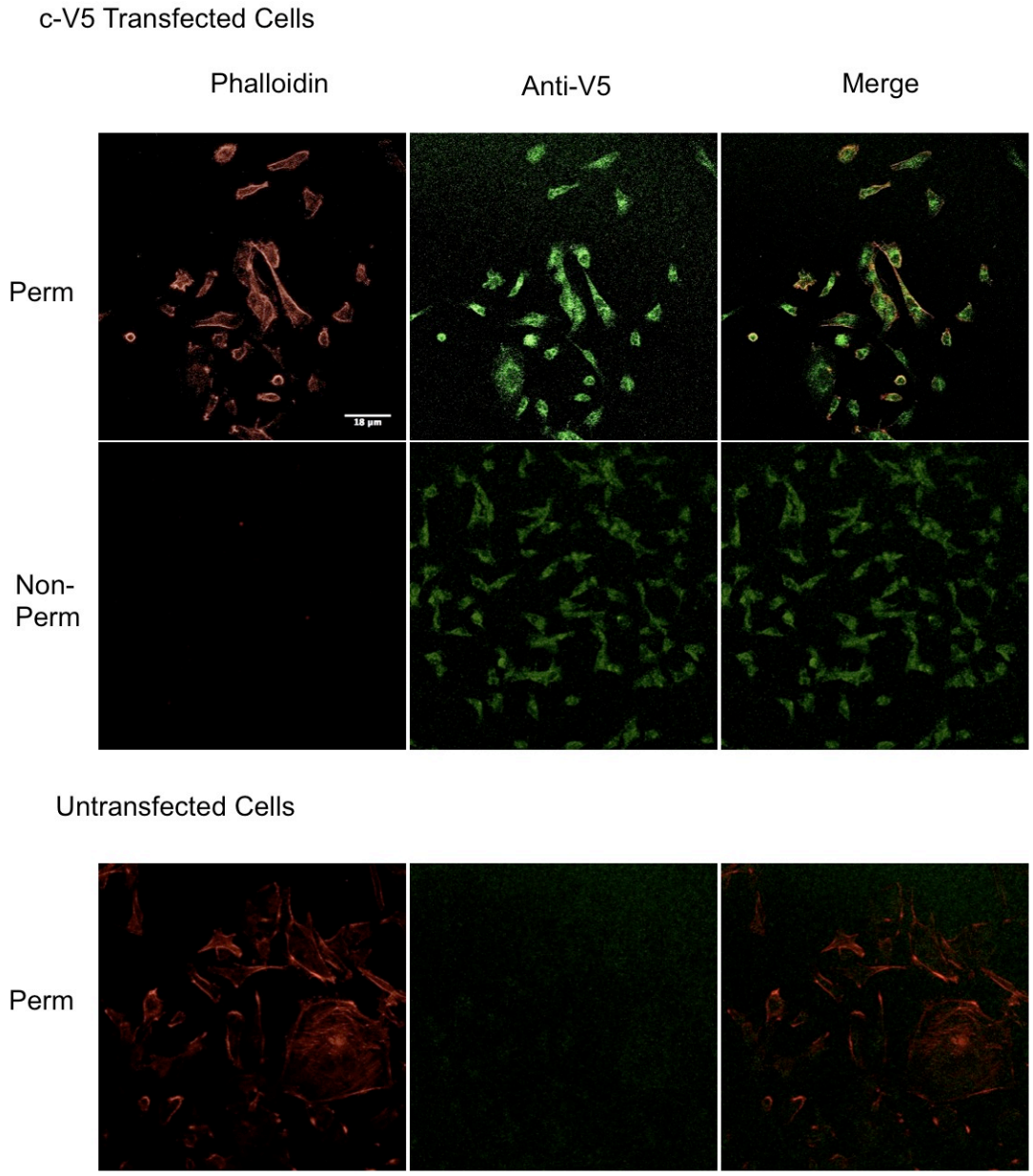

Figure 3.2. Immunostaining of Untransfected and c-V5 transfected cells using an antibody against V5. Control untransfected and c-V5 transfected cells were grown as a monolayer on coverslips in 6 well plates. Permeabilized cells were treated with 0.1% Triton X-100 for 5 min, while non-permeabilized cells were not. Cells were immunostained using a monoclonal antibody against V5 (Invitrogen), as well as Alexa Fluor® 594 phalloidin (Molecular Probes) to stain actin, followed by incubation with secondary antibodies as described under Experimental Procedures. Images were taken with identical exposure times and antibody concentrations. Top panels show permeabilized transfected cells, middle panels show non-permeabilized transfected cells and bottom panels show permeabilzed untransfected cells. Left panels show actin staining, middle panels show V5 staining, and right panels show the merged images.

Treatment of c-V5 expressing cells with an anti-V5 antibody causes acidification of the cytoplasm

To investigate the effect of addition of the anti-V5 antibody on cytosolic pH (pH_{cyt}) in cells expressing the c-V5 construct, the fluorescence pH indicator SNARF-1 was employed. MDA-MB231 cells were loaded with SNARF-1 and cytosolic pH was determined by measuring the ratio of fluorescence intensity at 644 and 584 nm upon excitation at 534 nm, as described under Experimental Procedures. As shown in Figure 3.3, c-V5 transfected cells had a more alkaline pH than untransfected cells. Addition of the anti-V5 antibody decreased the pH_{cyt} of c-V5 expressing cells but did not affect the pH_{cyt} of untransfected cells.

To determine whether the higher cytosolic pH observed in c-V5 expressing cells was due to an increase in total V-ATPase expression, we examined the protein levels of subunit A (part of the V_1 domain) by Western blotting of whole cell lysates using an anti-A subunit antibody. As shown in Figure 3.4, no difference in expression levels of subunit A was observed between untransfected cells and cells expressing the c-V5 construct, indicating that expression of the c-V5 protein did not alter total V-ATPase expression.

Treatment of c-V5 expressing cells with an anti-V5 antibody inhibits proton flux across the plasma membrane

To assess whether addition of the anti-V5 antibody inhibits proton flux across the plasma membrane of c-V5 expressing cells, the rate of pH_{cyt} recovery following an acute acid load induced by K^+-acetate was monitored as described under Experimental Procedures. Cells loaded with SNARF-1 were first perfused with buffer in the absence of

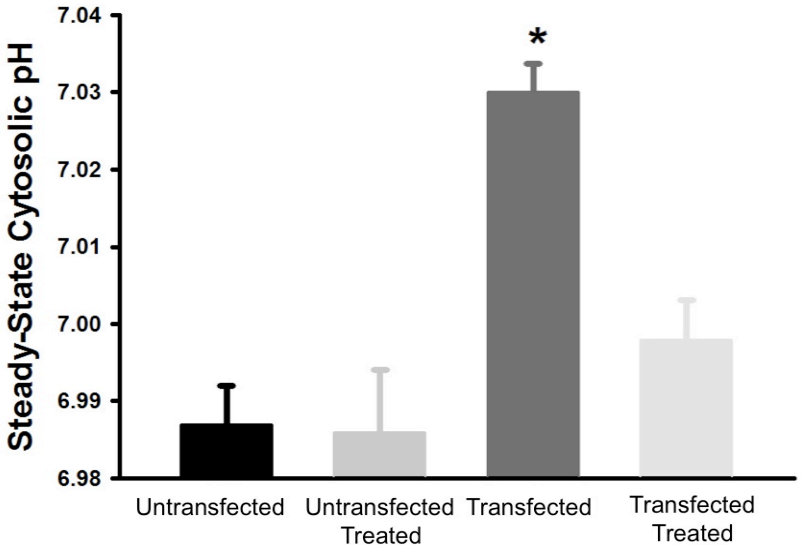

Figure 3.3. Cytosolic pH of untransfected and c-V5 transfected cells following incubation in the absence or presence of an anti-V5 antibody. Untransfected control or c-V5 transfected cells treated with or without a monoclonal antibody against V5 and then loaded with the pH sensitive fluorescence probe SNARF-1. Cytosolic pH was measured as described under Experimental Procedures. Values represent the mean cytosolic pH and *error bars* indicate standard deviation, $n = 9$. *, $p < 0.05$.

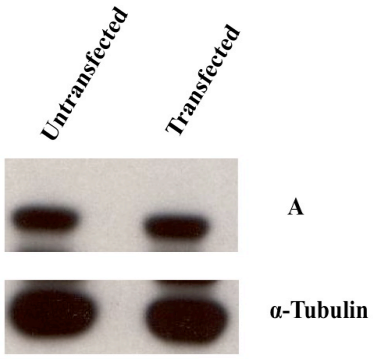

Figure 3.4. Levels of subunit A in untransfected and c-V5 transfected cells. Cell lysates from untransfected control cells and cells transfected with c-V5 were prepared. 20 μg of protein for each sample was separated by SDS-PAGE using 12% acrylamide gels and proteins were transferred to nitrocellulose. Immunoblotting was conducted using monoclonal antibodies against subunit A and alpha-tubulin as described under Experimental Procedures. The blot displayed is representative of data obtained from two separate experiments.

HCO_3^- and Na^+ to eliminate the contributions of HCO_3^- transporters and Na^+/H^+ exchangers to proton flux. Cells were subsequently equilibrated with 50 mM K^+-acetate resulting in a rapid intracellular acidification followed by a subsequent pH_{cyt} recovery. The rate of proton extrusion (J_{H+}) during the first three minutes of pH_{cyt} recovery was measured. As shown in Figure 3.5, no difference in proton flux across the plasma membrane was observed between untransfected and c-V5 transfected cells. Upon addition of the anti-V5 antibody, proton flux was significantly reduced in c-V5 transfected cells but not in untransfected cells. These results suggest that the anti-V5 antibody inhibits proton flux across the plasma membrane of c-V5 transfected cells by blocking the activity of V-ATPases.

Treatment of c-V5 expressing cells with an anti-V5 antibody does not inhibit endosomal/lysosomal acidification

To determine whether the anti-V5 antibody reduces the activity of V-ATPases expressed within endosomes and lysosomes, the fluorescence indicator pyranine was employed. Pyranine is taken into cells by endocytosis and will localize to endosomal and lysosomal compartments (Gillies and Martinez-Zaguilan, 1991). As shown in Figure 3.6, the steady-state pH of endosomal/lysosomal compartments in c-V5 transfected cells is 0.1 pH unit lower than those of untransfected MDA-MB231 cells. Upon anti-V5 antibody addition, the endosomal/lysosomal pH of both untransfected and transfected cells decreases by approximately 0.1 pH units (Figure 3.6), indicating that antibody exposure is associated with an increase in endosomal/lysosomal acidification regardless of c-V5 expression. While the mechanism causing increased acidification in these compartments

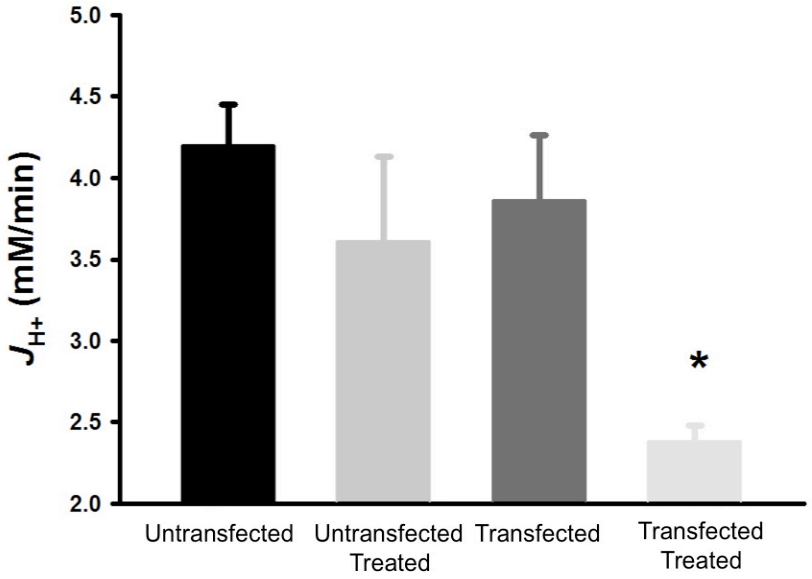

Figure 3.5. Proton flux across the plasma membrane in untransfected and c-V5 transfected cells with or without treatment with an anti-V5 antibody. Untransfected control and c-V5 transfected cells were incubated in the absence or presence of a monoclonal antibody against V5 and then loaded with SNARF-1. Cells were perfused with 50 mM K^+-acetate, which causes a rapid intracellular acidification followed by a pH_{cyt} recovery. The rate of proton extrusion (J_{H+}) during pH_{cyt} recovery was measured as described under Experimental Procedures. The values are the mean of nine experiments. *, $p < 0.05$.

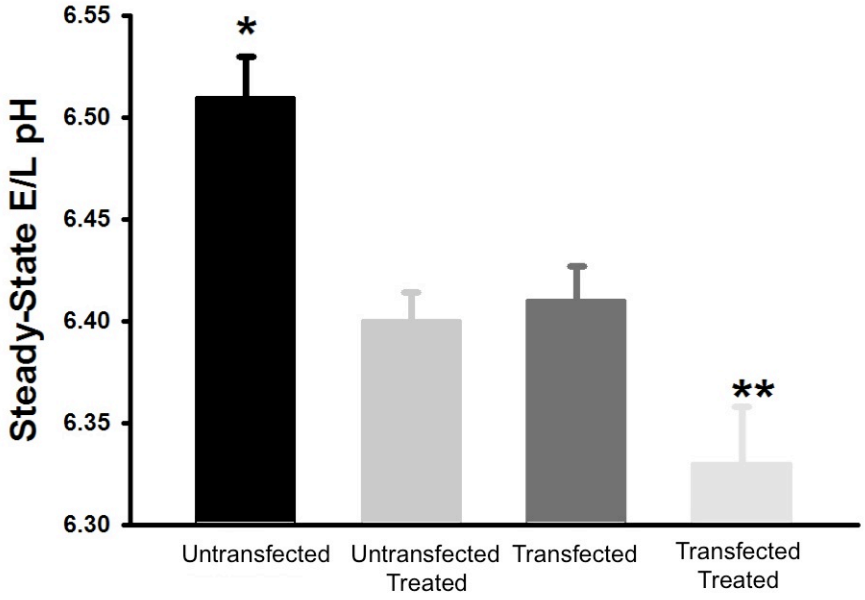

Figure 3.6. Endosomal/lysosomal pH of untransfected and c-V5 transfected cells following incubation in the absence or presence of an anti-V5 antibody. Untransfected control or c-V5 transfected cells were treated with or without a monoclonal antibody against V5 and then loaded with the pH sensitive fluorescence probe pyranine. Endosomal/lysosomal pH was measured as described under Experimental Procedures. Values represent the mean pH and *error bars* indicate standard deviation, n = 6-8. *, $p < 0.05$ compared to Untransfected Treated. **, $p < 0.05$ compared to Transfected.

is unclear, these results indicate that addition of the anti-V5 antibody does not inhibit V-ATPases localized to endosomes and lysosomes.

Treatment of c-V5 expressing cells with an anti-V5 antibody inhibits in vitro invasion of c-V5 expressing cells

We next wished to determine what effect addition of the anti-V5 antibody would have on invasion by c-V5 expressing cells. To address this, invasion was measured using an *in vitro* Matrigel assay as described under Experimental Procedures. Cells were incubated in the presence or absence of the anti-V5 antibody and then plated on Matrigel coated wells and induced to invade using a chemotractant (fetal bovine serum) on the trans-side of the well. After 8 hrs, cells on the trans-side were stained with Calcein AM and counted as described. As shown in Figure 3.7, while addition of the anti-V5 antibody had no effect on invasion of untransfected cells, invasion by the c-V5 expressing cells was significantly inhibited. These results suggest that inhibition of plasma membrane V-ATPases in c-V5 expressing cells is sufficient to block their invasion.

Treatment with a biotin-bafilomycin conjugate inhibits invasion of MDA-MB231 cells

To further test whether plasma membrane V-ATPases are critical to invasion, we employed a derivative of the specific V-ATPase inhibitor bafilomycin that has been conjugated to biotin. Biotin-bafilomycin was preincubated with streptavidin at a 2-fold molar excess of binding sites prior to assaying invasion through Matrigel for 8 hrs as described above. As shown in Figure 3.7, incubation with 1.5 μM biotin-bafilomycin significantly reduced the amount of invasion observed in MDA-MB231 cells. Future

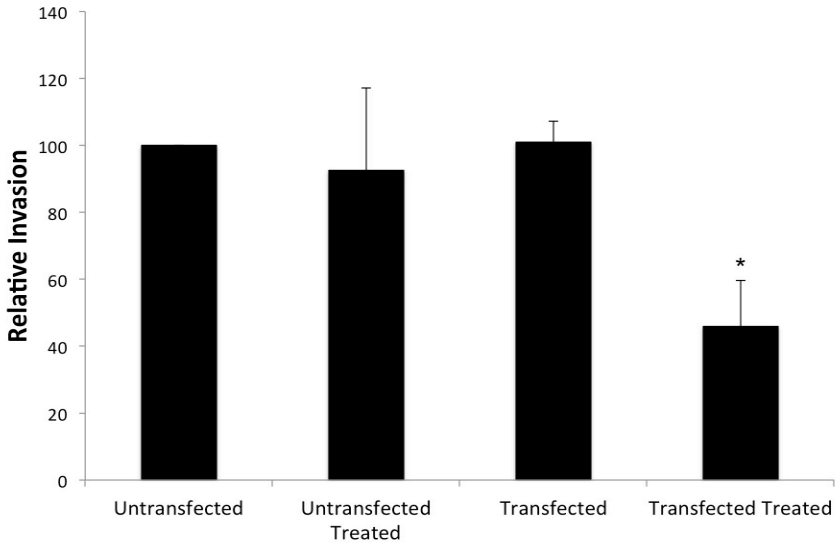

Figure 3.7. *In vitro* invasion of untransfected and c-V5 transfected cells with and without treatment with an anti-V5 antibody. Untransfected control cells or c-V5 transfected cells were treated in the presence or absence of a monoclonal antibody against V5 and then plated on Matrigel™-coated FluoroBlok™ inserts and allowed to invade towards a chemotractant on the trans-side of the well for 8 hrs. Cells were then stained with Calcein AM and the number of cells that had migrated to the trans-side were counted, with three wells analyzed per sample and 15 images analyzed per well. Values are the mean of three independent experiments and error bars indicate standard deviation. *, $p < 0.05$ compared to the untransfected cells not treated with antibody.

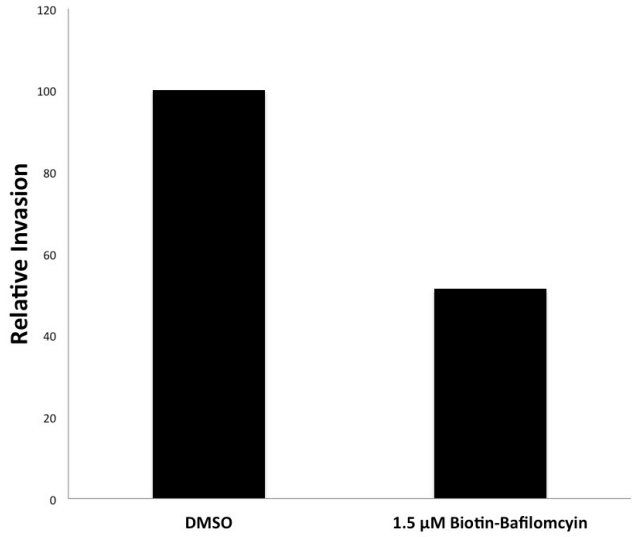

Figure 3.8. ***In vitro*** **invasion of MDA-MB231 cells with and without biotin-bafilomycin treatment.** MDA-MB231 cells were treated with either DMSO and streptavidin (labeled DMSO) or streptavidin-bound biotin-bafilomycin (labeled 1.5 µM Biotin-Bafilomycin) and then plated on Matrigel^{TM}-coated FluoroBlok^{TM} inserts and allowed to invade towards a chemotractant on the trans-side of the well for 8 hrs. Cells were then stained with Calcein AM and the number of cells that had migrated to the trans-side were counted, with three wells analyzed per sample and 15 images analyzed per well. Values are the mean of two independent experiments.

experiments assessing changes in cytosolic pH, endosomal/lysosomal pH and proton flux across the plasma membrane will be necessary to determine whether or not this compound is specifically inhibiting V-ATPases located at the plasma membrane.

Conclusions

The objective of this chapter was to determine whether or not activity of V-ATPases at the plasma membrane is critical for invasion of breast cancer cells. This was addressed by stably transfecting a c-V5 construct that expresses the V5 epitope extracellularly into MDA-MB231 cells. We found that treating c-V5 transfected cells with an anti-V5 antibody resulted in a more acidic cytosolic pH and reduced proton flux across the plasma membrane. These results are consistent with an inhibition of plasma membrane V-ATPases upon antibody treatment. Furthermore, antibody treatment did not inhibit activity of V-ATPases within endosomes and lysosomes. Antibody treatment was found to inhibit invasion of c-V5 expressing cells, but did not affect invasion of untransfected cells. Moreover, treatment with a biotin-bafilomycin conjugate predicted to inhibit only plasma membrane V-ATPases reduced invasion in untransfected MDA-MB231 cells. Additional experiments will evaluate whether biotin-bafilomycin also affects intracellular V-ATPases and will determine the mechanism by which the anti-V5 antibody reduces invasion of c-V5 transfected cells. Future studies will address the mechanism by which plasma membrane V-ATPases promote breast cancer invasion by analyzing the activity of potential downstream effectors of invasion, such as MMPs and pH-dependent cathepsins.

Chapter 4

Discussion

Function of a subunit isoforms in invasion of MCF10 cell lines

Targeting of V-ATPases to distinct cellular destinations is regulated by isoforms of subunit a (Toei et al., 2010). The role of different populations of V-ATPases containing particular isoforms of subunit a has begun to be probed in a number of cancers types, including breast cancer, melanoma and pancreatic cancer. In the cases of melanoma and pancreatic cancer cells, high expression of the a3 isoform was found to be critical for invasion of highly metastatic cancer cells (Chung et al., 2011; Nishisho et al., 2011). In the case of breast cancer cells, comparison of two unrelated cell lines (MCF-7 and MDA-MB231) showed that the more invasive MDA-MB231 cells express much higher levels of both a3 and a4 compared to the less invasive MCF-7 cell line (Hinton et al., 2009b). Because MDA-MB231 and MCF-7 cells were derived independently and differ in numerous characteristics (Soule et al., 1973; Cailleau et al., 1974), a comparison of expression of a subunit isoforms in more closely related cell lines was necessary. Furthermore, the effect of increasing expression of particular a subunit isoforms on tumor cell invasion has not previously been investigated. The goal of the Chapter 2 was to further probe the role of a subunit isoforms in the invasive potential of more closely related breast cancer cell lines.

The experiments in Chapter 2 focused on the MCF10a and the related MCF10CA1a cell lines (Soule et al., 1990; Santer et al., 2011). MCF10a cells. These cell lines have been used to study genetic alterations linked to tumorigenesis. Increased expression of signaling molecules with established roles in tumorogenesis, including c-Myc, Cyclin D1 and IGFR-1 has been observed in MCF10CA1a cells when compared to

MCF10a cells (So et al., 2012). These alterations are directly attributed to H-Ras transformation. Additional differences observed in MCF10CA1a cells include an overactivation of Erk, increased expression of Stat3 and an activating mutation in PI3KCA (So et al., 2012). These changes are not observed in H-Ras transformed MCF10AT cells, indicating that selection for an increased ability to form tumors and metastases has led to alterations in these signaling pathways. Moreover, MCF10CA1a cells have higher expression of CD44 splice-variants that are associated with increased malignancy compared to MCF10a and MCF10AT cells (So et al., 2012). Interestingly, Ras transformation upregulates expression of cathepsin B at the cell surface of colorectal cancer cells (Cavallo-Medved et al., 2003). While the affect of Ras transformation on cathepsin secretion in MCF10 cell lines has not been investigated, it is possible that MCF10CA1a cells may have higher cell surface expression of cathepsins and peripheral V-ATPases may participate in the activation of these cathepsins.

Here we have demonstrated that V-ATPase activity is critical for the *in vitro* invasion of highly metastatic MCF10CA1a cells but not the parental MCF10a cells (Figure 2.1). In addition, MCF10CA1a cells have increased expression of both the a1 and a3 isoforms relative to MCF10a cells (Figure 2.2). Interestingly, siRNA knockdown of a3 (but not a1, a2 or a4) led to a significant decrease in invasion by MCF10CA1a cells (Figure 2.3). These results suggest that a3 participates in invasion by MCF10CA1a cells. Since knockdown of other isoforms did not affect invasion, higher a1 expression in MCF10CA1a cells does not appear to be required for the invasive phenotype. It is possible that elevated expression of a1 in MCF10CA1a cells may confer some other advantage not tested in our invasion experiments. For example, elevated expression of a1

may be required for enhanced Golgi function associated with elevated expression of cell surface glycoproteins. Further work will be required to elucidate the function of a1 in tumor cells.

It is interesting to note that, while knockdown of the a4 isoform alone did not reduce invasion, it did result in an increase in the levels of a3 mRNA (Figure 2.3). It is possible that a reduction in invasion caused by the loss of a4 may have been masked by this upregulation in a3 levels. To address this possibility, knockdown of a3 and a4 was performed concurrently. Under these conditions, the inhibition of invasion observed was much larger than with knockdown of the a3 isoform alone. This effect suggests that both a3 and a4 may participate in the invasive phenotype of MCF10CA1a cells. The level of a3 mRNA present with either knockdown of a3 alone or knockdown of a3 and a4 together are comparable (Figure 2.3A), yet the level of invasion observed with knockdown of a3 and a4 together is much greater than that observed upon knockdown of a3 alone. Thus, a4 must be contributing to invasion in a way that does not depend upon a3, but this contribution is masked when knocking down a4 alone because of the compensating increase in a3 expression.

The a4 isoform is expressed at low levels in MCF10a and MCF10CA1a cells compared to a3 (Figure 2.3). Thus, it is surprising that knockdown of a4 in MCF10CA1a cells results in a 2-fold increase in a3 expression. These results suggest that despite being expressed at very low levels, a4 may have a critical function within these cells. One possibility is that a4-containing pumps are involved in trafficking of a3-containing pumps to the plasma membrane, such that compensating for the loss of a4 may require a large increase in a3 such that an equivalent number of pumps make it to the cell surface. Thus,

loss of peripheral localization of a3-containing V-ATPases in MCF10CA1a cells may activate signaling pathways that induce an increase in a3 expression. Further work will be necessary to elucidate the role of a4 in invasion of MCF10CA1a cells.

To complement our analysis of the effect of a subunit knockdown on invasion by MCF10CA1a cells, we also tested the effect of overexpression of a subunit isoforms on the invasive potential of the parental MCF10a cell line. Importantly, overexpression of a3 but not the other a subunit isoforms dramatically increased invasion by MCF10a cells (Figure 2.4). To the best of our knowledge, these are the first data demonstrating that elevated expression of a particular V-ATPase isoform can increase the invasion by tumor cells. While high expression of a3 did increase invasiveness of MCF10a cells, it did not bring invasion to the same level observed in MCF10CA1a cells (Figure 2.1 and Figure 2.4). These data indicate that high a3 expression is not the only factor contributing to the increased invasiveness of MCF10CA1a cells compared to the parental cell line. Since a3 is known to localize V-ATPases to the plasma membrane of osteoclasts (Frattini et al., 2000; Toyomura et al., 2000; Toyomura et al., 2003), we expected that overexpression of a3 was increasing localization of V-ATPases to the plasma membrane of MCF10a cells. Immunocytochemical localization confirmed increased peripheral staining of V-ATPases in cells overexpressing a3 (Figure 2.7). Consistent with this idea, MCF10CA1a cells express significantly higher levels of V-ATPase at the cell periphery relative to parental cells (Figure 2.6). These results suggest that elevated a3 expression may be responsible for elevated V-ATPase localization to the plasma membrane, and that plasma membrane V-ATPases contribute to enhanced invasion by breast tumor cells.

Comparison of the images in Figure 2.7 reveals that only overexpression of a3 leads to increased plasma membrane staining. By contrast, overexpression of a1 and a2 shows increased intracellular staining whereas overexpression of a4 looks similar to cells expressing the empty vector. It should be noted that the staining observed in MCF10a cells in Figure 2.6 appears somewhat more punctate than the empty vector transfected cells in Figure 2.7, which appears more diffuse. This may be due to the use of different secondary antibodies in the experiments employed in Figure 2.6 and Figure 2.7, which may result in a different sensitivity of detection. Nevertheless, comparison of the images in Figure 2.7 employing the same conditions and antibodies supports the conclusion that overexpression of a3 leads to increased peripheral localization of the V-ATPase. Although, as noted above, siRNA-mediated silencing of a4 contributed to inhibition of invasion by MCF10CA1a cells, overexpression of a4 did not significantly increase invasion (Figure 2.4) or plasma membrane V-ATPase localization (Figure 2.7) in parental MCF10a cells. These results suggest that a4 expression can contribute to invasion, but expression of a4 alone is not sufficient to increase invasion or plasma membrane V-ATPase localization in MCF10a cells.

There are several mechanisms by which overexpression of a3 and upregulation of peripheral V-ATPases may lead to enhanced invasion by tumor cells. One possibility is that high a3 expression leads an increase in total V-ATPase expression within MCF10a cells. Although somewhat brighter staining was observed for cells overexpressing a3 (Figure 2.7A), no increase in A subunit protein levels was detected in these cells (Figure 2.5). All panels in Figure 2.7 were obtained under identical experimental conditions with identical exposure times. It is possible that overexpression of a3 may result in more

assembled complexes which appear more finely punctate (and thus brighter) than the more diffuse pattern of the vector transfected cells. The results of these experiments demonstrate that there is a correlation between tumor cell invasion and V-ATPase localization to the cell periphery.

Overexpression of a3 may affect expression of proteins involved in invasion by altering cellular pH dynamics. Expression at the plasma membrane may cause a local extracellular acidification. Intriguingly, low extracellular pH has previously been demonstrated to increase MMP-2 and MMP-9 expression in metastatic melanoma cells (Kato et al., 2005; Nishisho et al., 2011). Moreover, knockdown of a3 has been shown to reduce expression of MMP-2 and MMP-9 (Nishisho et al., 2011). Thus increased expression of a3 in MCF10a cells may be directly increasing expression of proteases with established roles in invasion. Taken together, the results of this work and prior studies indicate that a3 is a suitable anti-invasive target for a variety of cancer types.

Function of plasma membrane V-ATPases in invasion of breast cancer cells

One limitation of previous studies that have correlated plasma membrane V-ATPase expression with tumor cell invasion has been the inability to specifically inhibit V-ATPases localized to the plasma membrane, since available V-ATPase inhibitors, while highly specific, are membrane permeant and thus inhibit all the V-ATPases in the cell. The purpose of Chapter 3 of this thesis was to determine whether V-ATPase activity at the plasma membrane plays a role in cancer cell invasion by specifically inhibiting activity of plasma membrane V-ATPases.

To address this question, we have tagged the proteolipid c subunit of the V-ATPase with the V5 epitope tag at the C-terminus. Although V-ATPases containing subunit a3 have been demonstrated to participate in invasion, we chose to conduct the experiments displayed in Chapter 3 with an epitope-tagged subunit c for several reasons. First, the topology of the c subunit ensures that the V5 epitope tag in this construct will be exposed on the luminal or, for plasma membrane localized V-ATPases, the extracellular surface of the protein (Flannery et al., 2004). Both the N- and C-termini of a3 are located in the cytosol and would therefore not be suitable locations to place tags for antibody inhibition assays. A second advantage of using the c subunit to insert an epitope tag is that it is expressed in multiple copies in V-ATPases. This is significant because MDA-MB231 cells express all of the endogenous V-ATPase genes. Since multiple copies of c are expressed in each V-ATPase, there is a larger probability that each V-ATPase will contain at least one V5 tagged subunit. Since only one copy of an a isoform is expressed in each V-ATPase, the presence of endogenous a isoforms would mean that some V-ATPases in these cells would not express the epitope tag and would therefore not be inhibited in our assay. Lastly, knockdown of a4 as well as a3, inhibited invasion and plasma membrane V-ATPase localization in MDA-MB231 cells (Hinton et al., 2009b). Thus it was necessary to construct an epitope tagged V-ATPase subunit that could be used to inhibit both a3 and a4 containing V-ATPases. Tagging only a3 would not inhibit activity of a4 containing V-ATPases, whereas tagging c-V5 should target all V-ATPases within the cell.

The tagged construct was stably transfected into MDA-MB231 cells. Plasma membrane expression of V5 in c-V5 expressing cells was confirmed by

immunocytochemistry using an anti-V5 antibody in non-permeabilized cells (Figure 3.2). Expression of c-V5 tagged V-ATPases at the plasma membrane is consistent with previous reports showing that MDA-MB231 cells localize V-ATPases to the cell surface (Sennoune et al., 2004; Hinton et al., 2009b). We next wished to determine whether treatment of cells with the anti-V5 antibody affected the activity of V-ATPases at the plasma membrane and regulation of cytosolic pH and endosomal/lysosomal pH. Using the fluorescent pH indicator SNARF-1, we observed a decrease in cytosolic pH upon addition of the anti-V5 antibody to cells expressing the c-V5 construct, but not to untransfected cells (Figure 3.3). Addition of the anti-V5 antibody inhibited proton flux across the plasma membrane in c-V5 transfected cells, but not control cells (Figure 3.5). Moreover, the anti-V5 antibody did not inhibit activity of V-ATPases in endosomes and lysosomes (Figure 3.6). These results suggest that the anti-V5 antibody is able to specifically inhibit proton transport across the plasma membrane mediated by the V-ATPase.

The mechanism by which the antibody inhibits V-ATPase activity is not known. It is possible that binding of the antibody to the c subunits sterically inhibits rotation of the proteolipid ring, which is required for ATP-driven proton transport (Yokoyama et al., 2003). Since each proteolipid ring contains multiple copies of the c subunit (Powell et al., 2000), it is possible that multiple V5 antibodies may bind to each V-ATPase complex, setting up interactions with nearby molecules in the membrane environment and obstructing rotation.

Unexpectedly, we found that addition of the anti-V5 antibody resulted in an increased lysosomal acidification in both transfected and untransfected MDA-MB231

cells (Figure 3.6). The fact that increased acidification occurs in untransfected MDA-MB231 cells indicates that this effect is likely not due to interactions between the antibody and V-ATPases. c-V5/antibody interactions were expected to increase endosomal/lysosomal pH, rather than decrease endosomal/lysosomal pH, if the antibody is inhibiting pumps in these organelles. Thus, these data are not consistent with an inhibition of V-ATPases in endosomes and lysosomes. While no off-target interactions were observed in untransfected MDA-MB231 cells exposed to the V5 antibody by Western blotting or immunocytochemistry (Figure 3.2), these experiments were conducted at much lower antibody concentrations than are utilized during the endosomal/lysosomal pH measurements (1:5000 versus 1:500, respectively). Thus it is possible that the V5 antibody has low affinity interactions with off-target proteins that become apparent at higher concentrations. These interactions may be causing endocytosis that induces acidification of endosomes and lysosomes. Further work will be necessary to determine the mechanism by which the anti-V5 antibody is causing increased acidification of these compartments.

Interestingly, we found that cells expressing the c-V5 construct had a more alkaline cytosolic pH than untransfected cells (Figure 3.3). Since transfected cells express endogenous subunit c in addition to the V5-tagged subunit c, it is possible that increased expression of proteolipid subunits leads to an increase in the number of V-ATPase complexes. The fact that the levels of subunit A in transfected and untransfected cells were the same (Figure 3.4) indicates that there is no change in V_1 levels in transfected cells. However, it is still possible that the levels of assembled V_0 may be increased in transfected cells. While there is no change in proton flux across the plasma

membrane (Figure 3.5), a lower pH of endosomes and lysosomes is observed in c-V5 transfected cells (Figure 3.6). This result is consistent with an increase in V-ATPase assembly and activity in internal compartments following c-V5 transfection.

Lastly, we wished to determine whether inhibiting plasma membrane V-ATPase activity blocked invasion of c-V5 expressing cells. Using an *in vitro* invasion assay we observed no difference in the invasiveness of c-V5 expressing cells and untransfected cells. However, addition of the anti-V5 antibody reduced invasion of c-V5 expressing cells by over 50% relative to untreated cells, but had no effect on invasion by untransfected cells (Figure 3.7). To further evaluate whether the activity is crucial for cell invasion, untransfected MDA-MB231 cells were treated with a streptavidin bound biotin-bafilomycin conjugate prior to assaying *in vitro* invasion. Biotin-bafilomycin treatment largely reduced invasion compared to non-treated cells (Figure 3.8). Experiments assessing the effects of this compound on proton flux across the plasma membrane, cytosolic pH and endosomal/lysosomal pH are necessary to determine whether or not the biotin-bafilomycin compound is specifically inhibiting plasma membrane V-ATPases. Additionally, we can conduct biotin-bafilomycin invasion assays using streptavidin-conjugated beads to ensure that the inhibitor is not being endocytosed after binding to plasma membrane V-ATPases. The results of these experiments are consistent with a role of plasma membrane V-ATPases in the invasion of MDA-MB231 cells.

For successful metastasis tumor cells must degrade the extracellular matrix and migrate out of the primary tumor as well as escape the circulation or lymphatic system to colonize new sites. For some tumor cells, this process of invasion relies on secretion of a

class of pH-dependent proteases known as cathepsins (Gocheva and Joyce, 2007). These proteases normally reside in lysosomes and therefore require a low pH for activity. Secreted cathepsins, once activated, may also function in the proteolytic activation of other proteases that participate in invasion, such as MMPs (Gocheva and Joyce, 2007; Gondi and Rao, 2013). Neutralization of the acidic extracellular pH of tumors has been shown to prevent the formation of metastases in mouse models and reduce cathepsin and MMP activation (Robey et al., 2009; Robey and Nesbit, 2013). Furthermore, pharmalogic or genetic disruption of V-ATPase activity has been shown to reduce MMP activity in pancreatic cancer cells (Chung et al., 2011). Thus, plasma membrane V-ATPases may be promoting invasion by generating a locally acidic extracellular pH that is required for the activity of cathepsins.

In addition to roles at the plasma membrane, it is possible that intracellular V-ATPases also participate in invasion. A recent report has shown that pharmacological V-ATPase inhibition or siRNA-mediated knockdown of the V_0 subunits a1 or d1 prevents Rab27-mediated invasion in breast cancer cells by preventing peripheral localization and secretion of Rab27 containing vesicles (Wiedmann et al., 2012). Moreover, inhibiting V-ATPases with archazolids impaired plasma membrane localization of EGFR and Rac1 in SKBR3 breast cancer cells, a critical process for cell migration (Hendrix et al., 2013). Since EGF has been shown to induce V-ATPase assembly in primary hepatocytes (Xu et al., 2012), V-ATPase assembly may be a necessary step in EGF signaling and receptor trafficking to the cell surface. The results of these studies suggest that intracellular V-ATPases may play an important role in the trafficking of molecules that participate in invasion. Indeed, V-ATPases may be promoting activity of extracellular proteases by

acidifying secretory lysosomes that deliver molecules to the cell surface. Secretory lysosomes are present in a variety of cell types, including osteoclasts where secretion allows for the extracellular activity of lysosomal hydrolases such as cathepsin K (Blott and Griffiths, 2002). Since osteoclasts express highly express a3, high a3 expression may also induce secretion of lysosomes in tumor cells by a similar mechanism. Future experiments will be aimed at determining the mechanism by which a3 promotes invasion.

Future Directions

It is hypothesized that plasma membrane V-ATPases promote invasion by increasing the activity of extracellular proteases. This may be accomplished by locally acidifying the extracellular space and promoting the activation of acid-dependent proteases. Future experiments will be aimed at testing this hypothesis. Commercially available fluorometric assays will be conducted to measure extracellular cathepsin activity with c-V5 expressing MDA-MB231 after antibody treatment. If cathepsin activation occurs outside of the cell as predicted, inhibition of only plasma membrane V-ATPases should inhibit cathepsin activity. Moreover, the effects of alterations in a3 expression on cathepsin activity in MC10a and MCF10CA1a can be evaluated. It is predicted that siRNA knockdown of a3 will reduce cathepsin activity in MCF10CA1a, while overexpression of a3 in MCF10a will increase cathepsin activity.

Cathepsin activity assays will be conducted in two distinct ways. First, media from the cells we are studying can be isolated, concentrated and incubated with commercially available fluorescent cathepsin substrates. This assay is a simple way to

measure the activity of extracellular proteases. However, one shortcoming of this experiment is that it will assay levels of cathepsin activity in the total media and may not be able to detect the local changes in cathepsin activity at the cell surface that we predict. Alternatively, the cell lines we are studying can be cultured in the presence of dye-quenched fluorescent (DQ) proteins that will emit fluorescent light when cleaved by extracellular proteases (Sloane et al., 2006; Cavallo-Medved et al., 2009). Cathepsin activity directly outside of living cells can be observed as a change in fluorescence observed by live-cell imaging of cells grown in wells containing DQ-tagged components of the extracellular matrix. This method has been previously used to study the roles of specific proteases in local degradation of the extracellular matrix (Sloane et al., 2006). By directly observing proteolytic degradation outside of cells by fluorescence microscopy, we will be able to better gauge the role of V-ATPases in local cathepsin activation in invasive cell lines. If no difference in cathepsin activity is observed, we will study the affect of V-ATPase activity on other types of acid-dependent proteases. A second possibility is legumain, a lysosomal protease that has been shown to be highly expressed in invasive breast cancers (Gawenda et al., 2007).

A second major goal of future experiments will be to determine whether V-ATPases containing the a3-isoform promote breast cancer invasion *in vivo*. Immunocompromised mice will be inoculated by tail vein injection with MCF10CA1a cells or MCF10CA1a cells stably transfected with a3 and a4-targeting short hairpin RNA expression plasmids to evaluate metastasis to lung. 12 days after injection animals will be sacrificed and lung tissue will be harvested for histological evaluation. A similar protocol has been conducted to assay the role of a3 in melanoma cell lines (Nishisho et

al., 2011). Moreover, tail vein injection of MCF10CA1a cells has previously been shown to cause lung metastases in nude mice (Tian et al., 2004). Based on our *in vitro* data, we expect that knockdown of a3 expression will decrease metastasis of MCF10CA1a cells *in vivo*. Furthermore, we expect that knockdown of a3 and a4 together will have a larger inhibitory effect on *in vivo* metastasis than knockdown of a3 alone. These results would corroborate our *in vitro* data, and demonstrate that a3 and a4 containing V-ATPases are potentially suitable anti-metastatic therapeutic targets.

A similar metastasis assay could be conducted with MCF10a cells and MCF10a cells overexpressing a3. Tail vein injection of MCF10a cells does not cause lung metastases in mice (Ordinario et al., 2012). Overexpression of a3 alone may not impart MCF10a cells with the ability to form metastases in mice. While a3 overexpressing cells have an increased invasion potential *in vivo*, they may not have an altered ability to colonize lung tissue. If no metastases form with MCF10a cells overexpressing a3 but shRNA knockdown of a3 blocks metastasis of MCF10CA1a cells, we would conclude that high a3 expression is necessary but not sufficient for metastasis to occur.

A number of additional experiments will be performed to analyze the effect of the anti-V5 antibody on c-V5 transfected MDA-MB231 cells. First, we would like to determine the mechanism of V-ATPase inhibition. To determine whether antibody addition directly inhibits the activity of V-ATPases, we will transform a yeast version of c-V5 into a yeast strain lacking endogenous c. Permeabilized vacuoles in which the V5 epitope is accessible will be obtained and used to determine whether the anti-V5 antibody affects concanamycin-sensitive ATPase activity. If antibody binding directly inhibits V-ATPase activity, its addition will result in a decrease in concanamycin-sensitive ATPase

activity. One shortcoming of this experiment is that the yeast membrane environment will be different than that of the MDA-MB231 plasma membrane. Therefore, if no inhibition of activity is observed, we cannot rule out inhibition due to steric interactions between antibody and nearby molecules in the cancer cells.

A second possibility is that antibody addition does not actually inhibit pump activity, but instead induces endocytosis of plasma membrane V-ATPases. Thus, the total number of plasma membrane V-ATPases available to secrete protons would be decreased. This would account for the loss of proton flux across the plasma membrane that we have observed (Figure 3.5). To test this, c-V5 antibody will be added to transfected MDA-MB231 cells and immunocytochemistry will be conducted at various time points after antibody addition. If plasma membrane V-ATPases are being endocytosed, we would expect to initially observe plasma membrane staining with the anti-V5 antibody and an antibody targeting subunit A. Over time, we would expect to see a relocalization of plasma membrane V-ATPases to intracellular compartments.

Another goal of future experiments will be to determine why c-V5 expression causes a decrease in endosomal/lysosomal pH and an increase in cytosolic pH in MDA-MB231 cells (Figures 3.3 and 3.6). While this effect is consistent with increased V-ATPase expression, it is not due to an increase in total V_1 subunits (Figure 3.4). A second possibility is that c-V5 expression increases the quantity of available V_0 complexes and causes an increase in V_1 assembly onto membranes. To address this, we will isolate membrane and cytosolic fractions from untransfected and transfected MDA-MB231 cells and determine by Western blotting whether there is an increase in V_1 localization onto membranes associated with c-V5 expression. Moreover, we will test the

effect of c-V5 expression on the protein levels of subunit d by Western blotting to determine whether or not there is an increase in total V_0 complexes. It is also possible that expression of c-V5 causes an increase in secretion of pro-invasive molecules, since more V_0 domains may be present. To test this, we can assay secretion of cathepsins by analyzing their levels in media isolated from untransfected and transfected MDA-MB231 cells. If increased secretion is occurring, we expect to see an increased level of cathepsins in the media of c-V5 transfected cells. No difference in secretion of pro-invasive molecules is expected since c-V5 transfected cells are not more invasive than untransfected cells (Figure 3.7).

We have demonstrated a correlation between peripheral localization of a3-containing V-ATPases in MCF10a cells overexpressing a3 and MCF10CA1a cells (Figure 2.6 and Figure 2.7). To determine whether the peripheral localization of V-ATPases observed in MCF10CA1a cells and MCF10a cells overexpressing a3 is plasma membrane localization, we will perform colocalization experiments using the Sodium Potassium ATPase as a marker for the plasma membrane. We anticipate that colocalization between V-ATPases and Sodium Potassium ATPases will be observed, indicating that V-ATPases are being localized to the plasma membrane. We will also conduct immunocytochemistry using an antibody against the lysosomal marker Lamp1. If V-ATPases are being expressed in secretory lysosomes, we would expect colocalization between Lamp1 and V-ATPases in the peripheral compartments.

We observed a large increase in mRNA levels of a1 in MCF10CA1a cells compared to MCF10a cells. However, siRNA knockdown of a1 did not cause a decrease in invasion of MCF10CA1a cells, suggesting that V-ATPases containing a1 do not

participate in invasion. One shortcoming of these experiments is that a1 levels following siRNA knockdown in MCF10CA1a cells remain higher than a1 levels in MCF10a cells (Figure 2.2 and Figure 2.3A). Therefore, a1 may still be promoting invasion in MCF10CA1a cells. To further evaluate the role of a1 in invasion of MCF10CA1a cells we can perform siRNA knockdown of a1 and a3 together. If a1 is participating in invasion, we expect to see a larger inhibition of invasion when a1 and a3 are knocked down together then when a3 is knocked down alone.

To further study whether a3-promotes invasion by localizing V-ATPases to the plasma membrane, these cells lines will be transfected with the c-V5 construct and invasion will be measured in the presence and absence of antibody. It is predicted that addition of antibody will inhibit invasion, indicating that a3 localizes V-ATPases to the plasma membrane and V-ATPases at this location are critical to invasion. Alternatively, antibody addition may not inhibition invasion of these cell lines. This result would indicate that a3-containing may be involved in the trafficking of pro-invasive molecules to the cell surface and may be involved in the secretion of secretory lysosomes.

A critical future direction is the development of an a3-specific V-ATPase inhibitor. One way the development of an inhibitor can be approached is by transforming each mammalian a isoform separately into a yeast strain lacking *VPH1* or *STV1* and conducting a screen for compounds that only inhibit activity of V-ATPases containing a3. To perform this screen we can employ the adenine-deficient *Saccharomyces cerevisiae* strain YPH500, which produces a red-pigment that is an intermediate in adenine biosynthesis. When V-ATPases are active, the red-pigment accumulates in vacuoles and colonies appear red. However, when V-ATPases are inactive the red-pigment diffuses

out of the cells and colonies appear white. This property of YPH500 has previously been used to conduct a screen that identified the Ras/cAMP/PKA pathway as a regulator of glucose-dependent dissociation (Bond and Forgac, 2008). To identify an a3-specific inhibitor, we would look for a compound that turns colonies expressing a3 white, without altering the red color of colonies expressing a1, a2 or a4.

In summary, the results of this work, in conjunction with other studies, indicate that V-ATPases participate in the invasion of metastatic cancer cells. Importantly, expression of the a3 isoform appears to promote both plasma membrane localization of V-ATPases and invasion in closely related breast cancer cell lines. Moreover, experiments conducted to directly inhibit only plasma membrane V-ATPases indicate that this population of V-ATPases is critical invasion of tumor cells. These data suggest that plasma membrane V-ATPases expressing the a3 isoform may be an effective target in the development of therapeutics to inhibit tumor cell metastasis.

Appendix 1

Determining the Role of Helical Swiveling in the Mechanism of V-ATPase Proton Translocation

Rationale

Cysteine cross-linking is a method used to determine whether specific residues in a protein are located in close proximity to one another (Jiang and Fillingame, 1998). In this method, site-directed mutagenesis is used to incorporate pairs of cysteine residues at specific sites within a protein. The mutant proteins are subjected to an oxidative treatment that will result in disulfide bond formation of cysteine residues located nearby one another. Previous work in our lab using this technique has shown that both TM2 of subunit c' and TM3 of subunit c" come close to residues of TM7 of subunit a (Kawasaki-Nishi et al., 2003; Wang et al., 2004). Importantly, residues predicted to be on opposite helical surfaces were capable of forming cross-linked products in both studies. One possible interpretation of these data is that the helices participating in the cross-linking are rotationally mobile. Mutation of the glutamic acid residue in any of the proteolipid subunits (c, c' or c") results in a complete loss of V-ATPase activity without affecting assembly (Hirata et al., 1997). These data are consistent with the requirement of protonation of every proteolipid subunit for proton translocation to occur, potentially due to conformational changes occurring upon protonation.

Additional support for the importance of helical swiveling comes from study of the F-ATPase, which is structurally and mechanistically related to the V-ATPase. The proteolipid subunits of the V-ATPase are homologous to one another and the c subunit of the F-ATPase, which contains 2 TMs. NMR analysis of the *E. coli* F-ATPase c subunit has revealed that the transmembrane segment containing the critical carboxyl group rotates with respect to the other transmembrane segment upon protonation (Rastogi and

Girvin, 1999). Moreover, cross-linking studies are supportive of helical movement occurring within the proteolipid ring of the F-ATPase as well (Vincent et al., 2007).

Here we hypothesize that helical swiveling is important for proton pumping by V-ATPases. Specifically, helical swiveling may control proton translocation through hemichannels located between subunit a and the proteolipid ring that control access of protons to the buried glutamic acid residues of the proteolipid ring. In addition to providing information regarding the mechanistic significance of helical swiveling, the experiments proposed in this Appendix will also provide information regarding the helical packing of the V-ATPase proteolipid subunits, which is not currently known.

Experimental Procedures

Yeast Strains

SF838-5Aα *S. cerevisiae* strains containing either wildtype *VMA1* or *VMA1* encoding the C261V mutation were previously generated (Liu et al., 1997). Yeast lacking the *VMA11, VPH1*, and *STV1* genes were previously constructed using the YPH500 yeast strain (Kawasaki-Nishi et al., 2003). *VMA1* was disrupted using a disruption cassette generated from the pUG27 plasmid to replace *VMA1* with a loxP flanked *HIS* gene (Gueldener et al., 2002), generating a YPH500 strain lacking endogenous *VPH1*, *STV1*, *VMA1* and *VMA11*. The *HIS* gene was subsequently recovered by transforming cells with the Cre-Expression plasmid pSH66 and selecting for growth on plates with nourseothricin (Sigma) at a concentration of 100 μg/ml. Mutations in *VMA11* were generated using the Quikchange Lightning Site-Directed Mutagenesis Kit (Stratagene).

Copper treatment

Vacuolar membranes were isolated as previously described (Wang et al., 2008). Isolated vacuolar membranes were treated with copper under conditions previously used to induce cross-linking (Kawasaki-Nishi et al., 2003). Briefly, vacuolar membrane vesicles were washed in buffer (5 mM Tris-Mes, pH 7.5, 0.25 mM $MgCl_2$ and 1.1 M glycerol) and divided into two tubes. Freshly prepared 2.5 mM Cu(1,10-phenanthroline)$_2SO_4$ was added to one tube and an equal volume of buffer without Cu(1,10-phenanthroline)$_2SO_4$ was added to the second tube. Both samples were incubated for 30 min at room temperature. The sample lacking Cu(1,10-phenanthroline)$_2SO_4$ was used as the no copper control in proton transport experiments.

Proton Transport Measurements

ATP-dependent proton transport by purified vacuolar membranes was measured as the initial rate of ATP-dependent fluorescence quenching using the fluorescence dye 9-amino-6-chloro-2-methoxyacridine (ACMA), as described previously (Toei et al., 2011).

Results and Future Directions

Previous work in our lab has produced single cysteine mutations within TM4 of subunit c' (Kawasaki-Nishi-et al., 2003). In order to block helical rotation within c', pairs of cysteine residues able to form cross-links between TM2 and TM4 will be need to be identified. Site-specific mutagenesis was conducted to generate mutations on the adjacent TM2 at positions predicted to be in close contact with TM4 (Figure A1.1).

A

Mutations made:

S144C, V64C
S144C, M65C
S144C, S66C
S144C, G67C
S144C, I68C
S144C, L69C
S144C, A70C
S144C, I71C
S144C, Y72C
S146C, M65C
S146C, S66C
S146C, G67C
S146C, I68C
S146C,L69C
S146C, A70C
S146C,I71C
S146C, Y72C

B

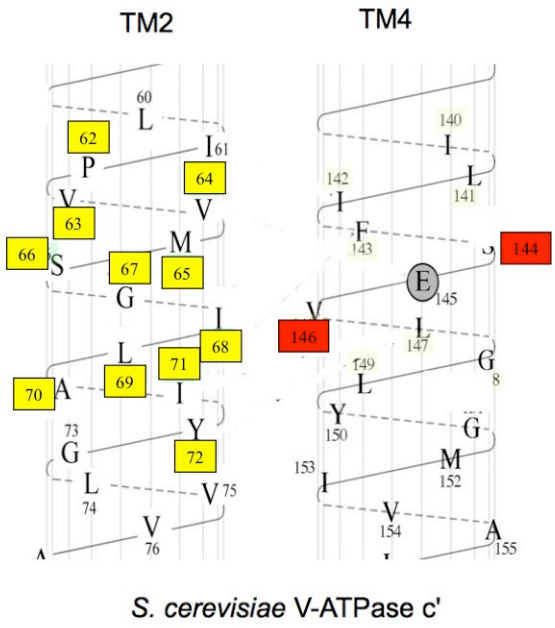

Figure A1.1. Mutations Generated in c' to Test the Effect of Cysteine Cross-Linking on V-ATPase Activity. Cysteine mutations in TM2 were constructed in c' containing single cysteine mutations in TM4 at positions 144 or 146. A, a list of cysteine pairs constructed in this study. B, predicted positions of residues in TM2 and TM4. Mutations introduced in TM2 are highlighted in yellow and mutations in TM4 are highlighted in red.

These predictions are based on homology to the c subunit of the *S. platensis* ATP synthase, for which crystal structures showing interactions between adjacent helices have been obtained (Pogoryelov et al., 2009; Krah et al., 2010). We have chosen to make cysteine pairs using a c' subunit containing single cysteine mutations within TM4 at residues 144 and 146. These two residues are on opposite sides of the critical Glu145 and are on different helical faces. Sequential residues in TM2 have been individually mutated to cysteine using the PCR-based QuikChange Lightning Site-Directed Mutagenesis Kit and paired with the existing single cysteine mutations in TM4 (Figure A1.1). Successful generation of cysteine pairs was verified by sequencing. These plasmids will be transformed into yeast lacking endogenous subunit c' as well as endogenous Vph1p and Stvp1. Along with mutant c' subunits, a cysteine-less mutant of *VPH1* will be transformed into this strain to ensure that oxidative copper treatment does cause cross-linking between Vph1p and subunit c' that would inhibit activity of V-ATPases.

Crude membrane fractions will be prepared and treated with the hydrophobic oxidizing agent copper phenanthroline to generate cross-links between nearby cysteine residues. Successful generation of cross-links will be determined by a shift in mobility on SDS-page following oxidizing treatment (Figure A1.2). After we identify pairs of residues able to cross-link, we will purify vacuolar membranes from yeast expressing these mutations, treat vacuoles with copper phenanthroline and test V-ATPase activity in two ways. First, we will measure ATPase activity using a coupled spectrophotometric assay in the presence or absence of the V-ATPase inhibitor concanamycin A. V-ATPase

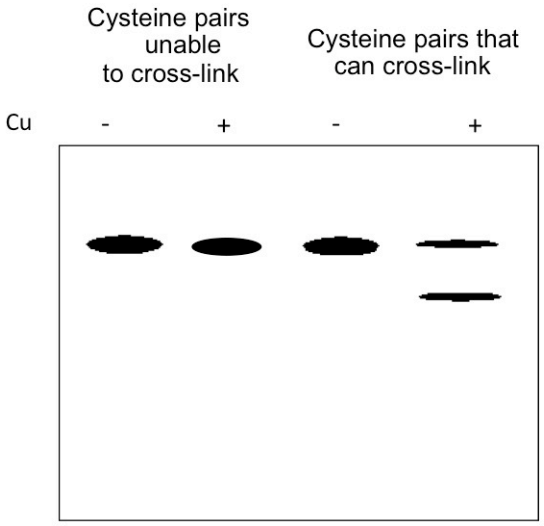

Figure A1.2. Model of Predicted Mobility Shifts in Cysteine Mutants After Copper Treatment. If cysteine pairs are unable to form disulfide bonds, copper treatment is expected to have no effect on mobility as detected by Western blotting for c' (left side). In cysteine pairs are able to form disulfide bonds, we predict a shift in mobility toward lower apparent molecular weight after copper treatment (right side).

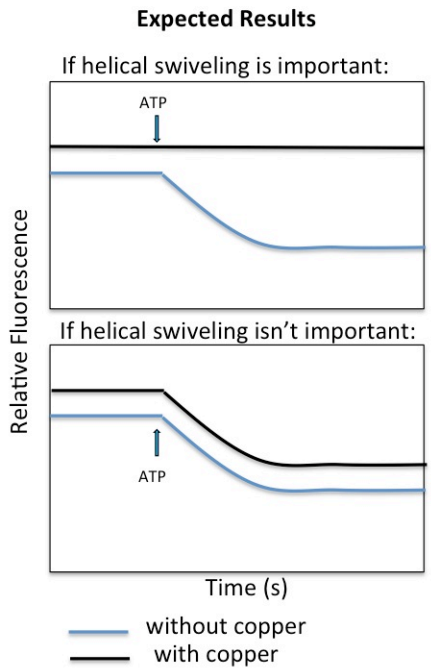

Figure A1.3. Model of Predicted Effects of Cross-Linking on Proton Transport. Proton transport will be measured as the initial rate of ATP-dependent ACMA fluorescence quenching. If helical swiveling is mechanistically important for proton translocation, we expected to see a loss of proton transport with oxidative copper treatment (top). Alternatively, if helical swiveling is not mechanistically important for V-ATPase activity, copper treatment will have no effect on proton transport (bottom).

activity can be defined as the fraction of ATPase activity that is sensitive to concanamycin A. Since ATP hydrolysis and proton transport are coupled, copper treatment that prevents helical swiveling is expected to block concanamycin A sensitive ATPase activity. Second, we will measure proton pumping by detecting ATP dependent fluorescence quenching of the fluorescent probe ACMA in the presence and absence of concanamycin A (Figure A1.3). If helical swiveling is important for proton translocation through V_0, the formation of a covalent bond that inhibits swiveling should prevent proton pumping.

Prior to analyzing the role of helical swiveling in proton translocation, we needed to determine whether or not V-ATPase activity is preserved after oxidative treatment with copper. Disulfide bond formation within the catalytic site of subunit A inhibits activity of V-ATPases. Mutation of one of the cysteine residues (C261V) involved in inhibitory disulfide bond formation has been shown to abolish hydrogen peroxide-mediated inhibition (Liu et al., 1997). However, the effect of copper phenanthroline treatment on activity of V-ATPases containing the C261V mutant has not previously been evaluated. To test this, vacuoles were isolated from yeast containing either wildtype subunit A or subunit A containing the C261V mutation and ATP-dependent proton transport was measured. As shown in Figure A.4, addition of copper completely abolished proton transport in cells expressing wildtype subunit A. However, addition of copper did not affect proton transport of cells expressing the C261V mutation, indicating that cysteine residues in the catalytic site are solely responsible for copper-mediated V-ATPase inhibition (Figure A1.4).

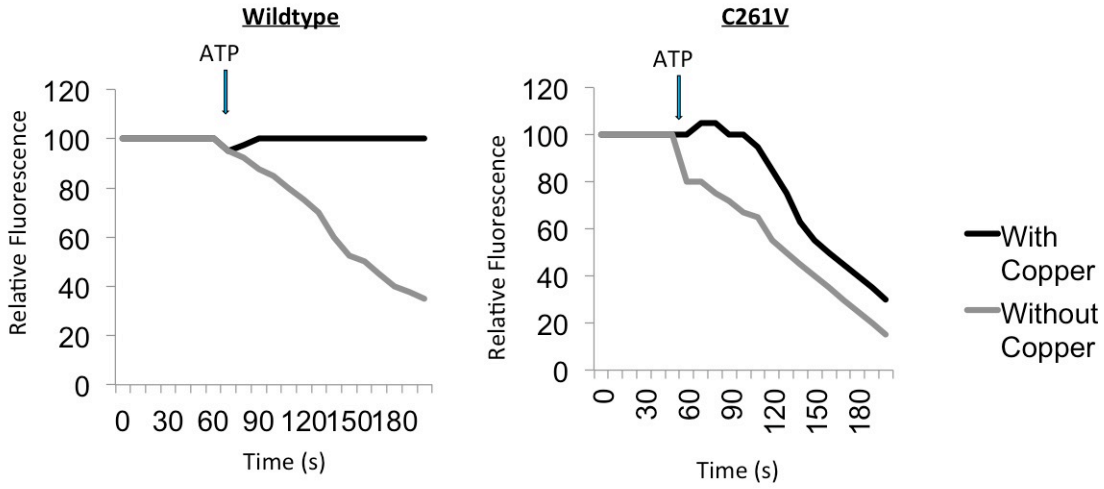

Figure A1.4. Proton Transport in Wildtype and Subunit A C261V Yeast. Vacuolar membranes were purified from yeast expressing wildtype *VMA1* or *VMA1* with the C261V mutation and proton transport was measured as the initial rate of ATP-dependent ACMA fluorescence quenching with or without oxidative pre-incubation with $Cu(1,10\text{-phenanthroline})_2SO_4$. The data displayed are representative of results obtained with two independent experiments.

These results indicated that the yeast strain we use to study helical swiveling must contain the C261V mutation in subunit A. To create this strain *VMA1* was deleted from YPH500 lacking *VPH1, STV1* and *VMA11* by homologous recombination using a PCR-generated loxP-flanked disruption cassette that replaces *VMA1* with *HIS* (Gueldener et al., 2002). Successful *VMA1* disruption was verified by sequencing. The mutant *VMA11* genes used in this study are expressed in the pRS413 plasmid that expresses the *HIS* marker. Therefore, in order to transform these plasmids into the Δ*vma1*Δ*vma11*Δ*vph1*Δ*stv1* strain, the *HIS* marker must be recovered from the site of *VMA1* deletion. This was accomplished by transforming yeast with the Cre-expressing pSH66 plasmid that contains a resistance gene for the antibiotic nourseothricin. Transformed cells were grown on nourseothricin selection plates and resistant yeast colonies were isolated. Resistant yeast were replica plated onto two complete supplement mixture plates either containing or lacking histidine. Colonies that grew on plates with histidine, but not on plates without histidine were isolated and DNA was sequenced to determine whether the *HIS* gene was successfully removed. The next step of this project will be to transform the necessary plasmids into the generated yeast strain and test for the ability to form cross-links.

Appendix II

V-ATPases

Published in *The Encyclopedia of Biological Chemistry*
Vol. 4, pp. 520-524, 2013

V-ATPases

J Capecci and M Forgac, Tufts University School of Medicine, Boston, MA, USA

This article is a revision of the previous edition article by Michael Forgac, volume 4, pp. 349–353, © 2004, Elsevier Inc.

Glossary

Access channel An aqueous channel that allows protons to reach buried carboxyl groups in the center of the membrane from one side of the membrane or the other.
Osteopetrosis A genetic disease in humans associated with the inability to degrade bone, one cause of which is a defect in the vacuolar proton translocating adenosine triphosphatase (V-ATPase) of osteoclasts.
Receptor-mediated endocytosis The process by which cells take up specific ligands from their environment (such as low-density lipoprotein) via cell-surface receptors.
V-ATPase Vacuolar proton translocating ATPase that carries out active proton transport from the cytoplasmic to the noncytoplasmic side of the membrane driven by energy released upon hydrolysis of adenosine triphosphate (ATP).

Vacuolar (H^+)-Adenosine Triphosphatase Function

Function of Intracellular Vacuolar (H^+)-ATPases

Vacuolar (H^+)-adenosine triphosphatase (ATPases) (V-ATPases) have been identified in many intracellular compartments, including endosomes, lysosomes, Golgi-derived vesicles, and secretory vesicles. V-ATPases within endosomal compartments are important for the process of receptor-mediated endocytosis (Figure 1). During receptor-mediated endocytosis, cells take up ligands (such as the cholesterol-carrying-complex, low-density lipoprotein, or LDL) from their environment by binding them to receptors on the cell surface and clustering these receptors in specialized regions of the plasma membrane (clathrin-coated pits) which then invaginate into the cell. Following this internalization, the ligand–receptor complexes are exposed to a low pH within the early (sorting) endosome that causes the internalized ligand to dissociate from its receptor. This dissociation allows the receptor to recycle to the plasma membrane (where it is reutilized) and the ligand to proceed to the lysosome, where it is degraded. The low pH within the endosome is generated by the V-ATPase.

Acidification of endosomes is also important in the formation of carrier vesicles that carry the released ligands from early to late endosomal compartments and in the delivery of newly synthesized lysosomal enzymes from the Golgi to lysosomes. The latter process involves the binding of these enzymes to mannose-6-phosphate receptors in the *trans*-Golgi followed by their delivery to an endosomal compartment. Within this compartment, the low pH created by the V-ATPases causes dissociation of the lysosomal enzymes from their receptors, allowing delivery of the enzymes to the lysosome and recycling of the receptors to the *trans*-Golgi. Finally, endosomal acidification is involved in the entry of certain envelope viruses (such as influenza virus) and toxins (such as diphtheria and anthrax toxins) into cells. These viruses and toxins bind to the surface of cells and are internalized by the process of endocytosis. Upon exposure to a low pH, the virus coat fuses with the endosomal membrane, releasing the viral nucleic acid into the cytoplasm of the host cell. In the case of internalized toxins, the low pH induces a conformational change in a portion of the toxin which creates a pore in the endosomal membrane through which the cytotoxic portion of the toxin enters the cell. Endosomal acidification is, therefore, essential in the process by which these viruses and toxins infect and kill cells.

Lysosomes are the major compartment in which degradation of proteins and other macromolecules occurs in cells. The lysosomal enzymes responsible for this degradation all require an acidic environment to be active. This acidic environment is created by the V-ATPases. Secretory vesicles, such as synaptic vesicles, are also acidic compartments. Synaptic vesicles are located at the synaptic terminal of nerve cells and release neurotransmitters (that chemically trigger the next nerve cell) by fusion with the plasma membrane. Neurotransmitters become concentrated within synaptic vesicles by transport proteins within the synaptic vesicle membrane that utilize either the proton gradient or the membrane potential generated by the V-ATPases to drive uptake of the transmitter. Finally, beyond their role in acidification, V-ATPases have been suggested to play a direct role in membrane fusion.

Function of Plasma Membrane V-ATPases

Plasma membrane V-ATPases play an important role in a number of normal and disease processes. In alpha-intercalated cells in the kidney, V-ATPases are located in the apical membrane where they pump protons into the urine, thus helping to control the pH of the blood. A genetic defect in this pump leads to a disease called renal tubule acidosis, in which the kidney is unable to secrete sufficient acid. V-ATPases are also present in the plasma membrane of osteoclasts, which are cells that function in degradation of bone. These cells are essential during development to facilitate bone remodeling. Plasma membrane V-ATPases in osteoclasts create an acidic extracellular environment that is necessary for bone degradation to occur. A genetic defect in the V-ATPase in osteoclasts leads to the human disease autosomal recessive osteopetrosis, in which the inability to degrade bone leads to severe skeletal defects and perturbations in Ca^{2+} homeostasis.

Plasma membrane V-ATPases in macrophages and neutrophils have been shown to help maintain a neutral internal

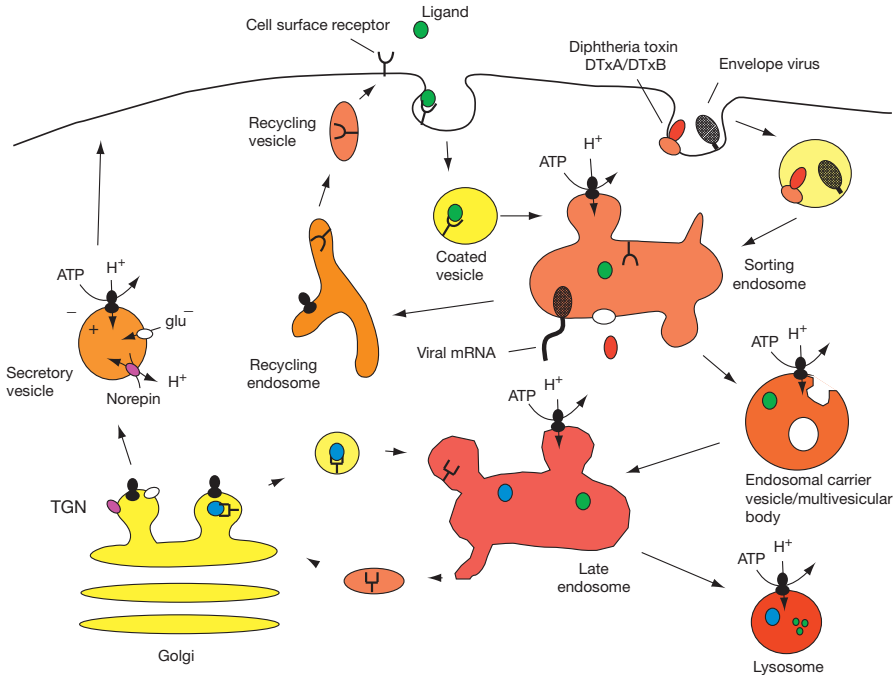

Figure 1 Function of intracellular V-ATPases. Acidification of early (sorting) endosomes by the V-ATPase facilitates receptor recycling following endocytic uptake and formation of endosomal carrier vesicles. Recycling M6P receptors to the *trans*-Golgi is also dependent on a low luminal pH. V-ATPase activity is required to drive neurotransmitter uptake by secretory vesicles and facilitates protein degradation in lysosomes. Finally, endosomal acidification facilitates the entry of the cytotoxic portions of viruses (such as influenza virus) and toxins (such as diphtheria toxin) into cells (see text).

pH under conditions of severe acid load. In the vas deferens, V-ATPases create a low pH environment necessary for sperm development. V-ATPases in the plasma membrane of tumor cells have also been proposed to function in tumor invasion by providing an acidic extracellular environment necessary for secreted lysosomal enzymes to degrade extracellular matrix. There is, thus, interest in V-ATPase inhibitors as potential anticancer drugs. Finally, V-ATPases in intestinal cells in insects create a membrane potential across the apical membrane that is used to drive potassium transport into the gut.

V-ATPase Structure

The V-ATPase is a large complex composed of 14 different subunits. These subunits are arranged into two separate domains termed V_1 and V_0 (Figure 2). The V_1 domain is made up entirely of subunits that are peripheral to the membrane (i.e., not membrane embedded). This domain has a molecular mass of ~720 kDa and contains eight different subunits (subunits A–H) of molecular mass 70–13 kDa (Table 1). The V_1 domain is responsible for hydrolysis of ATP, which occurs on catalytic sites located on the three copies of subunit A. There are, therefore, three catalytic nucleotide-binding sites per complex. The B subunits (which are also present in three copies per complex) can also bind nucleotides, but these sites are referred to as 'noncatalytic' sites, since they do not actually hydrolyze ATP. The function of these sites is not known, but they may play a role in controlling the activity of the V-ATPase. The A and B subunits are arranged in a hexamer, like the segments of an orange, with alternating A and B subunits. ATP is hydrolyzed sequentially at each of the three catalytic sites. The other subunits in the V_1 domain (subunits C–H) function to connect the V_1 domain to the V_0 domain and are discussed here.

The V_0 domain in yeast is composed of six different subunits (subunits a, d, c, c′, c″, and e) of molecular mass 100–9 kDa. All of the subunits in the V_0 domain except subunit d are embedded in the membrane and, thus, require detergent for solubilization. The V_0 complex has a molecular mass of 260 kDa and is responsible for transport of protons across the membrane. This proton transport only occurs when the V_1 domain is attached to V_0 and is driven by the hydrolysis of ATP in V_1. Three of the subunits in the V_0 domain are called 'proteolipid subunits' (c, c′, and c″) because they are so hydrophobic that they can be extracted from the membrane using organic solvent mixtures, such as chloroform:methanol. These subunits are almost completely embedded in the membrane and the polypeptide chain of each one crosses the membrane 4–5 times (these are called 'transmembrane segments'). Buried in the middle of one of the transmembrane segments of each of

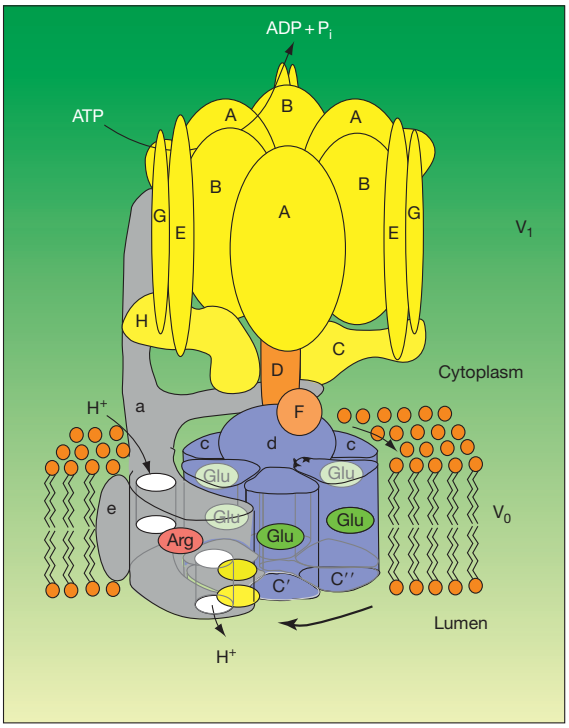

Figure 2 Structure of the V-ATPases. The V-ATPases contain two domains. The V_1 domain is responsible for ATP hydrolysis and the V_0 domain carries out proton transport across the membrane. Like the F-ATPases, the V-ATPases operate by a rotary mechanism in which ATP hydrolysis in V_1 drives rotation of a central stalk which is connected to a ring of proteolipid subunits in V_0. It is movement of the proteolipid ring relative to subunit a that drives proton transport (see text). An Arginine (Arg) residue on subunit a and glutamic acid (Glu) residues on the ring of proteolipid subunits are crucial for proton translocation and are shown in red and green, respectively. Charged residues on subunit a that contribute to proton-conducting hemi-channels are shown in yellow.

Table 1 Subunit composition of the V-ATPase

Domain	*Subunit*	*Gene (yeast)*	*M_r (kDa)*	*Function/location*
V_1	A	*VMA1*	69	Catalytic ATP-binding site
	B	*VMA2*	58	Noncatalytic ATP-binding site
	C	*VMA5*	44	Peripheral stalk, regulation of reversible dissociation
	D	*VMA8*	29	Central stalk
	E	*VMA4*	26	Peripheral stalk
	F	*VMA7*	14	Central stalk
	G	*VMA10*	13	Peripheral stalk
	H	*VMA13*	54	Peripheral stalk, inhibition of free V_1 ATP hydrolysis
V_0	a	*VPH1/STV1*	100	Proton translocation, targeting
	d	*VMA6*	40	Cytoplasmic side
	c	*VMA3*	17	Proton translocation, bafilomycin-binding site
	c′	*VMA11*	17	Proton translocation
	c″	*VMA16*	23	Proton translocation
	e	*VMA9*	9	Unknown

the proteolipid subunits is a single essential glutamic acid residue, which is reversibly protonated and deprotonated during proton transport by the V-ATPases. Like the A and B subunits in the V_1 domain, the proteolipid subunits in the V_0 domain form a ring, with four copies of subunit c and one copy each of subunit c′ and c″. The specific V-ATPase inhibitor bafilomycin has been shown to bind to the proteolipid subunits of the V_0 domain.

In addition to the proteolipid subunits, the a and e subunits of V_0 are also embedded in the membrane. Subunit a is 100 kDa and is made up of two domains. The carboxyl-terminal half of the molecule contains eight transmembrane segments while the amino-terminal half is a hydrophilic domain that is present on the cytoplasmic side of the membrane. Like the proteolipid subunits, subunit a also contains amino acid residues that are essential for proton transport. In particular, there is a positively charged arginine residue near the middle of the seventh transmembrane segment of subunit a that is absolutely required for proton transport by the V-ATPases. Subunit e is a small (9 kDa) highly hydrophobic protein of unknown function. The function of subunit d, which is tightly bound to the V_0 domain but is not embedded in the membrane, is thought to be in bridging the central stalk of V_1 (see below) with the proteolipid ring of V_0. It should be noted that in mammals there is no gene encoding subunit c′, but that the mammalian V_0 domain contains an additional accessory subunit (Ac45) of unknown function.

The V_1 and V_0 domains are connected by a single central stalk and multiple peripheral stalks. The central stalk is composed of the subunits D and F, whereas the peripheral stalks are composed of subunits C, E, G, H, and the soluble domain of subunit a. The function of these stalks is described below.

Mechanism of ATP-Driven Proton Transport by the V-ATPases

The V-ATPases operate by a rotary mechanism, similar to that demonstrated for the F-ATPases (or ATP synthases), which are enzyme complexes present in mitochondria, chloroplasts, and bacteria that function in the reverse direction (that is in proton-driven ATP synthesis). For the V-ATPases, ATP hydrolysis in the V_1 domain drives rotation of the central stalk (containing subunits D and F), which in turn drives rotation of the ring of proteolipid subunits relative to subunit a in the V_0 domain. Subunit a is held fixed relative to the A_3B_3 hexamer of V_1 by the peripheral stalks (or stators), composed of subunits C, E, G, H, and the soluble domain of subunit a. Recent data indicate there are three peripheral stalks, each of which contain a heterodimer of subunits E and G. It is rotation of the ring of proteolipid subunits relative to subunit a that drives active transport of protons from the cytoplasmic to the lumenal side of the membrane. A proton enters from the cytoplasmic side of the membrane via a cytoplasmic access channel in subunit a and protonates a buried carboxyl group on one of the proteolipid subunits. ATP hydrolysis in V_1 forces rotation of the proteolipid ring in the plane of the membrane such that the protonated carboxyl group on the proteolipid subunit reaches a second access channel in subunit a that leads to the lumenal side of the membrane. Interaction between this carboxyl group on the proteolipid subunit and the buried arginine residue of subunit a (which is positively charged) forces the proton off of the proteolipid subunit into the lumenal access channel, where it can be released to the lumenal side of the membrane, thus completing the transport cycle. In this way, the rotary motion driven by hydrolysis of ATP is converted into unidirectional transport of protons across the membrane.

Regulation of V-ATPase Activity *In Vivo*

The activity of V-ATPases in different membranes in the cell is known to be regulated such that the pH of different intracellular compartments and the degree of proton transport across the plasma membrane are carefully controlled, but the mechanisms employed in regulating V-ATPase activity in cells are still being elucidated. One important mechanism of regulation involves reversible dissociation of the V-ATPase complex into its component V_1 and V_0 domains. In yeast, dissociation occurs in response to removal of glucose from the media, probably as a way to preserve cellular energy stores. This process has been shown to be regulated by the Ras/cAMP/protein kinase A pathway. Reversible dissociation has also been demonstrated to occur in insects and in mammalian cells. In dendritic cells, activation of antigen processing increases V-ATPase assembly on the lysosomal membrane as a way to stimulate antigen processing, which depends upon the activity of proteases that have optimal activity at low pH. A second proposed regulatory mechanism involves the formation of a disulfide bond between conserved cysteine residues located at the catalytic site on the subunit A. Differences in the efficiency of coupling of ATP hydrolysis and proton transport have also been observed for V-ATPases containing different isoforms of subunit a and likely help to explain the difference in pH of different intracellular compartments.

Changes in the density of V-ATPases in different cellular membranes have also been proposed as a means of controlling proton transport. This has been shown to occur in intercalated cells in the kidney, where exposure to a low pH causes the fusion of intracellular vesicles containing the V-ATPase with the plasma membrane, thus increasing proton transport out of the cell into the renal fluid. Regulated exocytosis of V-ATPases has also been demonstrated in epididymal clear cells. Differential targeting of V-ATPases to different cellular membranes appears to be controlled by isoforms of the a subunit. Thus, the a3 isoform is able to target the V-ATPase to the plasma membrane in osteoclasts, whereas the a4 isoform targets the V-ATPase to the intercalated cell plasma membrane. It is mutations in these isoforms that lead to the human diseases osteopetrosis and renal tubule acidosis mentioned earlier. Isoforms have now been identified in many of the V-ATPase subunits in mammalian cells, and these have been shown to be expressed in both tissue- and organelle-specific manner. This has led to the expectation that specific inhibitors can be identified that are selective in their ability to inhibit particular V-ATPase complexes, which may in turn lead to the development of drugs for the treatment of diseases such as osteoporosis and tumor metastasis.

See also: **Lipids Carbohydrates Membranes and Membrane Proteins:** Lipid Rafts.

Further Reading

Bond S and Forgac M (2008) The Ras/cAMP/protein kinase A pathway regulates glucose dependent assembly of the vacuolar (H^+)-ATPase in yeast. *Journal of Biological Chemistry* 283: 36513–36521.

Forgac M (2007) Vacuolar ATPases: Rotary proton pumps in physiology and pathophysiology. *Nature Reviews. Molecular Cell Biology* 8: 917–929.

Hinton A, Sennoune SR, Bond S, et al. (2009) Function of a subunit isoforms of the V-ATPase in pH homeostasis and *in vitro* invasion of MDA-MB231 human breast cancer cells. *Journal of Biological Chemistry* 284: 16400–16408.

Hurtado-Lorenzo A, Skinner M, El Annan J, et al. (2006) V-ATPase interacts with ARNO and Arf6 in early endosomes and regulates the protein degradative pathway. *Nature Cell Biology* 8: 124–136.

Lu M, Ammar D, Ives H, Albrecht F, and Gluck SL (2007) Physical interaction between aldolase and vacuolar H^+-ATPase is essential for the assembly and activity of the proton pump. *Journal of Biological Chemistry* 282: 24495–24503.

Zhang Z, Zheng Y, Mazon H, et al. (2008) Structure of the yeast vacuolar ATPase. *Journal of Biological Chemistry* 283: 35983–35995.

References

Abrami L, Lindsay M, Parton RG, Leppla SH, van der Goot FG. 2004. Membrane insertion of anthrax protective antigen and cytoplasmic delivery of lethal factor occur at different stages of the endocytic pathway. J Cell Biol 166(5):645-51.

Basak S, Lim J, Manimekalai MS, Balakrishna AM, Gruber G. 2013. Crystal and NMR structures give insights into the role and dynamics of subunit F of the eukaryotic V-ATPase from saccharomyces cerevisiae. J Biol Chem 288(17):11930-9.

Berdowska I. 2004. Cysteine proteases as disease markers. Clin Chim Acta 342(1-2):41-69.

Blomqvist SR, Vidarsson H, Soder O, Enerback S. 2006. Epididymal expression of the forkhead transcription factor Foxi1 is required for male fertility. Embo j 25(17):4131-41.

Blott EJ and Griffiths GM. 2002. Secretory lysosomes. Nat Rev Mol Cell Biol 3(2):122-31.

Bond S and Forgac M. 2008. The Ras/cAMP/protein kinase A pathway regulates glucose-dependent assembly of the vacuolar (H+)-ATPase in yeast. J Biol Chem 283(52):36513-21.

Brown D, Paunescu TG, Breton S, Marshansky V. 2009. Regulation of the V-ATPase in kidney epithelial cells: Dual role in acid-base homeostasis and vesicle trafficking. J Exp Biol 212(Pt 11):1762-72.

Cailleau R, Young R, Olive M, Reeves WJ,Jr. 1974. Breast tumor cell lines from pleural effusions. J Natl Cancer Inst 53(3):661-74.

Cain BD. 2000. Mutagenic analysis of the F0 stator subunits. J Bioenerg Biomembr 32(4):365-71.

Canel M, Serrels A, Frame MC, Brunton VG. 2013. E-cadherin-integrin crosstalk in cancer invasion and metastasis. J Cell Sci 126(Pt 2):393-401.

Cavallo-Medved D, Rudy D, Blum G, Bogyo M, Caglic D, Sloane BF. 2009. Live-cell imaging demonstrates extracellular matrix degradation in association with active cathepsin B in caveolae of endothelial cells during tube formation. Exp Cell Res 315(7):1234-46.

Chabottaux V and Noel A. 2007. Breast cancer progression: Insights into multifaceted matrix metalloproteinases. Clin Exp Metastasis 24(8):647-56.

Chung C, Mader CC, Schmitz JC, Atladottir J, Fitchev P, Cornwell ML, Koleske AJ, Crawford SE, Gorelick F. 2011. The vacuolar-ATPase modulates matrix metalloproteinase isoforms in human pancreatic cancer. Lab Invest 91(5):732-43.

Cross RL and Muller V. 2004. The evolution of A-, F-, and V-type ATP synthases and ATPases: Reversals in function and changes in the H+/ATP coupling ratio. FEBS Lett 576(1-2):1-4.

Da Silva N, Shum WW, El-Annan J, Paunescu TG, McKee M, Smith PJ, Brown D, Breton S. 2007. Relocalization of the V-ATPase B2 subunit to the apical membrane of epididymal clear cells of mice deficient in the B1 subunit. Am J Physiol Cell Physiol 293(1):C199-210.

Dawson PJ, Wolman SR, Tait L, Heppner GH, Miller FR. 1996. MCF10AT: A model for the evolution of cancer from proliferative breast disease. Am J Pathol 148(1):313-9.

Debnath J, Muthuswamy SK, Brugge JS. 2003. Morphogenesis and oncogenesis of MCF-10A mammary epithelial acini grown in three-dimensional basement membrane cultures. Methods 30(3):256-68.

Dechant R, Binda M, Lee SS, Pelet S, Winderickx J, Peter M. 2010. Cytosolic pH is a second messenger for glucose and regulates the PKA pathway through V-ATPase. Embo j 29(15):2515-26.

Di Giovanni J, Boudkkazi S, Mochida S, Bialowas A, Samari N, Leveque C, Youssouf F, Brechet A, Iborra C, Maulet Y, et al. 2010. V-ATPase membrane sector associates with synaptobrevin to modulate neurotransmitter release. Neuron 67(2):268-79.

Diab H, Ohira M, Liu M, Cobb E, Kane PM. 2009. Subunit interactions and requirements for inhibition of the yeast V1-ATPase. J Biol Chem 284(20):13316-25.

Diakov TT and Kane PM. 2010. Regulation of vacuolar proton-translocating ATPase activity and assembly by extracellular pH. J Biol Chem 285(31):23771-8.

Drory O, Frolow F, Nelson N. 2004. Crystal structure of yeast V-ATPase subunit C reveals its stator function. EMBO Rep 5(12):1148-52.

El Far O and Seagar M. 2011. A role for V-ATPase subunits in synaptic vesicle fusion? J Neurochem 117(4):603-12.

Feng Y and Forgac M. 1992. Cysteine 254 of the 73-kDa A subunit is responsible for inhibition of the coated vesicle (H+)-ATPase upon modification by sulfhydryl reagents. J Biol Chem 267(9):5817-22.

Feng Y and Forgac M. 1994. Inhibition of vacuolar H(+)-ATPase by disulfide bond formation between cysteine 254 and cysteine 532 in subunit A. J Biol Chem 269(18):13224-30.

Fillingame RH, Angevine CM, Dmitriev OY. 2002. Coupling proton movements to c-ring rotation in F(1)F(o) ATP synthase: Aqueous access channels and helix rotations at the a-c interface. Biochim Biophys Acta 1555(1-3):29-36.

Finnigan GC, Cronan GE, Park HJ, Srinivasan S, Quiocho FA, Stevens TH. 2012. Sorting of the yeast vacuolar-type, proton-translocating ATPase enzyme complex (V-ATPase): Identification of a necessary and sufficient Golgi/endosomal retention signal in Stv1p. J Biol Chem 287(23):19487-500.

Flannery AR, Graham LA, Stevens TH. 2004. Topological characterization of the c, c', and c" subunits of the vacuolar ATPase from the yeast saccharomyces cerevisiae. J Biol Chem 279(38):39856-62.

Fogarty FM, O'Keeffe J, Zhadanov A, Papkovsky D, Ayllon V, O'Connor R. 2013. HRG-1 enhances cancer cell invasive potential and couples glucose metabolism to cytosolic/extracellular pH gradient regulation by the vacuolar-H ATPase. Oncogene .

Forgac M. 2007. Vacuolar ATPases: Rotary proton pumps in physiology and pathophysiology. Nat Rev Mol Cell Biol 8(11):917-29.

Frattini A, Orchard PJ, Sobacchi C, Giliani S, Abinun M, Mattsson JP, Keeling DJ, Andersson AK, Wallbrandt P, Zecca L, et al. 2000. Defects in TCIRG1 subunit of the vacuolar proton pump are responsible for a subset of human autosomal recessive osteopetrosis. Nat Genet 25(3):343-6.

Frosch BA, Berquin I, Emmert-Buck MR, Moin K, Sloane BF. 1999. Molecular regulation, membrane association and secretion of tumor cathepsin B. Apmis 107(1):28-37.

Galli T, McPherson PS, De Camilli P. 1996. The V0 sector of the V-ATPase, synaptobrevin, and synaptophysin are associated on synaptic vesicles in a triton X-100-resistant, freeze-thawing sensitive, complex. J Biol Chem 271(4):2193-8.

Gawenda J, Traub F, Luck HJ, Kreipe H, von Wasielewski R. 2007. Legumain expression as a prognostic factor in breast cancer patients. Breast Cancer Res Treat 102(1):1-6.

Ghosh P, Dahms NM, Kornfeld S. 2003. Mannose 6-phosphate receptors: New twists in the tale. Nat Rev Mol Cell Biol 4(3):202-12.

Gillet L, Roger S, Besson P, Lecaille F, Gore J, Bougnoux P, Lalmanach G, Le Guennec JY. 2009. Voltage-gated sodium channel activity promotes cysteine cathepsin-dependent invasiveness and colony growth of human cancer cells. J Biol Chem 284(13):8680-91.

Gillies RJ and Martinez-Zaguilan R. 1991. Regulation of intracellular pH in BALB/c 3T3 cells. bicarbonate raises pH via NaHCO3/HCl exchange and attenuates the activation of Na+/H+ exchange by serum. J Biol Chem 266(3):1551-6.

Gocheva V and Joyce JA. 2007. Cysteine cathepsins and the cutting edge of cancer invasion. Cell Cycle 6(1):60-4.

Gocheva V, Zeng W, Ke D, Klimstra D, Reinheckel T, Peters C, Hanahan D, Joyce JA. 2006. Distinct roles for cysteine cathepsin genes in multistage tumorigenesis. Genes Dev 20(5):543-56.

Gondi CS and Rao JS. 2013. Cathepsin B as a cancer target. Expert Opin Ther Targets 17(3):281-91.

Gruenberg J and van der Goot FG. 2006. Mechanisms of pathogen entry through the endosomal compartments. Nat Rev Mol Cell Biol 7(7):495-504.

Gu F and Gruenberg J. 2000. ARF1 regulates pH-dependent COP functions in the early endocytic pathway. J Biol Chem 275(11):8154-60.

Gueldener U, Heinisch J, Koehler GJ, Voss D, Hegemann JH. 2002. A second set of loxP marker cassettes for cre-mediated multiple gene knockouts in budding yeast. Nucleic Acids Res 30(6):e23.

Gunther W, Luchow A, Cluzeaud F, Vandewalle A, Jentsch TJ. 1998. ClC-5, the chloride channel mutated in dent's disease, colocalizes with the proton pump in endocytotically active kidney cells. Proc Natl Acad Sci U S A 95(14):8075-80.

Gupta GP and Massague J. 2006. Cancer metastasis: Building a framework. Cell 127(4):679-95.

Hashimoto Y, Kondo C, Kojima T, Nagata H, Moriyama A, Hayakawa T, Katunuma N. 2006. Significance of 32-kDa cathepsin L secreted from cancer cells. Cancer Biother Radiopharm 21(3):217-24.

Hendrix A, Sormunen R, Westbroek W, Lambein K, Denys H, Sys G, Braems G, Van den Broecke R, Cocquyt V, Gespach C, et al. 2013. Vacuolar H+ ATPase expression and activity is required for Rab27B-dependent invasive growth and metastasis of breast cancer. Int J Cancer 133(4):843-54.

Hiesinger PR, Fayyazuddin A, Mehta SQ, Rosenmund T, Schulze KL, Zhai RG, Verstreken P, Cao Y, Zhou Y, Kunz J, et al. 2005. The v-ATPase V0 subunit a1 is required for a late step in synaptic vesicle exocytosis in drosophila. Cell 121(4):607-20.

Hinton A, Bond S, Forgac M. 2009a. V-ATPase functions in normal and disease processes. Pflugers Arch 457(3):589-98.

Hinton A, Sennoune SR, Bond S, Fang M, Reuveni M, Sahagian GG, Jay D, Martinez-Zaguilan R, Forgac M. 2009b. Function of a subunit isoforms of the V-ATPase in pH homeostasis and in vitro invasion of MDA-MB231 human breast cancer cells. J Biol Chem 284(24):16400-8.

Hirata R, Graham LA, Takatsuki A, Stevens TH, Anraku Y. 1997. VMA11 and VMA16 encode second and third proteolipid subunits of the saccharomyces cerevisiae vacuolar membrane H+-ATPase. J Biol Chem 272(8):4795-803.

Holliday LS, Lu M, Lee BS, Nelson RD, Solivan S, Zhang L, Gluck SL. 2000. The amino-terminal domain of the B subunit of vacuolar H+-ATPase contains a filamentous actin binding site. J Biol Chem 275(41):32331-7.

Hurtado-Lorenzo A, Skinner M, El Annan J, Futai M, Sun-Wada GH, Bourgoin S, Casanova J, Wildeman A, Bechoua S, Ausiello DA, et al. 2006. V-ATPase interacts with ARNO and Arf6 in early endosomes and regulates the protein degradative pathway. Nat Cell Biol 8(2):124-36.

Imamura H, Nakano M, Noji H, Muneyuki E, Ohkuma S, Yoshida M, Yokoyama K. 2003. Evidence for rotation of V1-ATPase. Proc Natl Acad Sci U S A 100(5):2312-5.

Inoue T and Forgac M. 2005. Cysteine-mediated cross-linking indicates that subunit C of the V-ATPase is in close proximity to subunits E and G of the V1 domain and subunit a of the V0 domain. J Biol Chem 280(30):27896-903.

Jefferies KC, Cipriano DJ, Forgac M. 2008. Function, structure and regulation of the vacuolar (H+)-ATPases. Arch Biochem Biophys 476(1):33-42.

Jefferies KC and Forgac M. 2008. Subunit H of the vacuolar (H+) ATPase inhibits ATP hydrolysis by the free V1 domain by interaction with the rotary subunit F. J Biol Chem 283(8):4512-9.

Jiang L, Salao K, Li H, Rybicka JM, Yates RM, Luo XW, Shi XX, Kuffner T, Tsai VW, Husaini Y, et al. 2012. Intracellular chloride channel protein CLIC1 regulates macrophage function through modulation of phagosomal acidification. J Cell Sci 125(Pt 22):5479-88.

Jiang W and Fillingame RH. 1998. Interacting helical faces of subunits a and c in the F1Fo ATP synthase of escherichia coli defined by disulfide cross-linking. Proc Natl Acad Sci U S A 95(12):6607-12.

Kane PM. 2012. Targeting reversible disassembly as a mechanism of controlling V-ATPase activity. Curr Protein Pept Sci 13(2):117-23.

Kane PM. 2006. The where, when, and how of organelle acidification by the yeast vacuolar H+-ATPase. Microbiol Mol Biol Rev 70(1):177-91.

Kane PM. 1995. Disassembly and reassembly of the yeast vacuolar H(+)-ATPase in vivo. J Biol Chem 270(28):17025-32.

Karet FE, Finberg KE, Nelson RD, Nayir A, Mocan H, Sanjad SA, Rodriguez-Soriano J, Santos F, Cremers CW, Di Pietro A, et al. 1999. Mutations in the gene encoding B1 subunit of H+-ATPase cause renal tubular acidosis with sensorineural deafness. Nat Genet 21(1):84-90.

Kato Y, Lambert CA, Colige AC, Mineur P, Noel A, Frankenne F, Foidart JM, Baba M, Hata R, Miyazaki K, et al. 2005. Acidic extracellular pH induces matrix metalloproteinase-9 expression in mouse metastatic melanoma cells through the phospholipase D-mitogen-activated protein kinase signaling. J Biol Chem 280(12):10938-44.

Kawasaki-Nishi S, Bowers K, Nishi T, Forgac M, Stevens TH. 2001a. The amino-terminal domain of the vacuolar proton-translocating ATPase a subunit controls targeting and in vivo dissociation, and the carboxyl-terminal domain affects coupling of proton transport and ATP hydrolysis. J Biol Chem 276(50):47411-20.

Kawasaki-Nishi S, Nishi T, Forgac M. 2001b. Yeast V-ATPase complexes containing different isoforms of the 100-kDa a-subunit differ in coupling efficiency and in vivo dissociation. J Biol Chem 276(21):17941-8.

Kawasaki-Nishi S, Nishi T, Forgac M. 2001c. Arg-735 of the 100-kDa subunit a of the yeast V-ATPase is essential for proton translocation. Proc Natl Acad Sci U S A 98(22):12397-402.

Kawasaki-Nishi S, Nishi T, Forgac M. 2003. Interacting helical surfaces of the transmembrane segments of subunits a and c' of the yeast V-ATPase defined by disulfide-mediated cross-linking. J Biol Chem 278(43):41908-13.

Kohio HP and Adamson AL. 2013. Glycolytic control of vacuolar-type ATPase activity: A mechanism to regulate influenza viral infection. Virology 444(1-2):301-9.

Kopan R and Ilagan MX. 2009. The canonical notch signaling pathway: Unfolding the activation mechanism. Cell 137(2):216-33.

Kornak U, Kasper D, Bosl MR, Kaiser E, Schweizer M, Schulz A, Friedrich W, Delling G, Jentsch TJ. 2001. Loss of the ClC-7 chloride channel leads to osteopetrosis in mice and man. Cell 104(2):205-15.

Krah A, Pogoryelov D, Meier T, Faraldo-Gomez JD. 2010. On the structure of the proton-binding site in the F(o) rotor of chloroplast ATP synthases. J Mol Biol 395(1):20-7.

Leng XH, Manolson MF, Forgac M. 1998. Function of the COOH-terminal domain of Vph1p in activity and assembly of the yeast V-ATPase. J Biol Chem 273(12):6717-23.

Leng XH, Manolson MF, Liu Q, Forgac M. 1996. Site-directed mutagenesis of the 100-kDa subunit (Vph1p) of the yeast vacuolar (H+)-ATPase. J Biol Chem 271(37):22487-93.

Li YP, Chen W, Liang Y, Li E, Stashenko P. 1999. Atp6i-deficient mice exhibit severe osteopetrosis due to loss of osteoclast-mediated extracellular acidification. Nat Genet 23(4):447-51.

Liberman R, Cotter K, Baleja JD, Forgac M. 2013. Structural analysis of the N-terminal domain of subunit a of the yeast vacuolar ATPase (V-ATPase) using accessibility of single cysteine substitutions to chemical modification. J Biol Chem 288(31):22798-808.

Liegeois S, Benedetto A, Garnier JM, Schwab Y, Labouesse M. 2006. The V0-ATPase mediates apical secretion of exosomes containing hedgehog-related proteins in caenorhabditis elegans. J Cell Biol 173(6):949-61.

Liu Q, Kane PM, Newman PR, Forgac M. 1996. Site-directed mutagenesis of the yeast V-ATPase B subunit (Vma2p). J Biol Chem 271(4):2018-22.

Liu Q, Leng XH, Newman PR, Vasilyeva E, Kane PM, Forgac M. 1997. Site-directed mutagenesis of the yeast V-ATPase A subunit. J Biol Chem 272(18):11750-6.

Lu M, Ammar D, Ives H, Albrecht F, Gluck SL. 2007. Physical interaction between aldolase and vacuolar H+-ATPase is essential for the assembly and activity of the proton pump. J Biol Chem 282(34):24495-503.

Lu M, Holliday LS, Zhang L, Dunn WA,Jr, Gluck SL. 2001. Interaction between aldolase and vacuolar H+-ATPase: Evidence for direct coupling of glycolysis to the ATP-hydrolyzing proton pump. J Biol Chem 276(32):30407-13.

Lu M, Sautin YY, Holliday LS, Gluck SL. 2004. The glycolytic enzyme aldolase mediates assembly, expression, and activity of vacuolar H+-ATPase. J Biol Chem 279(10):8732-9.

MacLeod KJ, Vasilyeva E, Baleja JD, Forgac M. 1998. Mutational analysis of the nucleotide binding sites of the yeast vacuolar proton-translocating ATPase. J Biol Chem 273(1):150-6.

Maher MJ, Akimoto S, Iwata M, Nagata K, Hori Y, Yoshida M, Yokoyama S, Iwata S, Yokoyama K. 2009. Crystal structure of A3B3 complex of V-ATPase from thermus thermophilus. Embo j 28(23):3771-9.

Manolson MF, Wu B, Proteau D, Taillon BE, Roberts BT, Hoyt MA, Jones EW. 1994. STV1 gene encodes functional homologue of 95-kDa yeast vacuolar H(+)-ATPase subunit Vph1p. J Biol Chem 269(19):14064-74.

Martinez-Zaguilan R, Lynch RM, Martinez GM, Gillies RJ. 1993. Vacuolar-type H(+)-ATPases are functionally expressed in plasma membranes of human tumor cells. Am J Physiol 265(4 Pt 1):C1015-29.

Martinez-Zaguilan R, Seftor EA, Seftor RE, Chu YW, Gillies RJ, Hendrix MJ. 1996. Acidic pH enhances the invasive behavior of human melanoma cells. Clin Exp Metastasis 14(2):176-86.

Meier T, Polzer P, Diederichs K, Welte W, Dimroth P. 2005. Structure of the rotor ring of F-type na+-ATPase from ilyobacter tartaricus. Science 308(5722):659-62.

Michel V, Licon-Munoz Y, Trujillo K, Bisoffi M, Parra KJ. 2013. Inhibitors of vacuolar ATPase proton pumps inhibit human prostate cancer cell invasion and prostate-specific antigen expression and secretion. Int J Cancer 132(2):E1-10.

Mindell JA. 2012. Lysosomal acidification mechanisms. Annu Rev Physiol 74:69-86.

Moore KJ and Fillingame RH. 2013. Obstruction of transmembrane helical movements in subunit a blocks proton pumping by F1Fo ATP synthase. J Biol Chem 288(35):25535-41.

Morel N, Dedieu JC, Philippe JM. 2003. Specific sorting of the a1 isoform of the V-H+ATPase a subunit to nerve terminals where it associates with both synaptic vesicles and the presynaptic plasma membrane. J Cell Sci 116(Pt 23):4751-62.

Murata T, Yamato I, Kakinuma Y, Leslie AG, Walker JE. 2005. Structure of the rotor of the V-type na+-ATPase from enterococcus hirae. Science 308(5722):654-9.

Nanda A, Brumell JH, Nordstrom T, Kjeldsen L, Sengelov H, Borregaard N, Rotstein OD, Grinstein S. 1996. Activation of proton pumping in human neutrophils occurs by exocytosis of vesicles bearing vacuolar-type H+-ATPases. J Biol Chem 271(27):15963-70.

Nguyen DX, Bos PD, Massague J. 2009. Metastasis: From dissemination to organ-specific colonization. Nat Rev Cancer 9(4):274-84.

Nishisho T, Hata K, Nakanishi M, Morita Y, Sun-Wada GH, Wada Y, Yasui N, Yoneda T. 2011. The a3 isoform vacuolar type H(+)-ATPase promotes distant metastasis in the mouse B16 melanoma cells. Mol Cancer Res 9(7):845-55.

Norgett EE, Golder ZJ, Lorente-Canovas B, Ingham N, Steel KP, Karet Frankl FE. 2012. Atp6v0a4 knockout mouse is a model of distal renal tubular acidosis with hearing loss, with additional extrarenal phenotype. Proc Natl Acad Sci U S A 109(34):13775-80.

O'Callaghan KM, Ayllon V, O'Keeffe J, Wang Y, Cox OT, Loughran G, Forgac M, O'Connor R. 2010. Heme-binding protein HRG-1 is induced by insulin-like growth factor I and associates with the vacuolar H+-ATPase to control endosomal pH and receptor trafficking. J Biol Chem 285(1):381-91.

Ochotny N, Flenniken AM, Owen C, Voronov I, Zirngibl RA, Osborne LR, Henderson JE, Adamson SL, Rossant J, Manolson MF, et al. 2011. The V-ATPase a3 subunit mutation R740S is dominant negative and results in osteopetrosis in mice. J Bone Miner Res 26(7):1484-93.

Oluwatosin YE and Kane PM. 1997. Mutations in the CYS4 gene provide evidence for regulation of the yeast vacuolar H+-ATPase by oxidation and reduction in vivo. J Biol Chem 272(44):28149-57.

Oot RA and Wilkens S. 2012. Subunit interactions at the V1-vo interface in yeast vacuolar ATPase. J Biol Chem 287(16):13396-406.

Oot RA and Wilkens S. 2010. Domain characterization and interaction of the yeast vacuolar ATPase subunit C with the peripheral stator stalk subunits E and G. J Biol Chem 285(32):24654-64.

Ordinario E, Han HJ, Furuta S, Heiser LM, Jakkula LR, Rodier F, Spellman PT, Campisi J, Gray JW, Bissell MJ, et al. 2012. ATM suppresses SATB1-induced malignant progression in breast epithelial cells. PLoS One 7(12):e51786.

Parra KJ, Keenan KL, Kane PM. 2000. The H subunit (Vma13p) of the yeast V-ATPase inhibits the ATPase activity of cytosolic V1 complexes. J Biol Chem 275(28):21761-7.

Partridge J and Flaherty P. 2009. An in vitro FluoroBlok tumor invasion assay. J Vis Exp (29). pii: 1475. doi(29):10.3791/1475.

Pastor-Soler N, Beaulieu V, Litvin TN, Da Silva N, Chen Y, Brown D, Buck J, Levin LR, Breton S. 2003. Bicarbonate-regulated adenylyl cyclase (sAC) is a sensor that regulates pH-dependent V-ATPase recycling. J Biol Chem 278(49):49523-9.

Pastor-Soler NM, Hallows KR, Smolak C, Gong F, Brown D, Breton S. 2008. Alkaline pH- and cAMP-induced V-ATPase membrane accumulation is mediated by protein kinase A in epididymal clear cells. Am J Physiol Cell Physiol 294(2):C488-94.

Paunescu TG, Russo LM, Da Silva N, Kovacikova J, Mohebbi N, Van Hoek AN, McKee M, Wagner CA, Breton S, Brown D. 2007. Compensatory membrane expression of the V-ATPase B2 subunit isoform in renal medullary intercalated cells of B1-deficient mice. Am J Physiol Renal Physiol 293(6):F1915-26.

Pena-Llopis S, Vega-Rubin-de-Celis S, Schwartz JC, Wolff NC, Tran TA, Zou L, Xie XJ, Corey DR, Brugarolas J. 2011. Regulation of TFEB and V-ATPases by mTORC1. Embo j 30(16):3242-58.

Peri F and Nusslein-Volhard C. 2008. Live imaging of neuronal degradation by microglia reveals a role for v0-ATPase a1 in phagosomal fusion in vivo. Cell 133(5):916-27.

Peters C, Bayer MJ, Buhler S, Andersen JS, Mann M, Mayer A. 2001. Trans-complex formation by proteolipid channels in the terminal phase of membrane fusion. Nature 409(6820):581-8.

Pogoryelov D, Krah A, Langer JD, Yildiz O, Faraldo-Gomez JD, Meier T. 2010. Microscopic rotary mechanism of ion translocation in the F(o) complex of ATP synthases. Nat Chem Biol 6(12):891-9.

Pogoryelov D, Yildiz O, Faraldo-Gomez JD, Meier T. 2009. High-resolution structure of the rotor ring of a proton-dependent ATP synthase. Nat Struct Mol Biol 16(10):1068-73.

Powell B, Graham LA, Stevens TH. 2000. Molecular characterization of the yeast vacuolar H+-ATPase proton pore. J Biol Chem 275(31):23654-60.

Qi J and Forgac M. 2007. Cellular environment is important in controlling V-ATPase dissociation and its dependence on activity. J Biol Chem 282(34):24743-51.

Qin A, Cheng TS, Pavlos NJ, Lin Z, Dai KR, Zheng MH. 2012. V-ATPases in osteoclasts: Structure, function and potential inhibitors of bone resorption. Int J Biochem Cell Biol 44(9):1422-35.

Rastogi VK and Girvin ME. 1999. Structural changes linked to proton translocation by subunit c of the ATP synthase. Nature 402(6759):263-8.

Ridley AJ, Schwartz MA, Burridge K, Firtel RA, Ginsberg MH, Borisy G, Parsons JT, Horwitz AR. 2003. Cell migration: Integrating signals from front to back. Science 302(5651):1704-9.

Robey IF, Baggett BK, Kirkpatrick ND, Roe DJ, Dosescu J, Sloane BF, Hashim AI, Morse DL, Raghunand N, Gatenby RA, et al. 2009. Bicarbonate increases tumor pH and inhibits spontaneous metastases. Cancer Res 69(6):2260-8.

Robey IF and Nesbit LA. 2013. Investigating mechanisms of alkalinization for reducing primary breast tumor invasion. Biomed Res Int 2013:485196.

Rojas JD, Sennoune SR, Maiti D, Bakunts K, Reuveni M, Sanka SC, Martinez GM, Seftor EA, Meininger CJ, Wu G, et al. 2006. Vacuolar-type H+-ATPases at the plasma membrane regulate pH and cell migration in microvascular endothelial cells. Am J Physiol Heart Circ Physiol 291(3):H1147-57.

Roos A and Boron WF. 1981. Intracellular pH. Physiol Rev 61(2):296-434.

Sagermann M, Stevens TH, Matthews BW. 2001. Crystal structure of the regulatory subunit H of the V-type ATPase of saccharomyces cerevisiae. Proc Natl Acad Sci U S A 98(13):7134-9.

Santner SJ, Dawson PJ, Tait L, Soule HD, Eliason J, Mohamed AN, Wolman SR, Heppner GH, Miller FR. 2001. Malignant MCF10CA1 cell lines derived from premalignant human breast epithelial MCF10AT cells. Breast Cancer Res Treat 65(2):101-10.

Sautin YY, Lu M, Gaugler A, Zhang L, Gluck SL. 2005. Phosphatidylinositol 3-kinase-mediated effects of glucose on vacuolar H+-ATPase assembly, translocation, and acidification of intracellular compartments in renal epithelial cells. Mol Cell Biol 25(2):575-89.

Saw NM, Kang SY, Parsaud L, Han GA, Jiang T, Grzegorczyk K, Surkont M, Sun-Wada GH, Wada Y, Li L, et al. 2011. Vacuolar H(+)-ATPase subunits Voa1 and Voa2 cooperatively regulate secretory vesicle acidification, transmitter uptake, and storage. Mol Biol Cell 22(18):3394-409.

Scimeca JC, Franchi A, Trojani C, Parrinello H, Grosgeorge J, Robert C, Jaillon O, Poirier C, Gaudray P, Carle GF. 2000. The gene encoding the mouse homologue of the human osteoclast-specific 116-kDa V-ATPase subunit bears a deletion in osteosclerotic (oc/oc) mutants. Bone 26(3):207-13.

Sennoune SR, Bakunts K, Martinez GM, Chua-Tuan JL, Kebir Y, Attaya MN, Martinez-Zaguilan R. 2004. Vacuolar H+-ATPase in human breast cancer cells with distinct metastatic potential: Distribution and functional activity. Am J Physiol Cell Physiol 286(6):C1443-52.

Sennoune SR and Martinez-Zaguilan R. 2012. Vacuolar H(+)-ATPase signaling pathway in cancer. Curr Protein Pept Sci 13(2):152-63.

Seol JH, Shevchenko A, Shevchenko A, Deshaies RJ. 2001. Skp1 forms multiple protein complexes, including RAVE, a regulator of V-ATPase assembly. Nat Cell Biol 3(4):384-91.

Sethi N, Yan Y, Quek D, Schupbach T, Kang Y. 2010. Rabconnectin-3 is a functional regulator of mammalian notch signaling. J Biol Chem 285(45):34757-64.

Shao E and Forgac M. 2004. Involvement of the nonhomologous region of subunit A of the yeast V-ATPase in coupling and in vivo dissociation. J Biol Chem 279(47):48663-70.

Shao E, Nishi T, Kawasaki-Nishi S, Forgac M. 2003. Mutational analysis of the non-homologous region of subunit A of the yeast V-ATPase. J Biol Chem 278(15):12985-91.

Shum WW, Da Silva N, Belleannee C, McKee M, Brown D, Breton S. 2011. Regulation of V-ATPase recycling via a RhoA- and ROCKII-dependent pathway in epididymal clear cells. Am J Physiol Cell Physiol 301(1):C31-43.

Shum WW, Da Silva N, Brown D, Breton S. 2009. Regulation of luminal acidification in the male reproductive tract via cell-cell crosstalk. J Exp Biol 212(Pt 11):1753-61.

Sloane BF, Sameni M, Podgorski I, Cavallo-Medved D, Moin K. 2006. Functional imaging of tumor proteolysis. Annu Rev Pharmacol Toxicol 46:301-15.

Smardon AM and Kane PM. 2007. RAVE is essential for the efficient assembly of the C subunit with the vacuolar H(+)-ATPase. J Biol Chem 282(36):26185-94.

Smardon AM, Tarsio M, Kane PM. 2002. The RAVE complex is essential for stable assembly of the yeast V-ATPase. J Biol Chem 277(16):13831-9.

Smith AN, Skaug J, Choate KA, Nayir A, Bakkaloglu A, Ozen S, Hulton SA, Sanjad SA, Al-Sabban EA, Lifton RP, et al. 2000. Mutations in ATP6N1B, encoding a new kidney vacuolar proton pump 116-kD subunit, cause recessive distal renal tubular acidosis with preserved hearing. Nat Genet 26(1):71-5.

So J, Lee HJ, Kramata P, Minden A, Suh N. 2012. Differential expression of key signaling proteins in MCF10 cell lines, a human breast cancer progression model. Molecular and Cellular Pharmacology 4(1):31-40.

Soule HD, Maloney TM, Wolman SR, Peterson WD,Jr, Brenz R, McGrath CM, Russo J, Pauley RJ, Jones RF, Brooks SC. 1990. Isolation and characterization of a

spontaneously immortalized human breast epithelial cell line, MCF-10. Cancer Res 50(18):6075-86.

Soule HD, Vazguez J, Long A, Albert S, Brennan M. 1973. A human cell line from a pleural effusion derived from a breast carcinoma. J Natl Cancer Inst 51(5):1409-16.

Srinivasan S, Vyas NK, Baker ML, Quiocho FA. 2011. Crystal structure of the cytoplasmic N-terminal domain of subunit I, a homolog of subunit a, of V-ATPase. J Mol Biol 412(1):14-21.

Stover EH, Borthwick KJ, Bavalia C, Eady N, Fritz DM, Rungroj N, Giersch AB, Morton CC, Axon PR, Akil I, et al. 2002. Novel ATP6V1B1 and ATP6V0A4 mutations in autosomal recessive distal renal tubular acidosis with new evidence for hearing loss. J Med Genet 39(11):796-803.

Su Y, Blake-Palmer KG, Sorrell S, Javid B, Bowers K, Zhou A, Chang SH, Qamar S, Karet FE. 2008. Human H+ATPase a4 subunit mutations causing renal tubular acidosis reveal a role for interaction with phosphofructokinase-1. Am J Physiol Renal Physiol 295(4):F950-8.

Su Y, Zhou A, Al-Lamki RS, Karet FE. 2003. The a-subunit of the V-type H+-ATPase interacts with phosphofructokinase-1 in humans. J Biol Chem 278(22):20013-8.

Sumner JP, Dow JA, Earley FG, Klein U, Jager D, Wieczorek H. 1995. Regulation of plasma membrane V-ATPase activity by dissociation of peripheral subunits. J Biol Chem 270(10):5649-53.

Sun-Wada GH, Toyomura T, Murata Y, Yamamoto A, Futai M, Wada Y. 2006. The a3 isoform of V-ATPase regulates insulin secretion from pancreatic beta-cells. J Cell Sci 119(Pt 21):4531-40.

Tian F, Byfield SD, Parks WT, Stuelten CH, Nemani D, Zhang YE, Roberts AB. 2004. Smad-binding defective mutant of transforming growth factor beta type I receptor enhances tumorigenesis but suppresses metastasis of breast cancer cell lines. Cancer Res 64(13):4523-30.

Toei M, Saum R, Forgac M. 2010. Regulation and isoform function of the V-ATPases. Biochemistry 49(23):4715-23.

Toei M, Toei S, Forgac M. 2011. Definition of membrane topology and identification of residues important for transport in subunit a of the vacuolar ATPase. J Biol Chem 286(40):35176-86.

Toyomura T, Murata Y, Yamamoto A, Oka T, Sun-Wada GH, Wada Y, Futai M. 2003. From lysosomes to the plasma membrane: Localization of vacuolar-type H+ -

ATPase with the a3 isoform during osteoclast differentiation. J Biol Chem 278(24):22023-30.

Toyomura T, Oka T, Yamaguchi C, Wada Y, Futai M. 2000. Three subunit a isoforms of mouse vacuolar H(+)-ATPase. preferential expression of the a3 isoform during osteoclast differentiation. J Biol Chem 275(12):8760-5.

Trombetta ES, Ebersold M, Garrett W, Pypaert M, Mellman I. 2003. Activation of lysosomal function during dendritic cell maturation. Science 299(5611):1400-3.

Vaccari T, Duchi S, Cortese K, Tacchetti C, Bilder D. 2010. The vacuolar ATPase is required for physiological as well as pathological activation of the notch receptor. Development 137(11):1825-32.

Vidarsson H, Westergren R, Heglind M, Blomqvist SR, Breton S, Enerback S. 2009. The forkhead transcription factor Foxi1 is a master regulator of vacuolar H-ATPase proton pump subunits in the inner ear, kidney and epididymis. PLoS One 4(2):e4471.

Vik SB and Antonio BJ. 1994. A mechanism of proton translocation by F1F0 ATP synthases suggested by double mutants of the a subunit. J Biol Chem 269(48):30364-9.

Vincent OD, Schwem BE, Steed PR, Jiang W, Fillingame RH. 2007. Fluidity of structure and swiveling of helices in the subunit c ring of escherichia coli ATP synthase as revealed by cysteine-cysteine cross-linking. J Biol Chem 282(46):33788-94.

Voss M, Vitavska O, Walz B, Wieczorek H, Baumann O. 2007. Stimulus-induced phosphorylation of vacuolar H(+)-ATPase by protein kinase A. J Biol Chem 282(46):33735-42.

Wagner CA, Finberg KE, Breton S, Marshansky V, Brown D, Geibel JP. 2004. Renal vacuolar H+-ATPase. Physiol Rev 84(4):1263-314.

Wang Y, Inoue T, Forgac M. 2004. TM2 but not TM4 of subunit c" interacts with TM7 of subunit a of the yeast V-ATPase as defined by disulfide-mediated cross-linking. J Biol Chem 279(43):44628-38.

Wang Y, Toei M, Forgac M. 2008. Analysis of the membrane topology of transmembrane segments in the C-terminal hydrophobic domain of the yeast vacuolar ATPase subunit a (Vph1p) by chemical modification. J Biol Chem 283(30):20696-702.

Wiedmann RM, von Schwarzenberg K, Palamidessi A, Schreiner L, Kubisch R, Liebl J, Schempp C, Trauner D, Vereb G, Zahler S, et al. 2012. The V-ATPase-inhibitor

archazolid abrogates tumor metastasis via inhibition of endocytic activation of the rho-GTPase Rac1. Cancer Res 72(22):5976-87.

Xu T and Forgac M. 2001. Microtubules are involved in glucose-dependent dissociation of the yeast vacuolar [H+]-ATPase in vivo. J Biol Chem 276(27):24855-61.

Xu Y, Parmar A, Roux E, Balbis A, Dumas V, Chevalier S, Posner BI. 2012. Epidermal growth factor-induced vacuolar (H+)-atpase assembly: A role in signaling via mTORC1 activation. J Biol Chem 287(31):26409-22.

Yan Y, Denef N, Schupbach T. 2009. The vacuolar proton pump, V-ATPase, is required for notch signaling and endosomal trafficking in drosophila. Dev Cell 17(3):387-402.

Yokoyama K, Nakano M, Imamura H, Yoshida M, Tamakoshi M. 2003. Rotation of the proteolipid ring in the V-ATPase. J Biol Chem 278(27):24255-8.

Zhang Z, Zheng Y, Mazon H, Milgrom E, Kitagawa N, Kish-Trier E, Heck AJ, Kane PM, Wilkens S. 2008. Structure of the yeast vacuolar ATPase. J Biol Chem 283(51):35983-95.

Zoncu R, Bar-Peled L, Efeyan A, Wang S, Sancak Y, Sabatini DM. 2011. mTORC1 senses lysosomal amino acids through an inside-out mechanism that requires the vacuolar H(+)-ATPase. Science 334(6056):678-83.

Zoncu R, Efeyan A, Sabatini DM. 2011. mTOR: From growth signal integration to cancer, diabetes and ageing. Nat Rev Mol Cell Biol 12(1):21-35.

Zuo J, Jiang J, Chen SH, Vergara S, Gong Y, Xue J, Huang H, Kaku M, Holliday LS. 2006. Actin binding activity of subunit B of vacuolar H+-ATPase is involved in its targeting to ruffled membranes of osteoclasts. J Bone Miner Res 21(5):714-21.